Ref 3/1/01

LA-UR- 01-2616

Approved for public release; distribution is unlimited.

Title:	Episodic volcanism, Petrology, and Lithostratigraphy of the Pajarito Plateau and Adjacent Areas of the Espanola basin and the Jemez Mountains
Author(s):	Giday Woldegabriel, Richard G. Warren, David E. Broxton, David T. Vaniman, Matthew Heizler, Emily C. Kluk, and Lisa Peters
Submitted to:	Book on New Mexico Volcanoes and Volcanology, to be published by the New Mexico Natural History Museum, Albuquerque

Los Alamos
NATIONAL LABORATORY

EPISODIC VOLCANISM, PETROLOGY, AND LITHOSTRATIGRAPHY OF THE PAJARITO PLATEAU AND ADJACENT AREAS OF THE ESPAÑOLA BASIN AND THE JEMEZ MOUNTAINS

Giday WoldeGabriel*, Richard G. Warren*, David E. Broxton*, David T. Vaniman*, Matthew T. Heizler†, Emily C. Kluk*, and Lisa Peters†

*Hydrology, Geochemistry, and Geology Group, EES-6/MS D462
Earth Environmental Sciences Division
Los Alamos National Laboratory, Los Alamos, NM 87545

†New Mexico Geochronology Research Laboratory
New Mexico Institute of Mining and Technology, Socorro, NM 8780

Abstract

The Pajarito Plateau occupies the southwestern part of the Española Basin of the Rio Grande Rift in north central New Mexico. It is a plateau constructed from a gently east-dipping ignimbrite sequence, separated from the Jemez Mountains by the NNE-trending Pajarito fault system on the west and the Rio Grande to the east. The Pajarito fault system appears to have been active during the Neogene, consistent with episodic volcanic eruptions within the plateau. It was reactivated following the eruption of the Upper Bandelier Tuff (1.2 Ma) and forms the current western boundary of the Española Basin.

The lithostratigraphic sequence of older rocks beneath the Bandelier Tuff is dominated by sedimentary deposits of the middle to late Miocene Santa Fe Group and Pliocene Puye Formation. The older units were superseded by late Pliocene Cerros del Rio mafic lavas, erupted from the western part of the rift floor, and Plio-Pleistocene silicic tuffs of the Bandelier Tuff and associated lavas and tuffs from the adjacent western margin. The Pleistocene Bandelier Tuff forms the uppermost bedrock on the plateau. Stratigraphic information based on core and cuttings from drilling and from outcrops on the Pajarito Plateau suggest at least three episodes of mostly mafic volcanism (10.9-13.1, 8.4-9.3, and 2.3-2.8 Ma) along the western part of the Española Basin. The Miocene lavas of the Pajarito Plateau erupted contemporaneously with the Keres Group and the Lobato Basalt from the southern and northeastern parts of the Jemez Mountains, respectively.

Geochemical analysis of the Miocene mafic lavas from the Pajarito Plateau indicate generally plagioclase- and clinopyroxene phyric alkalic and tholeiitic basalts with minor basaltic andesite and mugearite flows, whereas the late Pliocene Cerros del Rio flows consist of plagioclase- and clinopyroxene-aphyric basalts plus hawaiite, mugearite and benmoreite lavas.

Eruptions differ compositionally among different regions within the Jemez volcanic field; volcanism was notably more alkalic within the southern compared with the northeastern Jemez Mountains and the Pajarito Plateau.

The intercalated mafic flows within the fluvial and lacustrine rift-fill sediments establish a temporal framework for the widespread sedimentary deposits and tectonic activity at the plateau. Intense tectonic activity, subsidence, and continuous sedimentation adjacent to the western boundary fault of the Española basin are contemporaneous with the episodic volcanic eruptions.

INTRODUCTION

The Española basin, located within the northern half of the Rio Grande rift in north central New Mexico (Fig. 1), is a half graben that is about 70 km long and 60 km wide (Chapin, 1979; Manley, 1979; Biehler et al., 1991). Along the latitude of the Jemez Mountains, the Nacimiento and the Sangre de Cristo uplifts bound the basin on the west and east, respectively. However, the present western margin of the Española Basin is several kilometers to the east of the Nacimiento Mountains and is defined by discrete or splayed segments of north- to northeast-trending normal faults of the Pajarito fault system (Manley, 1979; Golombek, 1983). Unlike the western rift boundary, the eastern margin lacks a single major boundary fault, but it is cut by a series of parallel late Cenozoic NS-trending high-angle normal faults that are displaced down to the west (Manley, 1979; Vernon and Riecker, 1989).

The Pajarito Plateau is a faulted bench that represents the western part of the Española Basin of the Rio Grande rift between the Rio Grande and the Jemez Mountains in north central New Mexico (Fig. 1). The Los Alamos National Laboratory and the town of Los Alamos are located within the central part of the Pajarito Plateau. Several studies detailing surface geology and tectonic features of the plateau are available in the published literature (Griggs, 1964; Smith et al., 1970; Manley, 1979; Golombek, 1983; Gardner and Goff, 1984; Gardner et al., 1986; Carter and Gardner, 1995; WoldeGabriel et al., 1996; Dethier, 1997). Geophysical surveys and exploratory drill holes and water wells provide preliminary information about subsurface geological features of the central part of the Pajarito Plateau. Gravity surveys of the Pajarito Plateau indicate a subsurface north-northeast-trending marginal graben or narrow structural sub-basins parallel and adjacent to the Pajarito fault zone (Budding, 1978; Ferguson et al., 1995). Shallow and deep exploratory bore holes and water wells scattered throughout the Laboratory property also provide subsurface information on structure, volcanism, and depositional and erosional processes related to the development of the western part of the Española basin. Subsurface maps based on drill hole data corroborate the presence of a NE-trending trough under the Pajarito Plateau consistent with the gravity data (Ferguson et al., 1995; Purtymun, 1995; Broxton and Reneau, 1996).

Multiple mafic lava flows interbedded within fluvial sedimentary deposits of the Miocene Santa Fe Group are intersected by various drill holes within and adjacent to the subsurface trough (Purtymun, 1995). Mafic flows consist of basalt, mugearite, and latite and also include minor vitric and pumiceous tephra deposits. Petrographic, geochemical, and geochronological analyses of selected samples from outcrops, cuttings, and cores provide information about the petrological characteristics and temporal relations of the lava flows and the associated sedimentary deposits (WoldeGabriel et al., 1999). Neogene and Quaternary volcanic and sedimentary rocks are exposed along fault scarps and in east-trending 200- to 300-m-deep, steep-sided canyons of the Pajarito Plateau. The oldest rocks of the Pajarito Plateau are exposed along White Rock Canyon and consist of sedimentary deposits of the Santa Fe Group (Baltz et al., 1963; Spiegel and Baldwin, 1963; Griggs, 1964; Dethier, 1997). Late Miocene mafic lavas are interbedded within the upper part of the sequence at the intersection of Ancho and White Rock Canyons and in Bayo Canyon (WoldeGabriel et al., 1996; Dethier, 1999). Facies of fanglomerate, lacustrine sediments, and gravel deposits of the ancestral Rio Grande within the Puye Formation cap fluvial sedimentary deposits of the Miocene Santa Fe Group in White Rock Canyon and in the northeastern part of the Pajarito Plateau (Griggs, 1964; Waresback and Turbeville, 1990; Dethier, 1997). Lava flows of the Pliocene (2.3-2.8 Ma) Cerros del Rio volcanic field also occur within the upper part of the Puye Formation (Manley, 1976; Bachman and Mehnert, 1978; Baldridge, 1979; WoldeGabriel et al., 1996; Dethier, 1997). During the late Pliocene, the mafic volcanic activity of the Española basin gave way to silicic explosive eruptions from multiple closely spaced calderas in the central part of the Jemez Mountains at about 1.78 Ma, 1.62 Ma and 1.2 Ma (Spell et al., 1990; Izett and Obradovich, 1994). The Pajarito Plateau is mostly blanketed by the Bandelier Tuff and younger tephra and Quaternary alluvial fan, colluvium, and landslide deposits (Dethier, 1997).

Different interpretations have been proposed for the origin, location, and attitude of the Pajarito fault system and its temporal and spatial relations to the Jemez volcanic field. According to Gardner and Goff (1984), the Pajarito fault system migrated eastward from the north-trending Cañada de Cochiti fault zone at the southern end of the Jemez Mountains to the eastern part of the volcanic field between 6 to 4 Ma due to the accumulation of shallow hybrid-magma chambers in the central part of the volcanic field. Other interpretations relate the current position of the fault system to intense tectonic activity along the northern part of the Española basin at about 5 to 3 Ma (Manley, 1979). According to Golombek (1983), the Pajarito fault system formed along the lithologic facies transition zone between volcanic succession of the Jemez Mountains and the sedimentary deposits of the Española Basin at about 5 Ma, following a decrease of volcanic activity in the Jemez volcanic field. The Pajarito fault system has also been interpreted as a growth fault consistent with the significant increase in the thickness of synrift sedimentary deposits of the Santa Fe Group in the western part of the Española Basin (Kelley, 1979).

New geochemical, petrographic, and geochronologic information from outcrops and subsurface mafic lavas suggest that faulting might be contemporaneous with the late Miocene volcanic eruptions in the area of the Pajarito Plateau. The volcanic sequences and associated fluvial deposits suggest that volcanic eruptions were closely related to intense tectonic processes along boundary faults during the Neogene.

This report summarizes presently known geological information used to develop a 3-D geologic model for the Pajarito Plateau. During the past several years, the Laboratory has developed a 3-D geologic model to provide a framework for hydrologic modeling (LANL 3-D Geology Team, 2000). Hydrologic modeling provides the primary means for assessing groundwater resources beneath the Pajarito Plateau and for predicting movement within groundwater of contaminants generated during early operational years of the Laboratory. Each successive year has produced an increasingly refined 3-D geologic model that describes the surface and subsurface geology of the Laboratory, which occupies the southern half of the Pajarito Plateau. It is essentially a progress report that describes recent advances in the temporal, spatial, geochemical, and petrographic characterization and understanding of the geologic units important to the geologic model, and provides descriptions and symbols for these units based on new and published work (LANL 3-D Geology Team, 2000).

SAMPLE PREPARATION AND ANALYTICAL METHODS

Samples from outcrops, and cuttings from drill hole O-4 and PM-5, in the central part of the Pajarito Plateau, were collected for petrographic, chemical, and geochronological analyses. Coarser fragments were picked during examination under binocular microscope and were cleaned using an ultrasonic probe to remove drilling contaminants. After drying, the samples were reexamined under binocular microscope. Aliquots were selected for petrographic, chemical, and/or dating analyses, depending on the alteration of the cuttings. Petrographic methods are described in a later section.

Either groundmass, plagioclase or hornblende was separated from these samples and analyzed using the incremental heating techniques at the New Mexico Geochronology Research Laboratory, New Mexico Tech, Socorro. Age and K/Ca spectra are given for each, and range from well-behaved flat spectra to highly complex ones (Figs. 2 to 5). A summary of the preferred eruption ages and a very brief explanation is given in Table 1, whereas the analytical data are provided in Appendix 1. Plateau ages represent the age calculated for the indicated steps by weighting each step by the inverse variance, and errors are calculated using the method of Taylor (1982). If the MSWD for the plateau steps is above the 95% confidence window for n-1 degrees of freedom (cf. Table 1 of Mahon, 1996), the error is multiplied by the square root of the MSWD. The plateau age is determined from the individual apparent ages, which have been calculated assuming the non-radiogenic ^{40}Ar is atmospheric. This assumption was tested for each sample by conducting isochron analyses (not shown) and in all cases less than one, the

trapped $^{40}Ar/^{36}Ar$ initial composition is within error of the atmospheric value of 295.5. Sample DEB5/98/1 gave a very slightly elevated initial $^{40}Ar/^{39}Ar$ value and regression methods of York (1969) yielded the reported isochron age (Table 1; Fig 2a). Sanidine of sample RWTB4-B8 was analyzed by the single crystal laser fusion method and those data are presented in Figure 5e and Appendix 1. All ages are calculated relative to the flux monitor standard Fish Canyon sanidine with an assigned age of 27.84 Ma. Extraction system and mass spectrometer blanks were monitored throughout the course of age dating and because of relatively large sample sizes, corrections are minimal.

Major and trace element compositions were determined for most samples from fused glass of bulk powders plus flux using a Rigaku 3064 wavelength dispersive X-ray fluorescence (XRF) at Los Alamos National Laboratory. Concentrations and analytical uncertainties were calculated from intensities using XRF-11 software (Criss, 1985), based on a model that uses intensities for 21 rock standards. Analytical quality assurance is based on acceptable analytical totals for all components, including major and trace elements as oxides and the loss on ignition. Quality of analysis is also based on acceptable matches between long-term average concentrations determined for 41 commonly used rock standards, compared with those for several such rock standards co-analyzed with our samples, as well as similar matches for secondary standards that were pulverized and co-analyzed with our samples. In this report we characterize the succession of volcanic units erupted within the Pajarito Plateau of the Española basin with those erupted adjacent to the rift floor in the Jemez volcanic field.

$^{40}Ar/^{39}Ar$ DATING RESULTS

As mentioned above, the age spectra range from flat to complex (Figs. 2 to 5). Flat spectra are defined by yielding significant portions of the age spectra, which give acceptable MSWD values (e.g., OT4-300-310; Fig. 3a; Appendix 1). Some spectra are nearly flat; however, the MSWD value is slightly elevated, indicating scatter above that predicted by the analytical uncertainties (e.g. DN97-16, Fig. 2a; Appendix 1). These spectra are probably disturbed by combination of excess argon, argon loss and/or ^{39}Ar recoil; however the disturbance does not significantly diminish the confidence in the eruption age. The plagioclase spectra are generally complex, and their age assignment is quite suspect and should be treated with caution.

The stratigraphic positions of some dated samples listed in Table 1 are shown in Figure 6. The dates from outcrops and subsurface stratigraphic sections record at least 3 major episodes of volcanic eruptions in the central part of the Pajarito Plateau. The earliest eruptions are middle Miocene in age, and consist of several flows (2-9) separated by sedimentary layers (3-140-m thick) of the Santa Fe Group (WoldeGabriel et al., 1999). Almost all of these flows were intersected in the northern part of the Pajarito Plateau, not far south from outcrops of middle Miocene Lobato Basalt in Santa Clara Canyon along the northeastern part of the Jemez Mountains (Smith et al., 1970; Aldrich and Dethier, 1990). We presently designate these middle

Miocene mafic lavas of the Pajarito Plateau as the Guaje Canyon basalt (Tb1), with an age range of 11.0 to 13.1 Ma within the 3-D model of the Pajarito Plateau (WoldeGabriel et al., 1999).

Several flows representing a second episode of mafic eruption occur in outcrop (e.g., Bayo and Ancho Canyons) and in drill holes (e.g., O-4, PM-5, etc.) throughout the central part of the Pajarito Plateau. These mafic flows, basalt through latite, are late Miocene in age and are presently designated as Bayo Canyon basalt (Tb2). The range of ages of the second episode in Table 1 is 8.49 to 8.97 Ma.

Mafic and intermediate flows were intersected within the lower parts of the Puye Formation in drill hole PM-5. Attempts to date cuttings from these flows resulted in questionable ages. Further studies are being conducted to accurately characterize these flows.

The last major volcanic episode within the Pajarito Plateau is represented by late Pliocene mafic flows of the Cerros del Rio volcanic field, with an age range of 2.33 to 3.18 Ma (WoldeGabriel et al., 1996). Although the bulk of this activity was confined to the south and east of White Rock Canyon, several flows occur in most drill holes within the upper part of the Puye Formation in the central part of the Pajarito Plateau. These flows are assigned within the 3-D model of the Pajarito Plateau as the Cerros del Rio mafic flows (Tb4). More detailed information on the dating results of different flows from outcrop and drill holes are given below by location, from south to north (Fig. 1). Following the description of results from these locations, we summarize the main stratigraphic units of the Pajarito Plateau.

Outcrops at Ancho Canyon

A localized 9.3 Ma late Miocene mafic lava flow crops out at river level on the west side of the Rio Grande, just south of the intersection of Ancho and White Rock Canyons (WoldeGabriel et al., 1996). The base of the columnar-jointed flow is not exposed, but the outcrop ranges in thickness from about 3 to 7 m. Correlative flows were intersected in drill hole O-4 in the central part of the Pajarito Plateau due north from Ancho Canyon. This flow is assigned to Bayo Canyon basalt (Tb2).

Near the intersection of Ancho and White Rock canyons, Quaternary colluvium obscures the rock units above the outcrop of the late Miocene mafic lava. However, sandstone, pumice-bearing bedded sandstone, conglomerate, and orange silty clays, belonging to the Puye Formation (Dethier, 1997) are exposed higher up in the section beneath the late Pliocene Cerros del Rio mafic flows (WoldeGabriel et al., 1996).

Mafic lava flows in drill hole O-4

The 855.5-m deep O-4 well intersected three mafic lava flows that are interbedded within the sedimentary deposits of the Pajarito Plateau. The uppermost flow is 37.5 m thick and occurs within the Pliocene Puye Formation, whereas the other two flows are located within volcaniclastic sediments temporally equivalent to the Miocene Santa Fe Group (Fig. 6). The

topmost flow (Tb4) is basaltic and is sandwiched between fanglomerates of the Puye Formation. Samples from different levels of the flow yielded an age range of 2.50 to 2.52 Ma (Table 1), consistent with the Cerros del Rio mafic flows (WoldeGabriel et al., 1996).

The uppermost mafic flow within the Santa Fe Group is 58.8-m thick, and occurs within volcaniclastic deposits of poorly defined character. Three samples of cuttings were processed for dating from this thick sequence of mafic lava, which probably represents more than two flows based on chemical composition (Table 2). An age range of 8.81 to 8.97 Ma was obtained from these samples (Table 1). A third flow was intersected about 23 m beneath the dated lava sequence and is 13.4 m thick. It is also interbedded within volcaniclastic deposits. There are no analytical data for this flow.

Mafic lava flows in drill hole PM-5

With a total depth of 948.2 m, PM-5 represents the deepest well in the central Pajarito Plateau. Seven lava flows are interbedded within the Pliocene Puye Formation and the late Miocene upper Santa Fe Group (Fig. 6). The topmost flow is 6.6-m thick basalt (Tb4) of the late Pliocene Cerros del Rio volcanic field. It caps the Puye Formation, whereas the underlying two dacite flows (38.1 and 54.9 m thick) of the upper Tschicoma Formation (Tt2), are interbedded within fanglomerates of the Puye Formation. Three deeper mafic flows of Bayo Canyon basalt (Tb2) occur within the upper part of the Santa Fe Group. The upper two of these three flows are 39.6 and 41.2 m thick, whereas the third one, 146.3 m thick, represents the thickest flow within PM-5. The basal flow (Fig. 4d), 15.2 m thick, is within the age range of the Guaje Canyon basalt (Tb1) intersected by the GR Series wells.

Incremental heating procedures for three samples of cuttings from Tb4 and Tt2 gave minor complexity for two of the age spectra and complex results for the third (Fig. 4a-c). The probable ages of these samples are given in Table 1. The Tb4 flow (2.50+0.28 Ma), capping the Puye Formation is within the age range of the Cerros del Rio basalts, whereas the underlying intermediate flows yielded older ages (~2.7 Ma). The basal flow within the Santa Fe Group in PM-5 yielded a highly interpreted middle Miocene age of 11.39±0.40 Ma. This basal flow is indistinguishable in age from other samples of Guaje Canyon basalt flows (Tb1).

Outcrops at Bayo Canyon

A fault scarp in lower Bayo Canyon, east of the Los Alamos County airport, exposes sedimentary deposits (>30 m) of the Santa Fe Group capped by at least two late Miocene basalt flows. These sediments consist of silty sandstone and sandstone and contain a thin, 10-cm thick layer of altered tuff. The sandstone directly beneath the basalt flow is baked and forms a 30-cm thick reddish orange layer. Two mafic flows, separated by thin oxidized or baked zone, crop out on the south side of the canyon, slightly above the floor (Fig. 6). These flows yielded late Miocene ages (8.8-8.78.Ma), and represent the type locality for the Bayo Canyon basalts (Tb2).

They are chemically and petrographically similar to 8.49 to 8.78 Ma basalt intersected at a depth of 209.15 m in drill hole R-9 and 239 m in drill hole R-12 (Fig. 1; Table 2; Broxton et al., 2000a, b). The upper flow is about 7.6 m thick, whereas the exposed part of the lower flow is about 4.6 m. The north side of the canyon across from these basalt flows is faulted. The footwall exposes basalt flows about 20-m thick that are fractured, altered and tilted to the west. These basalt flows underlie medium brown and well-sorted sandstone (≥ 1 m thick) with abundant basalt lithics. A pumiceous layer above the Bayo Canyon basalt flows, sampled in a side canyon south of Bayo Canyon, yielded very complex spectra (Fig. 2d). Although a total gas age of 9.25 Ma was measured, the result does not represent a meaningful age.

A 1-m thick gravel horizon, probably immediately overlying an unconformity surface, separates the sandstone above the late Miocene basalts from the Pliocene Puye Formation (Fig. 6). The basal section of the Puye Formation along the footwall consists upward of a 1.5-m thick bluish gray vitric tuff, 4-5-m thick layers of silty clays, conglomerate, and gravel, and 1.0-1.5-m thick calcite-cemented fallout pumice. An age of 5.3 Ma was obtained on the vitric ash (RWTB4-B8). An 80-m thick section of the Puye Formation, consisting of tuffaceous sediments interbedded with conglomerates and gravels of dacitic composition, crops out above the fallout pumice. About 100 m upstream from the Bayo Canyon basalts, the tuffaceous sediments are generally well sorted, bedded and cross-bedded, and grade to gravel and conglomerate deposits. The Bandelier Tuff caps the Puye Formation.

About 100 m downstream from the late Miocene basalts, the pumice fall is faulted down by about 35 to 40 m to the east. Downstream from the pumice outcrop, the Puye Formation consists of tuffaceous sandstone and interbedded thin, 5-7-cm thick pumiceous layers, basaltic tuff, and conglomerate deposits. Basaltic tuff and lava flow (1.5-2-m thick) of the Cerros del Rio mafic flows (Tb4) cap the section. The basaltic lava flow is a northern extension of the outcrop along the SR502 road cut in Los Alamos Canyon, about a kilometer east of the junction of the White Rock and Los Alamos roads. A K-Ar age of 2.4 Ma was reported for the lava along the road cut, whereas a slightly younger $^{40}Ar/^{39}Ar$ age of 2.33 Ma was obtained on a nearby flow to the west (Bachman and Mehnert, 1978; WoldeGabriel et al., 1996)

LITHOSTRATIGRAPHY OF THE PAJARITO PLATEAU

The Pajarito Plateau is formed on Neogene and Quaternary sedimentary and volcanic rocks that are closely associated with the development of the Española Basin of the Rio Grande rift and the Jemez volcanic field. Although synrift sedimentary deposits dominate the oldest rocks beneath the plateau, synrift volcanic eruptions occurred along the western margin of the rift, beginning in the middle Miocene. Below, we describe the major lithostratigraphic units of the Pajarito Plateau, updating previous work with new dating results described in the previous section. In ascending stratigraphic order, the major volcanic and sedimentary units of the Pajarito Plateau belong to the Santa Fe Group and intercalated basalts, the Tschicoma and Puye

Formations, the Cerro del Rio mafic flows, and the Bandelier Tuff (Fig. 6). Mafic lavas intercalated within the Santa Fe Group include the middle Miocene Guaje Canyon and late Miocene Bayo Canyon basalts. Lithologic characteristics, including temporal and spatial relationships of the major lithostratigraphic units of several drill holes throughout the central part of the Pajarito Plateau, are summarized below. Petrographic and chemical characteristics are summarized in later sections.

Santa Fe Group (Tsf)

Sedimentary deposits of the Española basin east of the Rio Grande consist chiefly of the Santa Fe Group, and overlain by late Tertiary pediment gravels along the foothills of the western slopes of the Sangre de Cristo Mountains. These sedimentary rocks have been thoroughly characterized and divided into the Tesuque and the Chamita Formations in ascending stratigraphic order (Galusha and Blick, 1971; Cavazza, 1989). East of the Pajarito Plateau and east of the Rio Grande, Cavazza (1989) identified two sedimentary packages (lithosomes) on the basis of paleocurrent studies, lithologic characteristics, and facies analysis, and suggested eastern and northeastern provenances for the Tesuque Formation. The Tesuque Formation consists of conglomerate, sandstone, mudrock, and lacustrine sediments, including terrestrial (nonmarine) limestone. The Tesuque Formation is blanketed by remnants of the late Miocene to early Pliocene Chamita Formation in the northern part of the Española basin (Galusha and Blick, 1971; MacFadden, 1977; Aldrich and Dethier, 1990). The Chamita Formation consists of conglomerate with abundant quartzite and abundant volcanic clasts in the upper and lower parts of the sequence, respectively. Widespread erosion in the last 5 million years has stripped the Chamita Formation from much of the Española basin (Ingersoll et al., 1990).

Discontinuous outcrops of the Santa Fe Group are also exposed in the eastern parts of deep canyons crossing the Pajarito Plateau (Griggs, 1964; Purtymun, 1995; Dethier, 1997). In addition, the Santa Fe Group is unconformably exposed along a footwall of the Pajarito fault zone above the pre-rift Eocene Galisteo Formation in the vicinity of St. Peters Dome (Smith et al., 1970; Goff et al., 1990; Cather, 1992). At this location, the Santa Fe Group is about 100 m thick and generally arkosic with volcaniclastic components, including interlayerd mafic lavas, one of which is dated at 16.5 Ma (Gardner and Goff, 1984; Goff et al., 1990). Discordant and questionable total gas and isochron ages of 30.5±9.2 Ma and 17.7±3.9 Ma, respectively, were obtained on this flow by the $^{40}Ar/^{39}Ar$ method. More work is needed to accurately determine the age of the earliest volcanic flow interbedded within the basal section of the Santa Fe Group in the southern part of the Jemez Mountains.

The Santa Fe Group at the intersection of Ancho and White Rock Canyons is probably capped by the 9.3 Ma mafic flow of Bayo Canyon basalt, and thus belongs to the upper part of the unit (WoldeGabriel et al., 1996). Upstream along the Rio Grande, similar sedimentary deposits are exposed on both sides of the White Rock Canyon along the eastern parts of the

Pajarito Plateau, and were subdivided into the Tesuque and Chamita Formations (Spiegel and Baldwin, 1963; Baltz et al., 1963; Griggs, 1964).

In the subsurface, exploratory drill holes and water wells intersected thick sections of sedimentary rocks in the central part of the Pajarito Plateau. Based on lithologic descriptions of drill hole cuttings and cores, Purtymun (1995) subdivided the subsurface Santa Fe Group beneath the Pajarito Plateau into three packages, represented by the Tesuque, Chamita, and Chaquehui Formations in ascending stratigraphic order. However, new $^{40}Ar/^{39}Ar$ dating results (8.81-8.97 Ma) from lava flows interbedded within the Chaquehui formation are older than the age range (5.5-7.7 Ma; McIntosh and Quade, 1995) of the Chamita Formation at its type locality in the northern part of the Española Basin. The Tesuque and Chamita Formations were also mapped and described in outcrops in the vicinity of the central part of the Pajarito Plateau (Spiegel and Baldwin, 1963; Baltz et al., 1963; Griggs, 1964). The Chaquehui formation supposedly represents a stratigraphic sequence exposed in Chaquehui Canyon, located between Frijoles and Ancho Canyons (Purtymun, 1995). However, the section at Chaquehui Canyon consists of thick phreatomagmatic deposits that are capped by late Pliocene mafic lava flows (Heiken et al., 1995; WoldeGabriel et al., 1996) and therefore cannot be correlated with deposits identified as Chaquehui in the deep drill holes.

The Tesuque and Chamita Formation in the subsurface are of fluvial origin, containing arkosic sediments with sandstone, siltstone, and minor pebbly conglomerate lenses (Purtymun, 1995). The Chamita Formation contains interbedded ashes within pebble conglomerate. Unlike the Tesuque and the Chamita Formations, rocks assigned to the Chaquehui are characterized by mixtures of coarse volcaniclastic fragments from the Jemez Mountains and arkosic and granitic debris from sources located to the north and east of the Española basin (Purtymun, 1995). However, recent examination of cuttings assigned as Chaquehui in well O-4 indicates that the unit consists of volcaniclastic deposits with abundant dacitic clasts derived from the adjacent Jemez Mountains. These lithologic features are characteristic of the Puye Formation. We suggest that the term Chaquehui formation be abandoned and that rocks widely assigned to the Chaquehui be assigned to the Puye Formation or Santa Fe Group, depending on the lithologic composition.

Lava flows interbedded within the Santa Fe Group were intersected in all drill holes throughout the central Pajarito Plateau. The volcanic rocks are grouped according to their age into the middle Miocene Guaje Canyon basalt (Tb1) and the late Miocene Bayo Canyon basalt (Tb2).

Guaje Canyon basalt (Tb1)

Multiple mafic lava flows, separated by interbedded sediments of the Santa Fe Group, were intersected in several wells in Guaje Canyon (Fig. 1). These lavas group into the middle Miocene Guaje Canyon basalt (Tb1) based on recent $^{40}Ar/^{39}Ar$ dates (WoldeGabriel et al., 1999).

Ages for these basalts from the GR Series wells of Guaje Canyon span a relatively brief period within latest middle Miocene (11.5-13.1 Ma). These ages are within the range of the older episode of the Lobato basalt (11.9-14.1 Ma) flows from the north wall of Santa Clara Canyon (Aldrich and Dethier 1990). Additional field and analytical work is needed to confirm apparent age differences between the middle Miocene Lobato basalt and the Guaje Canyon basalts intersected by the GR Series drill holes, 10 km to the south. Given the problems associated with subdivision of the Santa Fe Group as discussed above, age control, and petrographic analysis of sediment samples intercalated with Guaje Canyon basalt may offer reliable temporal and spatial constraints.

Bayo Canyon basalt (Tb2)

Flows of the Bayo Canyon basalt (Tb2) have been identified in outcrop (Bayo and Ancho Canyons) and in drill holes O-4, R-9, R-12, and PM-5 (Fig. 1). Observed elevations and thickness of subsurface Bayo Canyon basalt are consistent with those outcrops in Ancho and Bayo Canyons. Moreover, these late Miocene flows in R-9 and R-12 appear to be along strike with the Bayo and Ancho Canyon outcrops (Fig. 1). All known Bayo Canyon basalt flows occur west of a late Miocene NE-SW-trending subsurface trough beneath the central part of the Pajarito Plateau delineated by gravity surveys and drill hole stratigraphic information (Ferguson et al., 1995; Purtymun, 1995; Broxton and Reneau, 1996).

Puye Formation (Tp/Tpf/Tpt):

The Pliocene and possibly late Miocene Puye Formation (Tp) consists of interbedded fanglomerate deposits, axial river gravels, lacustrine sediments, and distal tephra. The fanglomerate was derived from the east flank of the Tschicoma volcanic complex of the Jemez volcanic field (Waresback and Turbeville, 1990). Griggs (1964) mapped the basal section of the Puye Formation as the Totavi Lentil (Tpt), which includes prominent quartzite cobbles and boulders deposited as axial river gravels. The Totavi Lentil is identified in some drill holes, in outcrops in the eastern part of the Pajarito Plateau, and in White Rock Canyon (Purtymun, 1995; Dethier, 1997). Earlier workers placed the Totavi Lentil (Tpt) at the base of the Puye Formation.

The Puye Formation exhibits thickness between 36.6-137.2 m in outcrop and subsurface throughout the central part of the Pajarito Plateau. In most cases, the Puye fanglomerate (Tpf) unconformably overlies sediments assigned to the upper part of the Santa Fe Group in the GR Series, O-4 and PM wells. In the O-1 well, the Totavi Lentil occurs directly above sediments assigned to the Tesuque Formation (Purtymun, 1995). Considering the discussion below and the nearly exclusive presence of volcanic clasts derived from the Jemez Mountains within samples of the GR Series wells beneath Totavi lentil, the longstanding assumption that this unit occurs at the base of the Puye Formation is certainly erroneous.

The Puye Formation contains interbedded mafic (Tb4) and dacitic (Tt2) lava flows and silicic tephra. However, in lower Bayo Canyon, dacitic to rhyolitic tephra ranging in thickness from a few centimeters to about 1.5 m are exposed at the base of the Puye Fanglomerate and above the Bayo Canyon basalt. A vitric ash close to the base of the Puye Formation in Bayo Canyon yielded an age of 5.3 Ma near the Miocene and Pliocene boundary, and probably represents a maximum age for the initial deposits of the sequence in the area. Downstream from this section, basaltic lavas and tephra deposits are interbedded within the upper part of the Puye Formation. In White Rock Canyon, the Puye Formation generally crops out above the Santa Fe Group. However, the Totavi Lentil is intercalated with the Puye Formation (Dethier, 1997). In Frijoles Canyon at the southern part of the Pajarito Plateau, the Totavi Lentil crops out within mafic lava flows and hydromagmatic deposits of the Cerros del Rio basalts (F. Goff, 2000, personal communication).

The Puye Formation consists principally of volcanic detritus derived from the Jemez Mountains. Where exposed in outcrop to the north of Los Alamos National Laboratory, the Puye is characterized by fanglomerates that are coarse-grained toward the west but become significantly finer to the east, toward the Rio Grande (Griggs, 1964; Waresback and Turbeville, 1990). Along the Rio Grande in White Rock Canyon, the fanglomerates are interbedded with lacustrine and river-gravel deposits (Dethier, 1997). River gravels that contain abundant cobbles of Precambrian lithology, including quartzit,e, are often assigned to the Totavi Lentil of the Puye Formation (Griggs, 1964; Waresback and Turbeville, 1990). More recent drilling on the Pajarito Plateau within Los Alamos National Laboratory has identified a mappable distinction between upper Puye deposits consisting predominantly of lava clasts from intermediate volcanic rocks and a lower sequence of more siliceous pumice-rich deposits (e.g., Broxton et al., 2000c). The age and extent of the Puye Formation may be revised, based on these recent findings.

Lower Tschicoma Formation (Tt1)

The mountains to the west of Los Alamos are part of the Pliocene and late Miocene Tshicoma Formation (Tt1), consisting of calcic flows of dacitic to rhyodacitic composition (Griggs, 1964; Goff et al., 1989). The outcrop surface was projected eastward beneath the coeval Puye Formation and the overlying Bandelier Tuff (LANL 3-D Geology Team, 2000). Post-eruption faulting along the Pajarito fault system dropped the projected surface sharply eastward, consistent with observed drill hole and outcrop elevations for Tt1. Flows of Tschicoma Formation in wells H-19 and TW-4 along the western part of the Pajarito Plateau and outcrops of rhyodacite at Cumbres Middle School and Pueblo Canyon are presently assigned to Tt1 (Fig. 1). These assignments are based on subsurface projection of outcrop data (Griggs, 1964; WoldeGabriel, 1999) and on chemical and petrographic analyses for samples from these outcrops (Table 2).

Upper Tschicoma Formation (Tt2)

The Pliocene upper Tschicoma Formation (Tt2) is based on only 4 intersections of the unit in drill holes SHB-1, Sigma Mesa, TW-8, and PM-5 (Fig. 1). Initial assignments in wells H-19 and TW-4 were reassigned from Tt2 to Tt1, based on new interpretations of the western area of the Laboratory (LANL 3-D Geology Team, 2000). The upper Tschicoma Formation (Tt2) is interbedded within the upper part of the Puye Formation in PM-5 and other drill holes. In the PM-5 well, the Tt2 flow occurs about 13.7 m below the Tb4 mafic lavas. The Tt2 flow has a fairly constant thickness of about 40 m for the 3 drill holes in which thickness can be determined, and pinches out abruptly to the east away from its probable source centers. The youngest Tschicoma Formation (Tt2) flows are 2.3-2.6 Ma, whereas Tt1 samples range between 3.0-6.9 Ma (Goff et al., 1989). Other units with similar ages (2.0-3.6 Ma) are El Rechuelos Rhyolite and Cerro Rubio quartz latite (Gardner et al., 1986; Gardner and Goff, 1996).

Cerros del Rio mafic flows (Tb4)

The deeply eroded center of Black Mesa in San Ildefonso Pueblo is an isolated flow that forms the northern boundary of the late Pliocene Cerros del Rio volcanic field located mostly east of the Rio Grande across from the Pajarito Plateau. A single early Pliocene age from K-Ar dating (4.4 Ma) was reported on one of the basal flows, which appeared to indicate that the Black Mesa center was older than nearby flows from the Cerro del Rio volcanic field to the south (Bachman and Mehnert, 1978; Baldridge, et al., 1980). Recent dating of a basal flow from the northwestern part of the center yielded a late Pliocene age of 2.73 Ma (Fig. 2a; Table 1). The current total gas age, which suggests contamination, matches the K-Ar result. This explains the distinct older age of the center compared with the rest of the volcanic field. The new age suggests contemporaneous eruption with the initial flows of the Cerros del Rio volcanic field. Thus, the basaltic center located at Black Mesa is included with the Cerros del Rio volcanic flows (Tb4). Other potentially early Pliocene mafic lavas occur in some wells (e.g., PM-5 and O-1 drill holes), but $^{40}Ar/^{30}Ar$ dating results on samples taken from cuttings yielded questionable ages.

Multiple mafic flows of lava and tephra from the late Pliocene Cerros del Rio volcanic field are exposed along canyon walls in the upper half of White Rock Canyon. The bulk of the volcanic field forms a plateau east of the Rio Grande across from the central and southern parts of the Pajarito Plateau. The lava flows capping the White Rock Canyon range in age mostly between 2.4 and 2.8 Ma (Bachman and Mehnert, 1978; Baldridge, 1979; WoldeGabriel et al., 1996). Phreatomagmatic deposits are commonly associated with lava flows close to clustered vents in the southern and northern parts of the White Rock Canyon. These volcanic deposits are thicker and older in the vicinity of Frijoles Canyon at the southern part of White Rock Canyon. The uppermost flow in Frijoles Canyon yielded an age of 2.75 Ma, and it overlies multiple layers of lavas and tephra deposits (WoldeGabriel et al., 1996; Dethier, 1997). Although the Cerros del

Rio mafic flows overlie the sedimentary deposits of the Puye Formation on both sides of White Rock Canyon, similar lavas are interbedded within the Puye Formation in some of the drill holes (Fig. 6).

The Cerros del Rio mafic flows are interbedded within the Puye Formation at shallow depths in several drill holes of the Pajarito Plateau. For example, late Pliocene lava flows cap the Puye Formation in PM-5 (Fig. 6). Like outcrops in White Rock Canyon, the thickness of the Tb4 lavas is variable in all drill holes. In the GR-series wells, Tb4 lavas are absent, but basaltic and silicic tephra layers and basaltic lava flows occur in the lower part of Bayo Canyon. The thickness and number of flows appears to generally increase southward from Bayo Canyon to Frijoles Canyon.

Bandelier Tuff (Qbt)

The Pleistocene Bandelier Tuff blankets most of the Pajarito Plateau. It is divided into Upper (Tshirege) and Lower (Otowi) Members, and each consists of multiple cooling units of fallout and ignimbrite deposits (Smith et al., 1970). The Otowi and Tshirege tephra erupted from the buried Toledo and the Valles calderas at 1.61 Ma and 1.22 Ma, respectively (Izett and Obradovich, 1994). The tephra deposits throughout the Pajarito Plateau exhibit variable degrees of thickness and welding; however, the thickness generally increases toward the caldera. Although similar volumes of each tephra were extruded during the caldera-forming eruptions, the Tshirege Member dominates exposures and volumes within the Pajarito plateau. The latest description of mappable cooling units within the Bandelier Tuff is briefly summarized below.

Otowi Member Qbo (Qbof/Qbog):

The Pleistocene Otowi Member (Smith et al., 1970) consists of basal fallout of the Guaje Pumice Bed (Qbog) and the Otowi ignimbrite (Qbof). The matrix-poor, clast-supported pumice lapilli bed of Qbog is as much as 15 m thick, and forms a distinct stratigraphic marker in outcrops and in the subsurface throughout the Pajarito Plateau. In most cases, the Guaje Pumice Bed is partially exposed along the base of canyons because it is either buried beneath the younger ignimbrite or covered by slope deposits.

The distinctive Guaje Pumice Bed provides a prominent stratigraphic marker in many drill holes. It is absent from the GR Series and the O-1 wells, which spudded in the Puye Formation beneath Qbog (Fig. 1). Thicknesses vary in drill holes O-4, PM-4, PM-5, and SHB-1 (Fig. 1). In the subsurface, the Qbog unconformably overlies the Puye Formation in drill holes O-4, PM-5, and SHB-1, whereas in PM-4, it directly overlies the late Pliocene Cerro del Rio lava flows (Fig. 6).

The Otowi Member ignimbrite (Qbof) is widespread in the eastern and northern parts of the Pajarito Plateau, mostly exposed at canyon bottoms. It is characterized by massive and non-welded glassy matrix with abundant pumice clasts. It also generally contains about 5% lithics of

intermediate composition. The deposit is up to 60 m thick in the vicinity of the O-4 drill hole in Los Alamos Canyon.

Cerro Toledo interval (Qct)

This informal Pleistocene unit, which consists of fallout tephra, reworked volcaniclastic sediments, and soil horizons in outcrop and in the subsurface of the Pajarito Plateau, is sandwiched between the upper and lower units of the Bandelier Tuff (Smith et al., 1970; Heiken et al., 1986). It varies in thickness laterally across the central Pajarito Plateau from 0 to greater than 42 m (Broxton and Reneau, 1995). This unit is exposed along canyon walls in Los Alamos, Pueblo, and Bayo Canyons along the northeastern part of the plateau. In the western part of the Laboratory, sections thicker than these outcrops were intersected in the drill holes. For example, a thick deposit (81.1 m) was intersected in drill hole of R-19 in the south-central part of the Laboratory (Broxton et al., 2000c). Pumice fallout units stratigraphically equivalent to the Cerro Toledo interval range in age between 1.23 to 1.59 Ma (Spell et al., 1996).

Tshirege Member of the Bandelier Tuff (Qbt)

The Pleistocene Tshirege Member consists of basal fallout and several mappable ignimbrite units. Vertical and lateral welding and crystal content variations characterize the proximal and distal parts of the ignimbrite deposit of the Tshirege Member (Broxton and Reneau, 1995; Broxton et al., 1995). Recent detailed mapping (Gardner et al., 1999) shows that a strongly welded unit (3t) in the middle of the stratigraphic sequence, defined by Warren et al. (1997), is widespread in the northwestern part of the Laboratory. This new cooling unit, which increases in thickness westward, crops out above Unit 3. Complex stratigraphic relations still poorly understood exist in the western area of the Laboratory, close to the caldera source, such as those along State Road 4 in the western part of the Laboratory. Here, localized nonwelded pumice-rich ignimbrite underlies a fiamme ignimbrite. The fiamme ignimbrite (Qbt5) was defined as a separate cooling unit (Rogers 1995; Warren et al., 1997). Currently, the sitewide model for the upper Bandelier Tuff is based on 7 cooling units that are briefly highlighted below in ascending stratigraphic order (The LANL 3-D Geology Team, 2000).

Tsankawi Pumice Bed (Qbtt)

The Tsankawi Pumice Bed occurs at the base of the Tshirege Member of the Bandelier Tuff. The clast-supported pumice fallout ranges in thickness from about 20 to 100 cm, forming a distinct stratigraphic marker in outcrop and in subsurface. In some areas, the pumice layer consists of two subunits, including a 60 to 74 cm-thick basal pumice lapilli and a 2 to 7-cm thick ash in the vicinity of Pueblo and Los Alamos Canyons (Broxton et al., 1995). According to Broxton et al. (1995), pumice clasts of rhyolitic composition are dominant, but minor amounts

(5%) of dacitic hornblende-bearing pumice clasts (Stimac, 1996) are also present. Lithic fragments (1 to 2%) are associated with the pumice fall.

Tshirege Unit 1(Qbt1g/Qbt1v)

The unit of Qbt1 forms the basal ignimbrite sequence of the Tshirege Member above the Tsankawi Pumice Bed. It is subdivided into a lower glassy zone (Qbt1g) and an upper devitrified (Qbt1v) zone (Broxton and Reneau, 1995). The glassy lower half is nonwelded and poorly sorted, grading to a more resistant upper part due to minor welding and devitrification. The glassy zone contains between 30 to 50% pumice clasts that are mostly high-silica rhyolite except for minor hornblende-bearing dacite. In outcrop, a vapor-phase notch represents the transition from the glassy to the vapor-phase-altered zone. The vapor-phase notch is orangish in outcrop and forms a distinct stratigraphic marker horizon that is recognizable throughout the Pajarito Plateau (Broxton et al., 1995).

Although generally nonwelded and poorly sorted, the lower half of the vapor-phase altered tuff of Unit 1 (Qbt1v) is slightly welded and jointed (Broxton et al., 1995). The massive upper section is slope forming and is dominated by matrix-supported crystal-rich pumice lapilli. The glassy and the vapor-phase-altered zones of Unit 1 contain comparable amounts of pumice clasts.

Tshirege Unit 2 (Qbt2)

The ignimbrite of Unit 2 is strongly welded and cliff-forming with distinctive orangish to medium brown features. It is poorly sorted, vapor-phase altered, and contains fewer pumice clasts (5-30%) compared with the underlying Unit 1 (Broxton and Reneau, 1995). The unit is devoid of glass due to devitrification and vapor-phase alteration. Moreover, outcrops of Qbt2 are traversed by narrowly spaced vertical fractures that are partially filled with calcite, brown clays, and detritus (Broxton et al., 1995). Unit 2 is very distinctive in its physical properties throughout the Pajarito Plateau. Its upper contact is sharper compared with its transitional base. In the eastern part of the plateau where it is well characterized, Unit 2 ranges in thickness from about 25 to 27 m (Broxton et al., 1995; Goff, 1995). Unit 2 appears to have similar thickness (31 m) in the western part of the plateau as in drill hole R-25 (Broxton, et al., 2001, in preparation)

Tshirege Unit 3 (Qbt3)

This unit consists of a slope-forming lower nonwelded and upper cliff-forming partially welded and jointed sequence. Its forms the mesa tops across most of the Pajarito Plateau, and the unit ranges in thickness from about 30 to 40 m (Broxton and Reneau, 1995). The nonwelded tuff forms low rounded mounds that are partially covered by rock fall and talus from the upper cliff-forming part of the unit. The contact between the nonwelded to the partially welded zone is

gradational, and these features disappear eastward to merge into a single unit (Goff, 1995). Unit 3 contains pumice clasts and pumice swarms of 10 to 20% and up to 30%, respectively, whereas the phenocryst (18-20%) contents are progressively higher than those of Unit 1 and Unit 2 (Broxton et al., 1995).

Tshirege Unit 3t (Qbt3t)

Unit 3t was first defined by Warren et al (1997), and its widespread extent first recognized during high-precision mapping in the western area of the Laboratory (Gardner et al., 1999) and during surface mapping west of the Los Alamos town site (WoldeGabriel, 1999). The top of Unit 3 is generally marked by localized and discontinuous surge deposits in the western part of the Pajarito Plateau, where it is either overlain by Unit 3t or Unit 4 (Gardner et al., 1999). In the immediate area of the Pajarito fault zone hanging and footwall, moderately welded Qbt3 underlies a strongly welded Qbt3t. However, to the east and south of the fault zone, Unit 4 caps Unit 3.

About 10 m of Unit 3t crops out in the canyons west of TA-3 and progressively thickens westward. However, its maximum thickness is unknown because of limited exposure in the western part of the Laboratory. The unit is strongly welded, platy, purplish, and becomes massive and rounded toward the top part. It is divided into upper and lower subunits by a surge deposit; however, no distinct differences were noted in the chemical and petrographic compositions (Gardner et al., 1999). Moreover, phenocryst contents are the highest within the Tshirege Member for Qbt3t at 20-25%, compared with 18-20% for Unit 3 and 10-15% for Unit 4.

Tshirege Unit 4 (Qbt4)

The ignimbrite of Unit 4 is slightly welded and jointed, and its surface distribution is constrained by high-precision mapping of Gardner et al. (1999) and mapping between Los Alamos and Rendija Canyons (WoldeGabriel, 1999). Although it is crystal (10-15%)- and pumice (<5%)- poor, it generally contains a few distinctive nonwelded and devitrified matrix-supported brown pumice clasts. In the vicinity of Los Alamos and Pajarito Canyons, where Unit 3t pinches out eastward, Unit 4 is separated from underlying Unit 3 by a widespread surge deposit. The unit has variable thickness (0-80 m) that increases westward like that of underlying Unit 3t. In Twomile Canyon, west of TA-3, Unit 4 exhibits a welding break between a partly welded base and a nonwelded upper section (Gardner et al., 1999).

Tshirege Unit 5 (Qbt5)

This unit is best exposed along a road cut on State Road 4 in the western area of the Laboratory, and was originally defined as Unit F by Rogers (1995). Unit F was redefined as Unit 5 in the MDA-P area northeast of the road cut (Warren et al., 1997). At the type section, the

unit is characterized by strongly welded fiamme ignimbrite that is separated from the underlying nonwelded tuff of Unit 4 by a surge layer. The fiamme ignimbrite was not recognized in the footwall of the Pajarito fault zone across from the type section of Unit 5. Except for welding variation, the glass chemistry on pumice clasts from both Units 4 and 5 generally plot together, suggesting similar compositions (Gardner et al., 2001). However, Warren et al. (1997) suggest that petrographic differences distinguish between the variably welded, but chemically similar deposits that they define as Units 4 and 5 in the upper part of the Tshirege Member of the Bandelier Tuff.

Alluvium (Qal)

Various types of surface deposits are recognized throughout the Pajarito Plateau on mesa tops, canyon floors, and along fault scarps and canyon walls. These include post-Bandelier Tuff fallout, alluvium, colluvium, landslide and fan, and terrace deposits. A variety of soil types are recognized on mesa tops throughout the Laboratory (Nyhan et al., 1978). Variable thicknesses (0-15 m) of alluvium were intersected in some of the drill holes.

PETROGRAPHIC FEATURES OF VOLCANIC UNITS BENEATH THE PAJARITO PLATEAU

Petrographic analysis provides data complimentary to chemical analysis to quantify contamination, alteration, mineralogical character, crystallization history, and temporal trends. Moreover, chemical and petrographic analyses greatly refine stratigraphic assignments and the nature of alteration, particularly when both types of data are obtained from the same sample. Accurate stratigraphic assignments provide spatial control for unit boundaries while alteration strongly relates to hydraulic transmissivity and water chemistry within the unit. The binocular and petrographic descriptions of cuttings from several drill holes are given in Appendix 2. We have just recently begun to apply these petrographic analyses for the above purposes, but provide a few examples below to illustrate the usefulness of such data.

Based on dating results, subsurface and surface lava flows were confidently assigned to one of the three groups of mafic flows described in the preceding section. Each unit conveniently occupies a distinctive subepoch, with striking age gaps between. The three groups are:

Volcanic units	Subepoch	Age range (Ma)	Unit names
Tb4	Late Pliocene	1.6 - 3.4 Ma	Mafic lavas of Cerros del Rio

Tb2	Late Miocene	5.3 - 11.5 Ma	Mafic lavas of Bayo Canyon
Tb1	Middle Miocene	11.5 – 13.1 Ma	Mafic lavas of Guaje Canyon

Each eruptive unit so defined consists of many subunits that match closely in chemistry and petrography. A unique number attached to the symbol of each stratigraphic unit identifies a chemical and/or petrographically distinct subunit within our database. This number does not specify stratigraphic level within each unit. Three examples provided in pairs below illustrate this point. In the first case, approximately 1.6 km separates two samples thought to represent the same subunit. In the second case, the petrographic differences are significant, and R9-50.5 probably represents a different flow of tholeiite than R9-92D, as shown below. The third example shows that lower tholeiite of R9, represented by sample R9-162D, contains significantly different primary mineral abundances than its stratigraphic neighbor, upper alkali basalt of R9, represented by sample R9-201.5.

Sample	**Plagioclase**	**Clinopyroxene**	**Olivine**	**Magnetite/Ilmenite**
AWL/19/93	1	0	3.3	2.8*
DN/93/5	2	0	2.9	0.3/2.3
R9-50.5D	13	0	2.4	3.1/0
R9-92D	5	0	5.6	1.3/0.3
R9-1625D	0.7	0	4.4	0.4/0.4
R9-201.5	5	0.1	3.7	3.0/0.4

* Value represents total of magnetite and ilmenite. All values are in volume per cent. Values for magnetite and ilmenite represent all grains, but those for other minerals represent phenocrysts only.

Certain eruptive subunits show indistinguishable chemical character but significantly different petrographic character. Examples provided in pairs are:

Unit	**Sample**	**Plagioclase**	**Clinopyroxene**	**Olivine**
Tb2	PM4-2210D	10	0	4
Tb2	PM5-2440D	10	3	1
Tb2	R9-690.4	4	0	5.5
Tb2	OT4-1210D	30	0.3	5

Most unaltered basalts are holocrystalline or nearly so, and are described as "pilotaxitic". Certain units have very characteristic textures, such as the coarse, microporphyritic texture often displayed by subunits of Tb1 and the ophitic texture characteristic of the lower tholeiite flow of R9, a subunit of Tb4. Some important alterations are "argillic", "calcareous", and "chloritic".

Abundances for calcite, clay, and zeolite are provided in Appendix 2 for some samples. These minerals generally fill voids rather than replace minerals.

Samples with the lowest percent of total minerals, phenocrysts, and groundmass, of course show the lowest abundances of late crystallizing minerals. The paragenetic sequence of crystallization is well illustrated by a set of samples from the same flow subunit of Tb4 in drill hole R9. Sample R9-282.6, a vitric hawaiite tephra with 30% minerals, contains no ilmenite or groundmass olivine, and only traces of magnetite and groundmass clinopyroxene. Two samples of hypocrystalline R9-219, with 41 and 42% minerals, show markedly increased abundances for total mafics and total feldspar, but these samples show only traces of magnetite and no ilmenite. Samples R9-228 and -273.7, holocrystalline samples, both exhibit very high magnetite abundances (5-6%). Total minerals within these holocrystalline samples are less than 100% primarily due to an inability to distinguish secondary clay from void space, rather than to the presence of glass. The paragenetic sequence can be inferred from these data. First plagioclase and olivine formed at depth as phenocrysts, then groundmass phases formed: plagioclase with olivine, then joined by clinopyroxene, probably with olivine ceasing soon after, then finally joined by sanidine and magnetite.

Sample	**Total minerals**	**Felsic**	**Mafic**	**Magnetite**	**Ilmenite (ppmV)**
R9-282.6	30	23	8	0.01	0
R9-219B	42	30	12	0.04	0
R9-219A	41	29	12	0.04	0
R9-273.7	92	60	25	5.02	52
R9-228	91	57	29	5.86	209

Based on very limited data for latites and mugearites, but corroborated by extensive data for the southwestern Nevada volcanic field (SWNVF) in Warren et al. (2000), several relationships and trends can be recognized for total mafic mineral abundances and for Fe-Ti oxide mineral abundances in progressively more evolved units. Average values for total mafics and magnetite are in percent, and ilmenite in ppm V:

Composition	**Number of samples**	**Mafics**	**Magnetite**	**Ilmenite (ppm V)**
Latite (or andesite)	3	14	2.0	3
Mugearite/basaltic andesite	1	21	2.7	0
Hawaiite/alkali basalt	5	26	3.6	52
Tholeiitic basalt	11	31	1.4	4537

The progressive increase in mafics and magnetite within the alkalic series from latite to hawaiite is expected due to a progressive increase in Fe and Mg. Although this progression is

not statistically significant, a similar, statistically significant trend occurs within basic rocks of the SWNVF (Warren et al., 2000). The most interesting differences occur between tholeiite and hawaiite. Note that tholeiites are lacking within the SWNVF, so a comparison cannot be made. Compared with tholeiites, hawaiites have somewhat lower total mafics, markedly higher magnetite, and strikingly lower ilmenite. Values for hawaiites are very similar to those for hawaiites of the SWNVF. The differences between tholeiites and hawaiites can be attributed to a considerably higher fO_2 of hawaiites. A higher fO_2 should result in formation of the FeIII-rich mineral magnetite at the expense of both mafic minerals and ilmenite, which are FeII-rich minerals, given a constant total Fe.

There is a striking difference between Pliocene and Miocene basalts, both tholeiites and hawaiites, in abundances of plagioclase and clinopyroxene phenocrysts, as tabulated below. Middle Miocene basalts (Tb1) generally have markedly higher abundances of plagioclase and clinopyroxene phenocrysts than their late Pliocene (Tb4) counterparts, as represented below by median values. Some 63% (19 of the 30 samples) of middle Miocene hawaiite and tholeiite have at least 0.5% clinopyroxene phenocrysts, contrasting with only 4% (1 of the 24 samples) of late Pliocene basalts. Based on sparse data, the petrographic character of late Miocene basalts (Tb2) appears to be most similar to that of middle Miocene basalts. Additionally, more evolved units become progressively more important with time. Two of the 6 samples (33%) within Tb2 are mugearite, but none are latite. Samples within Tb4 include 23% (7 of 31) that are latite or mugearite. A very similar petrographic evolution occurs for mafic rocks within the southwestern Nevada volcanic field, with Quaternary basalts generally plagioclase-aphyric compared to plagioclase-phyric Miocene basalts (Fleck et al., 1996).

Unit	**Basalt N**	**% latite & Mugearite**	**PL**	**CX**	**OL**	**% basalt CX ≥0.5%**
Tb4	24	23	0.8	0.0	4.5	4
Tb2	4	33	10	0.2	4.5	50
Tb1	30	0	5	0.6	4.0	63

PL=Plagioclase, CX=Clinopyroxene, OL=Olvine

LITHOSTRATIGRAPHIC FEATURES OF THE JEMEZ MOUNTAINS WEST OF THE PAJARITO FAULT SYSTEM

Major Neogene stratigraphic units of the Jemez volcanic field are characterized by diverse volcanic, volcaniclastic, and sedimentary deposits (Griggs, 1964; Bailey, et al., 1969; Smith et al., 1970; Nielson and Hulen, 1984; Gardner et al., 1986; Aldrich and Dethier, 1990; Goff et al., 1990; Purtymun, 1995; Smith and Lavine, 1996). The earliest record of volcanic activity in the Jemez Mountains consists of middle Miocene (16.5 Ma) basanite flow that crops out within sediments of the Santa Fe Group in the southeastern part of the volcanic field

(Gardner et al., 1986). However, volumetrically significant volcanism initiated later, beginning in the middle Miocene (13 to 14 Ma) with continued episodic activities into the Pleistocene. Volcanism occurred contemporaneously at different locations of the volcanic field (Fig. 7).

The composite volcanic stratigraphy for the Jemez volcanic field consists of the Keres, Polvadera, and Tewa Groups (Smith et al., 1970; Gardner et al., 1986; Goff et al., 1989). This sequence is unconformably underlain by Tertiary and Paleozoic sedimentary rocks. In the southern Jemez volcanic field, the succession above the Santa Fe Group is represented by diverse and contemporaneous basalt to high-silica rhyolite eruptions and associated volcaniclastic deposits of the Keres Group (Fig. 8). It includes the Paliza Canyon Formation, the Canovas Canyon and Bearhead Rhyolite, and the Keres Group volcaniclastic deposits, respectively (Gardner et al., 1986; Goff et al., 1990; Smith and Lavine, 1996). Dacites and rhyodacites of the Tschicoma Formation and the El Rechuelos Rhyolite of the Polvadera Group, and rhyolitic lavas and tephra deposits of the Bandelier Tuff and associated units of the Tewa Group supersede the Keres Group. The sratigraphic column from one of several deep geothermal wells in the central part of the Jemez volcanic field (B-22; Nielson and Hulen, 1984) contains Paleozoic beds, the Miocene Santa Fe Group, moderately thick Paliza Canyon volcanic flows of the Keres Group, and very thick Pleistocene tephra of the Bandelier Tuff and related units of the Tewa Group (Fig. 8).

In Santa Clara Canyon along the northeastern part of the Jemez volcanic field, the Santa Fe Group contains middle to late Miocene mafic flows of the Lobato Basalt, which is superseded by dacites and rhyodacites of the Tschicoma Formation and fanglomerates of the Puye Formation (Aldrich and Dethier, 1990). According to Aldrich and Dethier (1990), the Santa Fe Group is divided into the Tesuque (>12 Ma) and the Chamita (≤12 Ma) Formations, which are alluvial fans derived from the north and the Sangre de Cristo Mountains to the east, both with no apparent input from the Jemez Mountains (Fig. 8). These authors describe a >200-m thick Lobato Basalt that erupted during two stages in the middle Miocene (11.9-14.1 Ma, 4 samples) and late Miocene (9.6-10.9 Ma, 10 samples). The Lobato Basalt is mostly confined to the northern wall of an east-trending ancestral paleodrainage of the Santa Clara Canyon west of the Pajarito fault system. On the south side of the canyon, the Lobato Basalt is absent, and early Pliocene (3.98 Ma) Tschicoma Formation dacite unconformably caps Tesuque Formation. Although the Lobato Basalt might have been eroded from the south wall of the Santa Clara Canyon, tightly grouped middle Miocene ages (11.5-13.1 Ma) for subsurface Guaje Canyon Basalt flows (WoldeGabriel et al., 1999) do not exactly match in age to the older stage of the Lobato basalt flows of the northeastern Jemez Mountains. The stratigraphic information highlighted above indicates differences in the volume and character of volcanic rocks and associated sedimentary units within different parts of the volcanic field.

GEOCHEMICAL FEATURES OF VOLCANIC UNITS BENEATH THE PAJARITO PLATEAU

Major and trace element data for representative surface and subsurface samples of Pliocene and Miocene flows from the Pajarito Plateau exhibit a wide range of magma compositions, ranging from basalt to latite, and including some dacite and rhyodacite (Table 2 and Fig. 9). The late Pliocene mafic flows (Tb4) extend beneath the eastern part of the Pajarito Plateau and consist of tholeiite, alkali basalt, hawaiite, mugearite, benmoreite, and latite flows (Fig. 9).

The older mafic flows erupted during two distinct episodes in the late Miocene (Tb2) and middle Miocene (Tb1). The late Miocene Bayo Canyon mafic flows, from outcrops (e.g., Bayo Canyon and Ancho Canyons) and drill holes (O-4, PM-5, etc.), are dominated by tholeiitic and hawaiite compositions that appear unaffected by mild to moderate alterations (Fig. 9). Unlike the Pliocene and late Miocene volcanic rocks, the middle Miocene Guaje Canyon basaltic flows are represented by several tholeiitic flows and are associated with lavas only slightly more evolved than basalt (Fig. 9). Samples of upper Tschicoma Formation (Tt) from outcrops near Cumbres Middle School and the adjacent Pueblo Canyon (Tt1) and from the SHB-1 and PM-5 drill holes in the central part of the Pajarito Plateau (Tt2) display dacite compositions. These relatively calcic compositions coincide with those for dacite flows of the lower Tschicoma Formation (Tt1) that are exposed along the eastern part of the Jemez Mountains (Fig. 10). The chemical similarity between Tt1 and Tt2 has an important implication delineating a potential center of upper Tschicoma Formation beneath the Pajarito Plateau.

Although fields defining chemistry generally overlap, tholeiite basalts become increasingly Si- and alkali-rich from Middle Miocene to Pliocene, whereas alkali basalts become more alkali-rich, but more Si-poor. These chemical differences, taken together with additional chemical and petrographic data, allow stratigraphic assignment for isolated mafic flows that might be encountered within future drill holes.

GEOCHEMICAL COMPARISON BETWEEN VOLCANIC UNITS FROM THE JEMEZ MOUNTAINS AND THE PAJARITO PLATEAU

The total alkali-silica diagram of representative volcanic samples from the different parts of the Jemez volcanic field exhibit wide range of chemical compositions that are also generally characteristic and distinctive for each area (Figs. 1 and 10). For example, alkalic and subalkalic basalts and evolved lavas of hawaiite, mugearites, benmoreite, and a few andesitic flows dominate mafic flows of the late Pliocene Cerros del Rio (Tb4). Diverse magmatic compositions, ranging from basalts to high-silica rhyolites, but dominated by latites, are noted in the volcanic succession of the Miocene Keres Group within the southern part of the Jemez volcanic field, west of the Pajarito fault system (Gardner et al., 1986; Ellisor et al., 1996). However, evolved lavas of Miocene benmoreite, trachyte, trachydacite, and rhyolite flows were

sampled west of the Pajarito fault system, whereas hawaiite and mugearite flows of late Pliocene age are dominant east of the Pajarito Plateau boundary fault system. The late Miocene (Tb2) and middle Miocene (Tb1) flows from the Pajarito Plateau are transitional to tholeiitic in composition, respectively, and are distinct from the representative alkalic mafic lavas of the Keres Group. Moreover, the mafic flows beneath the Pajarito Plateau represent a narrow range of composition compared with the diverse compositions of the Keres Group of the southern Jemez volcanic field (Fig. 10). Flows of the Bayo Canyon basalt (Tb2) are generally more alkalic compared with those of the Guaje Canyon basalt (Tb1); unlike Tb2, Tb1 represents tholeiitic and minor basaltic andesite flows (Fig. 10).

In other cases, chemical similarities are evident for units from different areas. Flows of the Guaje Canyon basalt of the Pajarito Plateau and Lobato Basalt of the northeastern Jemez Mountains show similar compositional ranges; both volcanic successions contain tholeiitic and basaltic andesite lavas. Mafic flows of similar compositional ranges were also noted in the late Pliocene lavas of the Cerros del Rio Volcanic field (Fig. 10).

Most of the felsic rocks (e.g., trachyte, trachydacite, dacite, and low- and high-silica rhyolite flows) are confined to the Jemez volcanic field west of the Pajarito fault system except for few late Pliocene dacitic and low-silica rhyolite (rhyodacite) flows from the Pajarito Plateau. Dacite flows beneath the Pajarito Plateau, intersected in drill holes PM-5 and SHB-1, are chemically similar to the lavas of the Tschicoma Formation, which are separated from the adjacent plateau by the boundary faults of the Pajarito fault system (Figs. 1 and 10). Northeast of the subsurface dacite lavas in PM-5 and SHB-1, thick (10-30 m) and porphyritic low-silica rhyolite flows crop out at the intersection of Walnut and Pueblo Canyon and at the nearby Cumbres Middle School at the northern part of the Los Alamos town site. These samples plot with other low-silica rhyolite samples from the Tschicoma Formation (Fig. 10). Over all, the felsic rocks from the Jemez volcanic field are characterized by two distinct chemical trends, which follow calc-alkalic trachyte-trachydacite-alkali-rich rhyolite and subalkalic dacite-low-alkali low- to high-silica rhyolite flows. The mostly high-silica rhyolite flows of the Bandelier Tuff generally plot between these two trends, suggesting probably hybrid magmatic source for the Quaternary silicic eruptions of the Bandelier Tuff (Fig. 10).

Three fundamentally different chemical and temporal episodes that correspond to the Keres (13 to 7 Ma) and Polvadera (7 to 3 Ma) Groups and the Cerros del Rio volcanic field (2.8 to 2.3 Ma) are apparent in the Jemez volcanic field (Gardner et al, 1986; WoldeGabriel et al., 1996). The Bearhead Rhyolite, although formally included within the Keres Group (Smith et al., 1970), is chemically allied with the Polvadera Group. Chemical affinities are presently poorly known for the Lobato Basalt and for the young (2 Ma) rhyolites of the Polvadera Group, which are not considered in discussion below. During each period, volcanism was calc-alkalic according to Peacock (1931), but during the early period it was borderline alkali-calcic, during the middle period it was borderline calcic, and during the latest period the chemical series fell

centrally within the calc-alkalic series (Fig. 10). To aid following discussion, we will describe the Keres Group as an alkali-calcic series, the Polvadera Group as a calcic series, and the Cerros del Rio mafic lavas as a calc-alkalic series.

No exceptions are presently known for the Polvadera Group or the Cerros del Rio mafic lavas, but a small portion, about 20%, of analyses represented for the southern Jemez, almost entirely from Ellisor (1995), are grouped with a calcic series rather than the dominant alkali-calcic series. These calcic analyses, chemically indistinguishable from those of the Polvadera Group, might represent southern units of that generally younger group, calcic units within the Keres Group, or older units of the Polvadera Group that indicate temporal overlap between alkali-calcic and calcic volcanism. The subordinate calcic series within the southern Jemez includes the Bearhead Rhyolite, well dated at about 6.5 Ma (Gardner et al, 1986; McIntosh and Quade, 1990). If the dacites of this series are associated with the Bearhead rhyolite, then they could be viewed as some of the oldest units within the Polvadera Group.

Irrespective of complications addressed above, the dominant chemistry within the Jemez volcanic field is well established, and certainly reflects episodic changes in tectonic activity related to the Rio Grande rift or the Jemez lineament. The period between 7 to 3 Ma, marked by the region's most calcic volcanism of the Polvadera Group, shows the virtual or complete absence of basaltic volcanism. This calcic chemistry, most closely approaching that of the crust, suggests a pause in rifting. A lack of structural conduits formed by rifting would inhibit magmatic ascent during this period, and thus would allow time to develop large volumes of crustal melts, assimilating ascending basalts that certainly fueled this crustal melting. Basalts are prominent within the Cerros del Rio mafic lavas during the immediately succeeding period between 2.8 to 2.3 Ma, suggesting a sudden resumption of rifting, allowing rapid ascent of magma from mantle sources. During the earliest episode of alkali-calcic volcanism within the Jemez volcanic field, peripheral basaltic volcanism was also episodically prominent, suggesting very active rifting prior to 7 Ma.

Differences in chemistry and apparent eruptive volumes between the older and younger series might explain the large volume, catastrophic eruption of the Bandelier Tuff following the younger series, in contrast to the smaller volume, more protracted and non-catastrophic volcanism of the Keres Group (see Figure 4, in Gardner et al, 1986). From apparent erupted volumes of tholeiite and hawaiite, and from the chemical series generated, the pulse of magma from the mantle that created the Cerros del Rio mafic lavas appears to have been volumetrically larger and melted considerably more crust than the pulses that created the Keres Group. Considering the very strong dominance of crustal melt inferred for the calcic Polvadera Group, the more alkalic chemistry of the older Keres Group suggests less crustal involvement compared to the Cerros del Rio mafic lavas. Although volumes are presently unknown, based on areal extents for each episode, the Cerros del Rio mafic lavas appear to represent a much larger volume of basaltic volcanism than Bayo Canyon, Lobato, or Guaje Canyon basalts, each possibly

triggering eruption episodes within the Keres Group. Thus, catastrophic eruptions such as those of the Bandelier Tuff might be favored by relatively mild rifting, conditions under which relatively large volumes of magma can migrate from the mantle to effectively melt crust. Under conditions of more active rifting, conduits allow easy access to the surface, and relatively little crust is melted (the Keres Group). With little or no rifting, relatively small volumes of magma can trickle from the mantle, but these volumes are tightly held and cause very effective crustal melting (e.g., the Polvadera Group).

There is no radiogenic isotope data for the Miocene mafic rocks of the Pajarito Plateau to assess their magmatic source history. However, published isotope data from the Miocene Keres Group and the late Pliocene Cerros del Rio volcanic rocks exhibit different petrological trends (Duncker et al., 1991; Ellisor et al., 1996). According to Duncker et al. (1991), the tholeiitic lavas from the late Pliocene Cerros del Rio volcanic rocks exposed along the eastern part of the Pajarito Plateau and east of White Rock Canyon are contaminated by upper and probably lower continental crust. Without crustal input, the tholeiites resemble enriched Mid-Oceanic Ridge Basalts (E-MORB) and Ocean-Island Basalts (OIB). Moreover, the hawaiites are attributed to mantle source contaminated by continental crust. Duncker et al. (1991) regard the evolved rocks of the Cerros del Rio flows as the products of mixing between hawaiite- and tholeiite-mantle source components. For the Keres Group of the Jemez Mountains, Ellisor et al. (1996) suggested multiple petrogenetic models, representing mixing of fractionation and assimilation products of OIB-like mantle-derived magmas with mafic lower and felsic lower and upper crustal inputs.

CONCLUSIONS

Volcanic rocks represent a volumetrically minor, but geologically and hydrogeologically important component of the Miocene and Pliocene deposits of the Pajarito Plateau. The stratigraphic sequence is dominated by Miocene and Pliocene sedimentary units derived from the Precambrian terrain to the north and east of the Española Basin, and from the Jemez Mountains to the west. Mafic and silicic volcanic eruptions during the late Pliocene and early Pleistocene from rift-bound centers and the rift shoulder, respectively, superseded these older sediments.

The surface and subsurface stratigraphic sequences of the Pajarito Plateau record at least three episodes of volcanic eruptions, beginning in the Middle Miocene. Sedimentary rocks of the Santa Fe Group and the overlying Puye Formation and the younger Pleistocene Bandelier Tuff dominate the lithostratigraphic sequence of the plateau. Other volcanic rocks are mostly mafic lavas that provide temporal constraints for the rift-fill sediments of the plateau. Moreover, the distribution and elevation of the mafic flows suggest intense episodic tectonic activities consistent with the alternating intercalation of rift-fill sediments with the Miocene and late Pliocene lava flows adjacent to the western boundary fault of the Española basin. The Pajarito fault system, which defines the current western rift margin, appears to have been active during the Neogene and was reactivated following the eruption of the Bandelier Tuff (1.2 Ma).

Chemical and petrographic data define distinctive compositional ranges among the mafic flows of the Pajarito Plateau. Generally plagioclase- and clinopyroxene-phyric subalkalic basalts with minor mugearite and basaltic andesite lavas represent the middle and late Miocene mafic rocks. The late Pliocene Cerros del Rio flows exhibit broad compositional ranges, consisting of alkalic and subalkalic basalts and hawaiite that are all generally plagioclase- and clinopyroxene aphyric, and an abundance of flows with mugearite and benmoreite compositions. Eruptions differ compositionally among different regions within the Jemez volcanic field. The Miocene Keres Group of the southern Jemez Mountains and the late Pliocene Cerros del Rio volcanic flows follow separate calc-alkalic trends. Published radiogenic isotope data from these volcanic units suggest variable magmatic sources and petrogenetic evolution dominated by fractionation and assimilation of mantle and crustal melts.

ACKNOWLEDGEMENTS

The study has been supported by ongoing hydrogeologic characterization activities of the Environmental Restoration Project of the Los Alamos National Laboratory. Reviews by Fraser Goff and Scott Baldridge are greatly appreciated.

REFERENCES

Aldrich, M. J., Jr. and Dethier, D. P. 1990, Stratigraphic and tectonic evolution of the northern Española basin, Rio Grande rift, New Mexico: Geological Society of America Bulletin, v. 102, p. 1695-1705.

Bachman, G. O. and Mehnert, H. H., 1978, New K-Ar dates and the late Pliocene to Holocene geomorphic history of the central Rio Grande region, New Mexico: Geological Society of America Bulletin, v. 89, p. 283-292.

Baldridge, W. S., Olson, K. H., and Callender, J. E., 1984, Rio Grande rift: Problems and perspectives: NM Geological Society Guidebook, 35, p. 1-12.

Baldridge, W. S., Damon, P. E., Shafiqullah, M., Bridwell, R. J., 1980, Evolution of the central Rio Grande rift: new potassium-argon ages: Earth Planetary Science Letters, v. 51, p. 309-321.

Baldridge, W. S., 1979, Petrology and petrogenesis Plio-Pleistocene basaltic rocks from the central Rio Grande Rift: in Riecker, R. E., (ed.), Rio Grande Rift: Tectonics and Magmatism, American Geophysical Union, Washington D. C., p. 323-353.

Bailey, R.A., Smith, R.L., and Ross, C. S., 1969, Stratigraphic nomenclature of volcanic rocks in the Jemez Mountains, New Mexico, in Contribution to Stratigraphy, U. S. Geological Survey, 1274-P, 1-18.

Baltz, E.M., Abrahams, J.H., and Purtymun, W.D., 1963, Preliminary report on geology and hydrology of Mortandad Canyon near Los Alamos, New Mexico, with reference to disposal of liquid low-level radioactive waste, US Geological Survey, Open-File Report (Albuquerque, New Mexico), 105 p.

Biehler, S., Ferguson, J., Baldridge, W. S., Jiracek, G. R., Aldern, J. L., Martinez, M., Fernandez, R., Romo, J., Gilpin, B., Braile, L. W., Hersey, D. R., Luyendyk, B. P., and Aiken, C. L., 1991, A geophysical model of the Española basin, Rio Grande rift, New Mexico: Geophys., v. 56, p. 340-353.

Broxton, D. E. and Reneau, S. L., 1996, Buried early Pleistocene landscapes beneath the Pajarito Plateau, northern New Mexico: New Mexico Geological Society, Guidebook 47, p. 325-334.

Broxton, D.E., and Reneau, S.L., 1995, Stratigraphic nomenclature of the Bandelier Tuff for the Environmental Restoration Project at Los Alamos National Laboratory: Los Alamos National Laboratory, Los Alamos, LA-13010-MS, 21 p.

Broxton, D.E., Heiken, G.H., Chipera, S.J., and Byers, F. M., 1995, Stratigraphy, petrography, and mineralogy of Bandelier Tuff and Cerro Toledo deposits: Los Alamos National Laboratory, Los Alamos, LA-12934-MS, p. 33-63.

Broxton, D., Gilkeson, R., Longmire, P., Marin, J., Warren, R., Vaniman, D., Crowder, A., Newman, B., Lowry, W., Rogers, D., Stone, W., McLin, S., WoldeGabriel, G., Daymon, D., and Wycoff, D., 2000a, Characterization Well R-9 Completion Report: LA-UR-00-4120/LA-series draft. ER2000-0218, 85 p.

Broxton, D., Warren, R., Vaniman, D., Newman, B., Crowder, A., Everett, M., Gilkeson, R., Longmire, P., Marin, J., Stone, W., McLin, S., and Rogers, D., 2000b, Characterization Well R-12 Completion Report: LA-UR-00-3785/LA-series draft. ER2000-0290, 72 p.

Broxton, D., Vaniman, D., Stone, W., McLin, S., Marin, J., Koch, R., Warren, R., Longmire, P., Rogers, D. and Tapia, N., 2000c, Characterization Well R-19 Completion Report: LA-UR-4085/LA-series draft. ER2000-0398, 58 p.

Budding, A. J., 1978, Subsurface geology of the Pajarito Plateau: interpretation of gravity data: in Hawley, J. W., ed., Guidebook to the Rio Grande Rift in New Mexico and Colorado: New Mexico Bureau of Mines and Mineral Resources Circular 163, p. 196-198.

Chapin, C. E., 1979, Evolution of the Rio Grande Rift: A summary; in Riecker, R. E. (ed.) Rio Grande rift: Tectonics and Magmatism: American Geophysical Union, Special publication, p. 1-6.

Carter, K. E. and Gardner, J. N., 1995, Quaternary fault kinematics in the northwestern Española basin, Rio Grande rift, New Mexico: New Mexico Geological Society, Guidebook 46, p. 97-103.

Cather, S. M., 1992, Suggested revisions to the Tertiary tectonic history of north central New Mexico: New Mexico Geological Society, Guidebook 43, p. 109-122.

Cavazza, W., 1989, Sedimentation pattern of a rift-filling unit, Tesuque Formation (Miocene), Española Basin, Rio Grande rift, New Mexico: J. Sedimentary Petrology, v. 59, p. 287-296.

Criss, J., 1985, User's Guide to XRF-11 Software for Fundamental Parameters: Criss Software Inc. Largo, MD, v.15, 49 p.

Dalrymple, G. B., Cox, A, Doell, R. R., and Gromme, C. S., 1967, Pliocene geomagnetic polarity epochs: Earth Planet. Sci. Lett., v. 2, p. 163-173.

Dethier, D. P., Aldrich, M. J., Jr., and. Shafiqullah, M., 1986, New K-Ar ages for Miocene volcanic rocks from the northeastern Jemez Mountains and Tejana Mesa, New Mexico: Isochron/West, No. 47, p. 12-14.

Dethier, D. P., 1997, Geologic map of the White Rock quadrangle: New Mexico Bureau of Mines and Mineral Resources.

Dethier, D. P., 1999, Preliminary geologic map of the Puye 7.5 Quadrangle, Los Alamos and Rio Ariba counties, NM: U.S, Geological Survey (in press).

Duncker, K. E., Wolff, J. A., Harmon, R. S., Leat, P. T., Dickin, A. P., and Thompson, R. N., 1991, Diverse mantle and crustal components in lavas of the NW Cerros del Rio volcanic field, Rio Grande Rift, New Mexico: Contrib. Mineral Petrol., v. 108, 331-345.

Ellisor, R., 1995. Petrogenesis of the lavas and tuffs of the Keres Group, Jemez Mountains volcanic field, New Mexico: MS thesis, The University of Texas, at Arlington, 130 p.

Ellisor, R., Wolff, J., and Gardner, J. N., 1996, Outline of the petrology and geochemistry of the Keres Group lavas and tuffs: NM Geological Society, Guidebook 47, p. 237-242.

Ferguson, J. F., Baldridge, W. S., Brail, L.W., Biehler, S., Gilpin, B., and Jiracek, G.R. 1995, Structure of the Española Basin, Rio Grande Rift, New Mexico, from SAGE seismic and gravity data: New Mexico Geological Society, Guidebook 46, p. 105-110.

Fleck, R. J., B. D. Turrin, D. A. Sawyer, R. G. Warren, D. E. Champion, M. R. Hudson, and S. A. Minor, 1996, Age and character of basaltic rocks of the Yucca Mountain region, southern Nevada: J. Geophys. Res., v. 101, No. B4, p. 8205-8228.

Galusha, T. and Blick, J. C., 1971, Stratigraphy of the Santa Fe Group, New Mexico: Bulletin of the American Museum of Natural History, v. 144, 127 p.

Gardner, J. N. and Goff, F., 1984, Potassium-argon dates from the Jemez volcanic field: implications for tectonic activity in the north central Rio Grande rift: New Mexico Geological Society, Guidebook 35, p. 75-81.

Gardner, J. N., Goff, F., Garcia, S., and Hagan, R. C., 1986, Stratigraphic relations and lithologic variations in the Jemez volcanic field, New Mexico: Journal of Geophysical Research, v. 91, p. 1763-1778.

Gardner, J. N. and Goff, F., 1996. Geology of the northern Valles caldera and Toledo embayment, New Mexico: NM Geological Society, Guidebook 47, p. 225-230.

Gardner J. N., Lavine, A., WoldeGabriel, G., Krier, D., Vaniman, D., Caporuscio, F., Lewis, C., Reneau, P., Kluk. E., Snow, M. J., 1999, Structural geology of the northwestern portion of Los Alamos national Laboratory, Rio Grande Rift, New Mexico: Implications for

seismic surface rupture potential from TA-3 to TA-55: Los Alamos National laboratory Report, LA-13589-MS, 112 p.

Gardner, J. N., Reneau, S. L., Krier, D., Lavine, A., Lewis, C. J, WoldeGabriel, G., Guthrie, G., 2001, Geology of the Pajarito Fault Zone in the Vicinity of S-Site (TA-16), Southwestern Corner of Los Alamos National Laboratory, Rio Grande Rift, New Mexico: Los Alamos National laboratory Report (in press).

Griggs, R.L., 1964, Geology and ground-water resources of the Los Alamos area, New Mexico: US Geological Survey, Water Supply Paper1753, 107 p.

Goff, F., Gardner, J. N., Baldridge, W. S., Hulen, J. B., Nielson, D. L., Vaniman, D., Heiken, G., Dungan, M. A., Broxton, D., 1989, Volcanic and hydrothermal evolution of Valles caldera and Jemez volcanic Field: in Chapin, C. E. and Zidek, J., eds., Field Excursions to Volcanic Terranes in the Western United States, V. I: Southern Rocky Mountain Region: New Mexico Bureau of Mines and Mineral Resources, Memoir 46, p. 381-434.

Goff, F., Gardner, J. N., Valentine, G., 1990, Geology of St. Peter's Dome area, Jemez Mountains, New Mexico: New Mexico Bureau of Mines and Mineral Resources: Geologic Map 69, scale 1:24,000.

Goff, F., 1995, Geologic map of Technical Area 21, Earth Sciences Investigations for Environmental Restoration: Los Alamos National Laboratory, Technical Area 21: Los Alamos National Laboratory Report, LA-12934-MS, p. 7-18.

Golombeck, M. P., 1983, Geology, structure, and tectonics of the Pajarito fault zone in the Española Basin of the Rio Grande rift, New Mexico: Geological Society of America Bulletin, v. 94, p. 192-205.

Heiken G., Goff, F., Stix, J., Tamanyu, S., Shafiqullah, M., Garcia, S., and Hagan, R., 1986, Intracaldera volcanic activity, Toledo caldera and embayment, Jemez Mountains, New Mexico: J. Geophys. Res. v. 19, p. 1799-1815.

Ingersoll, R. V., Cavazza, W., Baldridge, W. S., Shafiqullah, M., 1990, Cenozoic sedimentation and paleotectonics of north central New Mexico: Implications for initiation and evolution of the Rio Grande rift: Geol. Soc. Am. Bull. v. 102, p. 1280-1296.

Izett, G. A. and Obradovich, J. D., 1994, $^{40}Ar/^{39}Ar$ age constraints for the Jaramillo normal subchron and the Matuyama-Brunhes geomagnetic boundary: Journal of Geophysical Research, v. 99, p. 2925-2934.

Kelley, V. C., 1979, Tectonics, middle Rio Grande rift, New Mexico; in Riecker, R. E., ed., Rio Grande rift Tectonics and Magmatism, Washington, D. C.: Am. Geophysical Union, p. 57-70.

LANL 3-D Geology Team (B. Carey, G. Cole, C. Lewis, F. Tsai, R. Warren, and G. WoldeGabriel), 2000, Revised site-wide geologic model for Los Alamos National laboratory: Los Alamos National Laboratory Report, LA-UR-00-2056, 9 p.

Le Bas, M. J., Le Maitre, R. W., Streckeisen, A., and Zanettin, B., 1986, A chemical classification of volcanic rocks based on the total alkali-silica diagram: Journal of Petrology, v. 27, p. 745-750.

MacFadden, B. J., 1977, Magnetic polarity stratigraphy of the Chamita Formation stratotype (Mio-Pliocene) of north central New Mexico: Am. J. Sci., v. 277, p. 769-800.

Mahon, K. I., 1996, The New "York" regression: Application of an improved statistical method to geochemistry, International Geology Review, 38, 293-303.

Manley, K., 1979, Stratigraphy and structure of the Española Basin, Rio Grande rift, New Mexico: in Riecker, R. E. ed., Rio Grande Rift: Tectonics and Magmatism: American Geophysical Union, Washington D. C., p. 71-86.

Manley, K., 1976, K-Ar age determinations of Pliocene basalts from the Española Basin , New Mexico: Isochron West, v. 16, p. 29-30.

McIntosh, W. C. and Quade, J., 1995, $^{40}Ar/^{39}Ar$ geochronology of tephra layers in the Santa Fe group, Española Basin, New Mexico: NM Geological Society, Guidebook 46, p. 279-287.

Nielson, D. and Hulen, J., 1984, Internal geology and evolution of the Redondo Dome, Valles caldera, New Mexico: J. Geophys. Res., v. 89, p. 8695-8711.

Nyhan, J.W., Hacker, L.W., Calhoun, T.E., J. O. Carleton, J., and Young, D.L., 1978, Soil survey of Los Alamos County, New Mexico: Los Alamos National Laboratory, Los Alamos, LA-6779, 102 p.

Purtymun, W.D., 1995, Geologic and hydrologic records of observation wells, test holes, test wells, supply wells, springs, and surface water stations in the Los Alamos area: Los Alamos National Laboratory, Los Alamos, LA-12883-MS, 339 p.

Rogers, M.A., 1995, Geologic map of the Los Alamos National Laboratory Reservation: New Mexico Bureau of Mines and Mineral Resources.

Smith, G. A., and Lavine, A., 1996, What is the Cochiti Formation? NM Geological Society, Guidebook 47, p. 211-218.

Smith, R.L., Bailey, R.A., and Ross, C. S., 1970, Geologic map of the Jemez Mountains, New Mexico: I-571, U. S. Geological Survey.

Spiegel, Z. and Baldwin, B., 1963, Geology and water resources of the Santa Fe area New Mexico: U.S. Geological Survey Water-Supply Paper 1525, 258 p.

Spell, T. L., Harrison, T. M., and Wolff, J. A., 1990, $^{40}Ar/^{39}Ar$ dating of the Bandelier Tuff and San Diego Canyon ignimbrite: temporal constraints on magmatic evolution: J. volcanol. Geotherm. Res., v. 43, p. 175-193.

Spell, T. L., Kyle, P. R., Baker, J., 1996, Geochronology and geochemistry of the Cerro Toledo rhyolite: NM Geological Society, Guidebook 47, p. 263-268.

Stimac, J. A., 1996, Hornblende-dacite pumice in the Tshirege Member of the Bandelier Tuff: Implications for magma chamber and eruptive processes: New Mexico Geological Society Guidebook 47, p. 269-274.

Taylor, J. R., 1982, An introduction to error analysis : Mill Valey, California: University Science book, 269 p.

Vernon, J. H. and Riecker, R. E., 1989, Significant Cenozoic faulting, east margin of the Española basin, Rio Grande rift, New Mexico: Geology, v.17, p. 230-233.

Waresback, D.B., and Turbeville, B.N., 1990, Evolution of a Plio-Pleistocene volcanogenic-alluvial fan: The Puye Formation, Jemez Mountains, New Mexico: Geological Society of America Bulletin, v. 102, p. 298-314.

Warren, R. G., E. V. McDonald and R. T. Ryti, "Baseline geochemistry of soil and bedrock Tshirege Member of the Bandelier Tuff at MDA-P: Los Alamos National Laboratory Report LA-13330-MS, 89 pp., August 1997.

Warren, R. G., D. A. Sawyer, F. M. Byers, Jr., and G. L. Cole, A petrographic/geochemical database and stratigraphic framework for the southwestern Nevada volcanic field: Los Alamos National Laboratory Report LA-UR-00-3791, August 2000.

WoldeGabriel, G., Laughlin, A. W., Dethier, D. P., and Heizler, M., 1996, Temporal and geochemical trends of lavas in White Rock canyon and the Pajarito Plateau, Jemez volcanic field, New Mexico, USA: NM Geological Society, Guidebook 47, p. 251-261.

WoldeGabriel, G., 1999, Geologic map of the western area of Los Alamos between Los Alamos and Rendija Canyons, Pajarito Plateau (unpublished).

WoldeGabriel, G., Warren, R. G., Cole, G., Carey, J. W., Broxton, D., Laughlin, A. W., Heizler, M., 1999, The Pajarito Plateau of the Española Basin, Rio Grande rift, north-central New Mexico— A river ran through it: Geological Society of America Annual Meeting, Abstract with Programs, v.31, no.7, A-348.

York, D., 1969, Least squares fitting of a straight line with correlated errors: Earth Planetary Science Letters v. 5, p. 320-324.

Table 1. $^{40}Ar/^{39}Ar$ dating results of mafic lavas and minerals from the Pajarito Plateau.

Sample	Location	Material	Unit	Age (Ma±2σ)	comments
Surface samples					
DEB 5/98/1	Black Mesa (San Ildefonso)	groundmass	Tb4	2.73±0.27	Minor complexity, excess argon, good isochron age.
DN97-17B	Rendija Canyon	hornblende	Tb3	4.76±0.13	Saddle-shaped spectrum, good plateau segment.
DN97-19A	Rendija Canyon	plagioclase	Tb3	4.17±0.29	Complex spectrum, excess argon, low confidence age.
DN97-16	Bayo Canyon	groundmass	Tb2	8.86±0.05	Precise steps, minor complexity, high confidence age.
DN97-16	Bayo Canyon	plagioclase	Tb2	8.49±0.24	Complex spectrum, excess argon, low confidence age.
DN97-17	Bayo Canyon	groundmass	Tb2	8.78±0.09	Precise steps, minor complexity, high confidence age.
RWTB4-B8	Bayo Canyon	sanidine	Tpf	5.31±0.02	Well-defined age population, high confidence age.
RWTB4-B14	Bayo Canyon	plagioclase	Tb2	None	Very complex, no eruption age assigned.
Subsurface samples (drill hole names followed by sample depth, in feet)					
OT4-300-310	Los Alamos Canyon	groundmass	Tb4	2.50±0.03	Very flat spectrum, high confidence age.
OT4-410	Los Alamos Canyon	groundmass	Tb4	2.52±0.18	Very flat spectrum, high confidence age.
OT4-1200	Los Alamos Canyon	groundmass	Tb2	8.81±0.04	Mostly flat spectrum, minor recoil, high confidence age.
OT4-1270	Los Alamos Canyon	groundmass	Tb2	8.94±0.04	Mostly flat spectrum, minor recoil, high confidence age.
OT4-1280-1290	Los Alamos Canyon	groundmass	Tb2	8.97±0.08	Minor recoil, total gas age, moderate confidence age.
PM5 810-820	Mortandad Canyon	groundmass	Tb2	2.50±0.28	Climbing spectrum, moderate confidence age.
PM5 900-910	Mortandad Canyon	groundmass	Tt2	2.77±0.47	Climbing spectrum, moderate confidence age.
PM5 1100-1110	Mortandad Canyon	groundmass	Tt2	2.70±0.29	Xenocryst contamination, moderate confidence age.
PM5 2690-2700	Mortandad Canyon	groundmass	Tb1	11.39±0.40	Xenocryst contamination, moderate confidence age.

Table 2. Major and trace element data of outcrop and subsurface data from the Pajarito Plateau. See Figure 1 for location of samples and Appendix 2 for description. Analytical uncertainties (AU) are 2 sigma; negative values for Loss on Ignition (LOI) represent weight gain.

Sample Number	Unit	SiO2		TiO2		Al2O3		Fe2O3		FeO	MnO	
		%	AU	%	AU	%	AU	%	AU	%	%	AU
Samples of outcrop from Bayo Canyon												
DN/97/7	Tb2	49.31	0.72	1.673	0.058	16.87	0.26	11.20	0.13		0.372	0.018
DN/97/16	Tb2	52.42	0.74	1.735	0.060	16.83	0.26	10.05	0.12		0.198	0.013
RWTB4A14	Tb2	48.95	0.70	1.674	0.044	16.08	0.24	5.54	0.11	4.59	0.144	0.012
RWTB4A15	Tb2	52.71	0.71	1.721	0.046	16.75	0.24	4.44	0.11	4.88	0.157	0.012
RWTB4B8	Tpf	68.39	0.75	0.475	0.013	13.92	0.22	2.36	0.06	1.19	0.059	0.010
RWTB4B10	Tpf	62.64	0.73	0.55	0.015	14.63	0.23	1.90	0.06	1.81	0.071	0.010
RWTB4B14	Tpf	64.67	0.74	0.432	0.011	14.95	0.23	1.57	0.06	1.66	0.056	0.010
Samples of outcrop from western Pajarito Plateau												
LAPC9812	Tt1	71.33	0.79	0.361	0.012	14.37	0.21	2.75	0.06		0.054	0.010
LAPC9813	Tt1	70.62	0.79	0.385	0.012	14.21	0.21	2.89	0.06		0.059	0.010
Samples of cuttings or core (*) from drill holes												
OT4-310D	Tb4	51.35	1.32	1.418	0.030	16.49	0.40	11.15	0.20		0.162	0.013
OT4-370D	Tb4	51.47	1.32	1.477	0.029	16.44	0.39	11.15	0.20		0.158	0.012
OT4-420D	Tb4	51.18	1.31	1.453	0.029	16.35	0.39	11.16	0.20		0.162	0.012
OT4-1210D	Tb2	50.26	1.30	1.680	0.032	17.40	0.40	11.25	0.20		0.158	0.012
OT4-1280D	Tb2	52.18	1.32	1.764	0.033	16.22	0.39	10.00	0.18		0.120	0.011
OT4-1290D	Tb2	52.14	1.33	1.733	0.034	16.51	0.40	9.89	0.19		0.118	0.011
OT4-1300D	Tb2	55.20	1.36	1.708	0.032	16.53	0.39	9.70	0.18		0.141	0.012
PM5-820D	Tt2	63.89	0.75	0.650	0.017	16.48	0.23	4.76	0.07		0.077	0.010
PM5-910D	Tt2	63.42	0.75	0.649	0.017	16.17	0.23	4.76	0.07		0.078	0.010
PM5-1010D	Tt1	67.58	0.77	0.562	0.015	15.64	0.22	4.07	0.06		0.062	0.010
PM5-2190D	Tb2	62.27	0.75	1.061	0.027	16.29	0.23	5.79	0.08		0.085	0.010
PM5-2440D	Tb2	49.79	0.70	1.695	0.045	15.86	0.23	10.47	0.12		0.153	0.012
PM5-2700D	Tb1	46.84	0.69	1.781	0.047	15.24	0.22	10.23	0.12		0.135	0.011
R9-50.5D	Tb4	52.43	0.74	1.493	0.050	16.09	0.25	11.26	0.13		0.159	0.012
R9-92D	Tb4	51.59	0.70	1.502	0.039	16.00	0.23	11.25	0.13		0.162	0.012
R9-122D	Tb4	51.21	0.70	1.445	0.038	15.93	0.23	11.85	0.14		0.170	0.012
R9-162D	Tb4	51.23	0.70	1.446	0.038	16.00	0.23	11.68	0.13		0.165	0.012
R9-181.3	Tb4	50.00	0.73	1.612	0.055	16.15	0.25	11.21	0.13		0.167	0.012
R9-201.5	Tb4	49.91	0.73	1.617	0.055	16.03	0.25	11.21	0.13		0.170	0.012
R9-228	Tb4	48.57	0.72	1.772	0.062	15.32	0.24	11.37	0.14		0.167	0.012
R9-273.7	Tb4	48.62	0.72	1.787	0.062	15.55	0.24	11.31	0.13		0.172	0.012
R9-282.2	Tb4	50.26	0.73	1.690	0.058	15.01	0.24	10.54	0.13		0.155	0.012
R9-285.5	Tb4	49.71	0.72	1.701	0.059	14.52	0.24	11.03	0.13		0.191	0.012
R9-690.4	Tb2	47.97	0.69	1.597	0.042	15.55	0.22	10.40	0.12		0.135	0.011
R12-138.5D	Tb4	52.05	0.71	1.517	0.040	16.31	0.23	11.18	0.13		0.158	0.012
R12-228D	Tb4	51.28	0.70	1.417	0.037	16.08	0.23	11.62	0.13		0.163	0.012
R12-270D	Tb4	50.25	0.70	1.456	0.038	16.68	0.23	11.67	0.13		0.171	0.012
R12-380D	Tb4	48.93	0.68	1.818	0.048	16.12	0.23	11.08	0.13		0.170	0.012
R12-442D	Tb4	47.72	0.66	1.849	0.049	16.08	0.23	11.19	0.13		0.168	0.012
R12-810D	Tb2	49.38	0.70	1.735	0.046	16.64	0.23	10.98	0.13		0.154	0.012
R15-532D	Tb4	49.69	0.70	1.455	0.038	16.03	0.24	5.57	0.12	4.91	0.130	0.011
R15-562D	Tb4	50.82	0.70	1.471	0.039	15.98	0.24	5.64	0.12	5.10	0.163	0.012
R15-577D	Tb4	49.75	0.70	1.408	0.037	15.61	0.23	4.44	0.12	6.15	0.162	0.012
R15-610D	Tb4	50.36	0.70	1.437	0.038	15.74	0.23	4.07	0.12	6.67	0.163	0.012
R15-705D	Tb4	49.92	0.70	1.650	0.044	15.67	0.23	4.45	0.12	5.87	0.172	0.012
SHB1-656	Tt2	63.55	1.46	0.660	0.020	15.84	0.39	4.88	0.14		0.077	0.010

SHB1-694	Tt2	63.89	1.47	0.663	0.020	16.00	0.39	4.87	0.14		0.079	0.010	

Sample Number	Lithology	MgO		CaO		Na2O		K2O		P2O5		LOI	T
		%	AU	%	AU	%	AU	%	AU	%	AU	%	
Samples of outcrop from Bayo Canyon													
DN/97/7	Flow	4.70	0.12	10.36	0.08	3.29	0.10	0.89	0.03	0.367	0.011	1.07	10
DN/97/16	Flow	4.37	0.11	8.17	0.07	4.04	0.10	1.76	0.04	0.475	0.013	0.42	10
RWTB4A14	Flow	6.51	0.16	10.32	0.08	3.20	0.09	0.80	0.03	0.350	0.010	1.09	99
RWTB4A15	Flow	4.87	0.12	7.98	0.07	3.70	0.09	1.56	0.03	0.510	0.010	0.45	10
RWTB4B8	Ash	1.55	0.07	2.00	0.10	1.98	0.08	3.31	0.05	0.070	0.010	5.79	10
RWTB4B10	Pumice	2.04	0.07	3.62	0.08	2.43	0.08	3.12	0.05	0.270	0.010	6.14	99
RWTB4B14	Pumice fall	1.75	0.07	3.61	0.08	3.03	0.09	3.32	0.05	0.150	0.010	4.11	99
Samples of outcrop from western Pajarito Plateau													
LAPC9812	Flow	0.92	0.08	2.28	0.09	3.98	0.10	3.75	0.05	0.10	0.01	0.34	10
LAPC9813	Flow	1.55	0.07	2.44	0.09	3.75	0.09	3.88	0.06	0.11	0.01	0.39	10
Samples of cuttings or core (*) from drill holes													
OT4-310D	Flow	5.92	0.10	8.93	0.09	3.32	0.09	1.11	0.03	0.356	0.009		10
OT4-370D	Flow	5.73	0.09	8.72	0.08	3.42	0.08	1.12	0.03	0.413	0.009		10
OT4-420D	Flow	6.02	0.09	8.92	0.08	3.57	0.08	1.11	0.03	0.376	0.008		10
OT4-1210D	Flow	4.84	0.08	10.22	0.09	3.48	0.08	0.80	0.03	0.304	0.008		10
OT4-1280D	Flow	4.27	0.08	8.58	0.08	3.93	0.09	1.75	0.03	0.508	0.010		99
OT4-1290D	Flow	4.15	0.09	8.40	0.08	3.91	0.10	1.73	0.03	0.511	0.011		99
OT4-1300D	Flow	2.92	0.07	6.70	0.07	4.06	0.09	2.17	0.04	0.521	0.010		99
PM5-820D	Flow	2.55	0.06	4.58	0.08	3.83	0.10	2.61	0.04	0.235	0.009	1.17	10
PM5-910D	Flow	2.64	0.06	4.64	0.08	3.85	0.10	2.49	0.04	0.231	0.009	1.14	10
PM5-1010D	Flow	1.73	0.07	3.39	0.09	3.96	0.10	3.17	0.05	0.213	0.009	0.47	10
PM5-2190D	Flow	2.30	0.07	4.00	0.08	3.75	0.09	3.31	0.05	0.293	0.010	1.61	10
PM5-2440D	Flow	5.04	0.12	9.71	0.08	3.22	0.09	1.27	0.03	0.527	0.013	2.03	10
PM5-2700D	Flow	6.67	0.17	11.62	0.09	2.83	0.08	1.06	0.03	0.439	0.012	3.55	10
R9-50.5D	Flow	5.83	0.16	9.01	0.08	3.33	0.10	1.03	0.03	0.289	0.010	-0.04	10
R9-92D	Flow	6.32	0.16	9.03	0.07	3.28	0.09	1.13	0.03	0.312	0.010	-0.14	10
R9-122D	Flow	7.23	0.19	8.94	0.07	3.18	0.09	0.94	0.03	0.304	0.010	-0.43	10
R9-162D	Flow	7.16	0.19	9.25	0.08	3.28	0.09	0.84	0.03	0.294	0.010	-0.42	10
R9-181.3	Flow*	6.58	0.19	9.08	0.08	3.38	0.10	1.29	0.03	0.538	0.013	0.18	10
R9-201.5	Flow*	7.00	0.20	9.09	0.08	3.23	0.10	1.30	0.03	0.558	0.013	0.27	10
R9-228	Flow*	8.37	0.26	9.07	0.08	3.41	0.10	1.52	0.03	0.637	0.017	-0.32	10
R9-273.7	Flow*	8.53	0.26	8.96	0.08	3.44	0.10	1.56	0.03	0.671	0.018	-0.36	10
R9-282.2	Tuff*	7.60	0.23	8.70	0.08	2.49	0.09	1.26	0.03	0.647	0.017	1.64	10
R9-285.5	Tuff*	8.01	0.24	7.69	0.07	2.21	0.09	1.04	0.03	0.360	0.011	3.64	10
R9-690.4	Flow*	5.44	0.13	12.34	0.09	3.05	0.09	0.85	0.03	0.332	0.011	2.95	10
R12-138.5D	Flow	5.87	0.15	9.01	0.07	3.38	0.09	0.96	0.03	0.307	0.010	-0.07	10
R12-228D	Flow	7.31	0.19	8.97	0.07	3.20	0.09	0.91	0.03	0.302	0.010	-0.30	10
R12-270D	Flow	6.97	0.18	9.16	0.07	3.21	0.09	0.91	0.03	0.317	0.011	-0.14	10
R12-380D	Flow	7.92	0.21	9.09	0.07	3.47	0.09	1.54	0.03	0.668	0.030	-0.37	10
R12-442D	Flow	8.12	0.22	9.17	0.07	3.06	0.09	1.46	0.03	0.701	0.023	0.59	10
R12-810D	Flow	5.70	0.14	10.64	0.08	3.35	0.09	0.89	0.03	0.385	0.011	0.97	10
R15-532D	Flow	6.58	0.17	8.79	0.07	3.26	0.09	0.99	0.03	0.368	0.011	1.09	99
R15-562D	Flow	6.35	0.16	8.93	0.07	3.40	0.09	1.05	0.03	0.349	0.010	-0.20	99
R15-577D	Flow	6.99	0.18	8.52	0.07	3.10	0.09	1.00	0.03	0.346	0.010	1.09	98
R15-610D	Flow	6.54	0.16	8.93	0.07	3.43	0.09	1.04	0.03	0.346	0.011	-0.37	98
R15-705D	Flow	6.69	0.17	9.05	0.07	3.45	0.08	1.45	0.03	0.569	0.012	-0.20	99
SHB1-656	Flow*	2.77	0.07	4.75	0.06	3.82	0.09	2.43	0.04	0.260	0.007		99
SHB1-694	Flow*	2.73	0.07	4.76	0.06	3.99	0.09	2.41	0.04	0.262	0.007		99

Sample Number	Unit	Lithology	V		Cr		Ni		Zn	
			ppm	AU	ppm	AU	ppm	AU	ppm	AU
Samples of outcrop from Bayo Canyon										
DN/97/7	Tb2	Flow	237	23	245	13	77	10	100	10
DN/97/16	Tb2	Flow	197	23	50	9	24	10	97	10
RWTB4A14	Tb2	Flow	216	21	247	13	77	11	91	10
RWTB4A15	Tb2	Flow	207	22	44	9	24	11	82	12
RWTB4B8	Tpf	Ash	24	12	10	9	<11		77	12
RWTB4B10	Tpf	Pumice	55	13	29	9	22	11	54	11
RWTB4B14	Tpf	Pumice fall	57	10	34	8	17	10	53	10
Samples of outcrop from western Pajarito Plateau										
LAPC9812	Tt1	Flow	31	12	37	9	24	10	34	13
LAPC9813	Tt1	Flow	32	12	67	9	32	10	37	12
Samples of cuttings or core (*) from drill holes										
OT4-310D	Tb4	Flow	187	24	176	10	65	7	75	12
OT4-370D	Tb4	Flow	179	25	172	9	63	6	65	12
OT4-420D	Tb4	Flow	184	25	166	9	69	6	94	13
OT4-1210D	Tb2	Flow	223	28	262	12	80	7	76	12
OT4-1280D	Tb2	Flow	220	29	41	7	32	6	73	12
OT4-1290D	Tb2	Flow	210	29	34	7	30	6	63	12
OT4-1300D	Tb2	Flow	210	29	39	7	41	6	90	13
PM5-820D	Tt2	Flow	72	13	46	9	31	9	62	11
PM5-910D	Tt2	Flow	77	13	52	9	40	9	60	11
PM5-1010D	Tt1	Flow	53	13	26	9	25	11	50	12
PM5-2190D	Tb2	Flow	101	16	33	9	18	10	47	12
PM5-2440D	Tb2	Flow	232	22	202	11	119	10	98	10
PM5-2700D	Tb1	Flow	223	22	290	13	144	10	89	10
R9-50.5D	Tb4	Flow	176	20	148	11	64	9	108	12
R9-92D	Tb4	Flow	180	20	187	11	78	10	79	10
R9-122D	Tb4	Flow	173	19	252	12	106	10	106	10
R9-162D	Tb4	Flow	189	19	254	12	96	10	85	10
R9-181.3	Tb4	Flow*	192	22	205	12	119	12	110	10
R9-201.5	Tb4	Flow*	181	21	215	12	125	12	103	10
R9-228	Tb4	Flow*	186	23	243	13	184	18	107	10
R9-273.7	Tb4	Flow*	183	23	241	13	198	19	111	10
R9-282.2	Tb4	Tuff*	170	22	235	13	159	15	99	10
R9-285.5	Tb4	Tuff*	154	22	267	13	197	19	96	10
R9-690.4	Tb2	Flow*	219	21	221	12	89	10	81	11
R12-138.5D	Tb4	Flow	160	20	141	10	59	10	102	10
R12-228D	Tb4	Flow	183	19	248	12	96	10	88	10
R12-270D	Tb4	Flow	171	19	228	12	86	10	72	11
R12-380D	Tb4	Flow	195	54	233	20	158	22	97	20
R12-442D	Tb4	Flow	206	27	223	20	144	22	87	20
R12-810D	Tb2	Flow	227	22	240	12	85	10	78	11
R15-532D	Tb4	Flow	190	19	198	12	86	10	98	12
R15-562D	Tb4	Flow	190	18	186	10	84	9	98	9
R15-577D	Tb4	Flow	185	17	199	10	88	9	92	9
R15-610D	Tb4	Flow	195	19	195	12	92	10	98	10
R15-705D	Tb4	Flow	206	20	211	11	111	9	98	9
SHB1-656	Tt2	Flow*	68	12	59	7	35	6	51	11
SHB1-694	Tt2	Flow*	75	12	58	7	40	6	61	12

Sample Number	Rb		Sr		Y		Zr		Nb		Ba	
	ppm	AU	ppm	AU	ppm	AU	ppm	AU	ppm	AU	ppm	AU
Samples of outcrop from Bayo Canyon												
DN/97/7	<9		584	30	20	9	165	15	16	8	879	55
DN/97/16	29	8	828	43	22	8	236	19	20	8	883	55
RWTB4A14	<9		513	31	25	9	149	14	12	7	378	47
RWTB4A15	23	8	820	48	36	9	225	19	27	7	820	52
RWTB4B8	107	6	208	11	65	11	546	21	54	10	802	51
RWTB4B10	66	6	531	31	<7		154	15	28	9	1103	58
RWTB4B14	60	6	435	24	16	6	159	12	12	7	1159	49
Samples of outcrop from western Pajarito Plateau												
LAPC9812	101	7	323	14	20	7	152	12	23	9	796	53
LAPC9813	106	7	306	14	21	7	152	12	22	9	854	55
Samples of cuttings or core (*) from drill holes												
OT4-310D	21	4	502	13	26	4	159	14	22	7	550	34
OT4-370D	21	4	518	11	31	4	169	14	21	7	591	30
OT4-420D	21	4	503	11	30	4	158	14	22	7	542	30
OT4-1210D	9	4	568	12	25	4	154	14	17	7	385	29
OT4-1280D	30	4	775	14	27	4	232	17	26	7	758	34
OT4-1290D	31	4	794	16	24	4	244	18	27	7	979	41
OT4-1300D	42	5	773	14	30	4	258	17	27	7	974	36
PM5-820D	37	6	659	31	16	8	190	16	19	9	1177	69
PM5-910D	36	7	641	31	21	8	191	16	18	8	1196	70
PM5-1010D	59	6	509	25	18	8	174	15	24	9	1285	74
PM5-2190D	64	6	572	27	22	8	284	16	30	9	1197	70
PM5-2440D	16	8	990	48	28	7	203	20	24	9	715	52
PM5-2700D	13	8	805	39	32	7	162	17	15	9	1324	78
R9-50.5D	14	9	427	20	21	6	149	13	16	7	391	48
R9-92D	26	7	451	20	25	7	153	13	19	8	373	47
R9-122D	19	7	440	20	25	9	138	13	15	8	389	47
R9-162D	15	8	413	21	29	9	137	12	13	8	404	47
R9-181.3	19	8	669	34	25	6	191	17	26	8	776	53
R9-201.5	18	9	676	35	32	9	187	17	29	8	732	51
R9-228	26	8	794	41	26	9	200	19	27	8	794	53
R9-273.7	28	8	827	43	38	9	207	19	33	8	822	54
R9-282.2	27	8	628	32	21	8	187	16	28	8	628	50
R9-285.5	32	8	537	28	31	8	166	15	17	8	714	51
R9-690.4	13	8	569	28	26	9	136	14	12	8	462	48
R12-138.5D	10	8	421	19	31	9	149	13	17	7	377	48
R12-228D	21	7	427	19	39	9	138	12	22	8	394	48
R12-270D	16	8	427	22	22	9	140	13	20	7	389	48
R12-380D	26	15	884	42	29	9	223	21	33	7	816	54
R12-442D	18	15	1085	52	43	6	220	23	26	8	983	117
R12-810D	10	8	611	30	30	9	153	15	21	8	413	48
R15-532D	11	9	452	27	20	8	155	13	21	8	466	47
R15-562D	21	8	479	27	25	7	157	13	20	7	507	36
R15-577D	18	8	434	24	22	7	146	12	19	7	508	36
R15-610D	16	8	490	29	21	9	147	14	21	8	470	47
R15-705D	23	7	683	39	36	7	197	16	23	7	719	38
SHB1-656	33	4	670	13	14	4	193	15	18	7	1197	36
SHB1-694	35	4	661	12	19	4	191	15	17	7	1200	36

Figure Captions

Figure 1. Relief and location map of the Pajarito Plateau of the Española Basin, Rio Grande rift, north central New Mexico. Outcrop and drill hole locations of the Pajarito Plateau are shown in the relief map. Inset map A shows the tectonic domain of the Rio Grande rift and the Jemez Lineament (Baldridge, et al., 1984), and inset map B shows the relief map of the Jemez Mountains.

Figure 2. $^{40}Ar/^{39}Ar$ age spectra for samples from Rendija Canyon and Black Mesa at San Ildefonso. The groundmass appears to have minor excess argon and thus an isochron age is reported. The hornblende yields a large plateau segment despite the saddle-shaped spectrum. Plagioclase spectrum is complex, however a plateau age is cautiously assigned.

Figure 3. $^{40}Ar/^{39}Ar$ age spectra for samples from a well at Los Alamos Canyon. The two shallow samples yield analytically identical ages of 2.50±0.03 and 2.52±0.06 Ma, whereas the 3 deeper samples group within an age range of 8.81 to 8.97 Ma. The decreasing age spectra for the three deeper samples may be related to ^{39}Ar recoil during irradiation.

Figure 4. $^{40}Ar/^{39}Ar$ age spectra for samples from a well at Mortandad Canyon. The two shallow samples have overall rising age spectra, which may indicate minor argon loss. The two deeper samples have dramatically increasing ages across the spectrum that suggests xenocrystic contamination.

Figure 5. $^{40}Ar/^{39}Ar$ age spectra (a-d) and probability diagram (e) for single crystal sanidine laser fusion results for samples from Bayo Canyon. Groundmass samples yield precise apparent ages with minor complexity, whereas plagioclase spectra are quite complex. Sanidine ages are normally distributed and provide a precise eruption age.

Figure 6. Simplified stratigraphic sections of the O-4 and PM-5 drill holes (adapted from Purtymun, 1995) and from the middle part of the Bayo Canyon drainage in the eastern part of the Pajarito Plateau.

Figure 7. Age (K-Ar and $^{40}Ar/^{39}Ar$) distributions of mafic volcanic units from the Jemez volcanic field, including the Cerros del Rio volcanic flows, the Tschicoma Formation, the Keres Group, and the Bayo Canyon, Lobato, and Guaje Canyon basalts (Bachman and Mehnert, 1978; Dalrymple et al., 1967; Dethier et al., 1986; Gardner and Goff, 1984; Gardner et al., 1986; Goff et al., 1989; WoldeGabriel et al., 1996).

Figure 8. Simplified stratigraphic sections from the Jemez Mountains and the Pajarito Plateau. Columns for the southern (St. Peters dome) and northeastern (Santa Clara Canyon) Jemez Mountains are compiled from outcrops (Aldrich and Dethier, 1990; Goff et al., 1990), and column for central Jemez Mountains Drill hole B-22 is from Nielson and Hulen (1984). Drill holes O-4 and PM-5 and outcrops at Ancho and Bayo canyons represent various parts of the Pajarito Plateau. Symbols in parenthesis are those of the LANL site-wide 3-D geologic model.

Figure 9. Total alkali-silica diagram (Le Bas et al., 1986) for volcanic samples from the late Pliocene Cerros del Rio (Tb4), the late Miocene Bayo Canyon basalt (Tb2), and the middle Miocene Guaje Canyon basalt (Tb1). Data are from this work and from WoldeGabriel et al (1996).

Figure 10. Total alkali-silica plots (Le Bas et al., 1986) for representative Neogene and Quaternary volcanic rocks from the Keres Group (TMk), the Lobato Basalt (TMl), the Tschicoma Formation (Tt1 and Tt2), mafic units of the Pajarito Plateau (Tb4, Tb2, and Tb1) and the Bandelier Tuff (Qbo and Qbt) of the Jemez volcanic field. Data are from this work; Goff et al. (1989); Ellisor (1995); and WoldeGabriel et al. (1996).

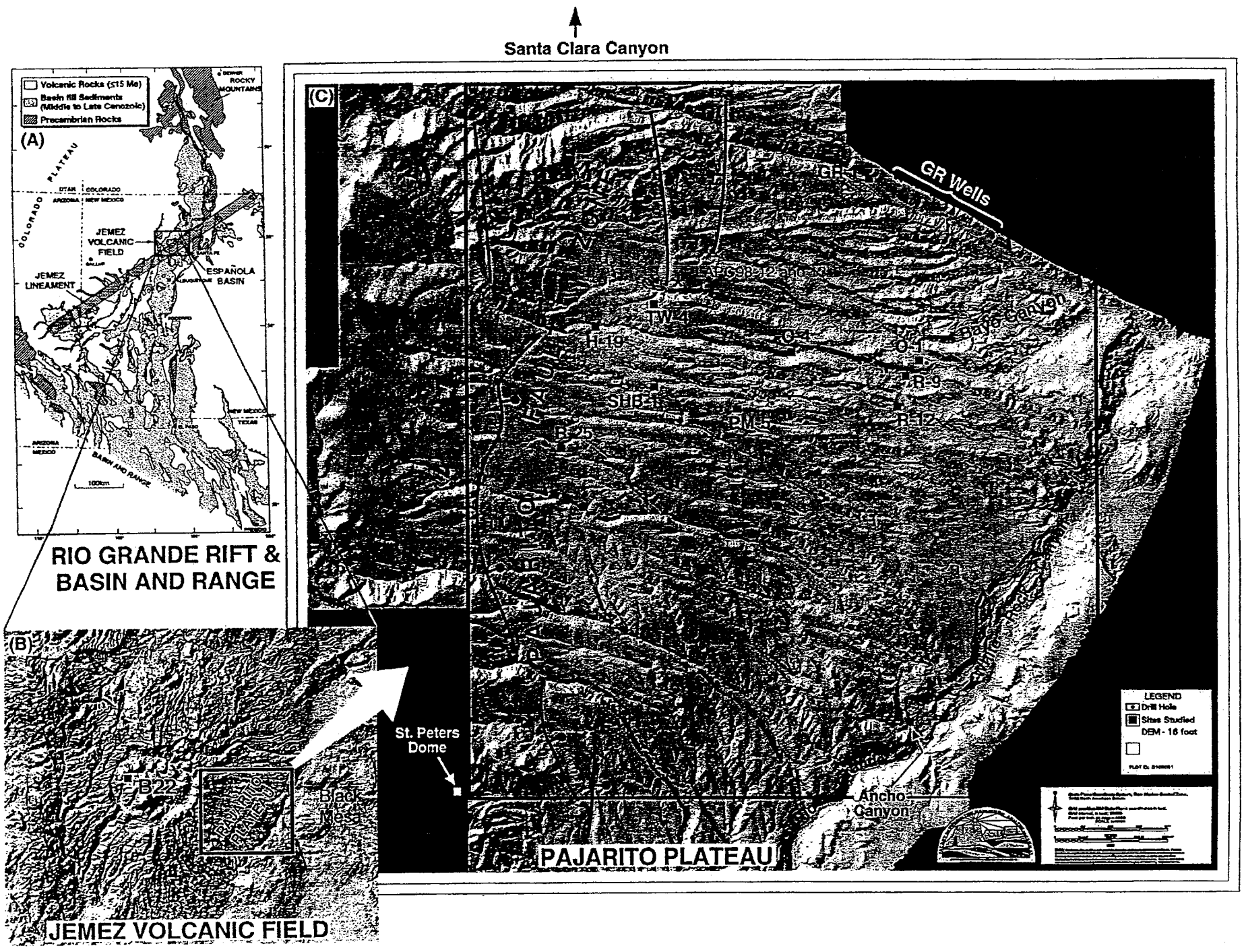
Santa Clara Canyon
(A)
Volcanic Rocks (≤15 Ma)
Basin fill Sediments (Middle to Late Cenozoic)
Precambrian Rocks
ROCKY MOUNTAINS
COLORADO PLATEAU
JEMEZ VOLCANIC FIELD
JEMEZ LINEAMENT
ESPAÑOLA BASIN
BASIN AND RANGE
RIO GRANDE RIFT & BASIN AND RANGE
(B)
St. Peters Dome
B-22
Black Mesa
JEMEZ VOLCANIC FIELD
(C)
GR
GR Wells
LAPG GR-12
TW-4
H-19
O-1
O-1
Bayo Canyon
R-9
SHB-1
PM-5
R-12
R-25
Ancho Canyon
PAJARITO PLATEAU
LEGEND
Drill Hole
Sites Studied
DEM - 10 foot

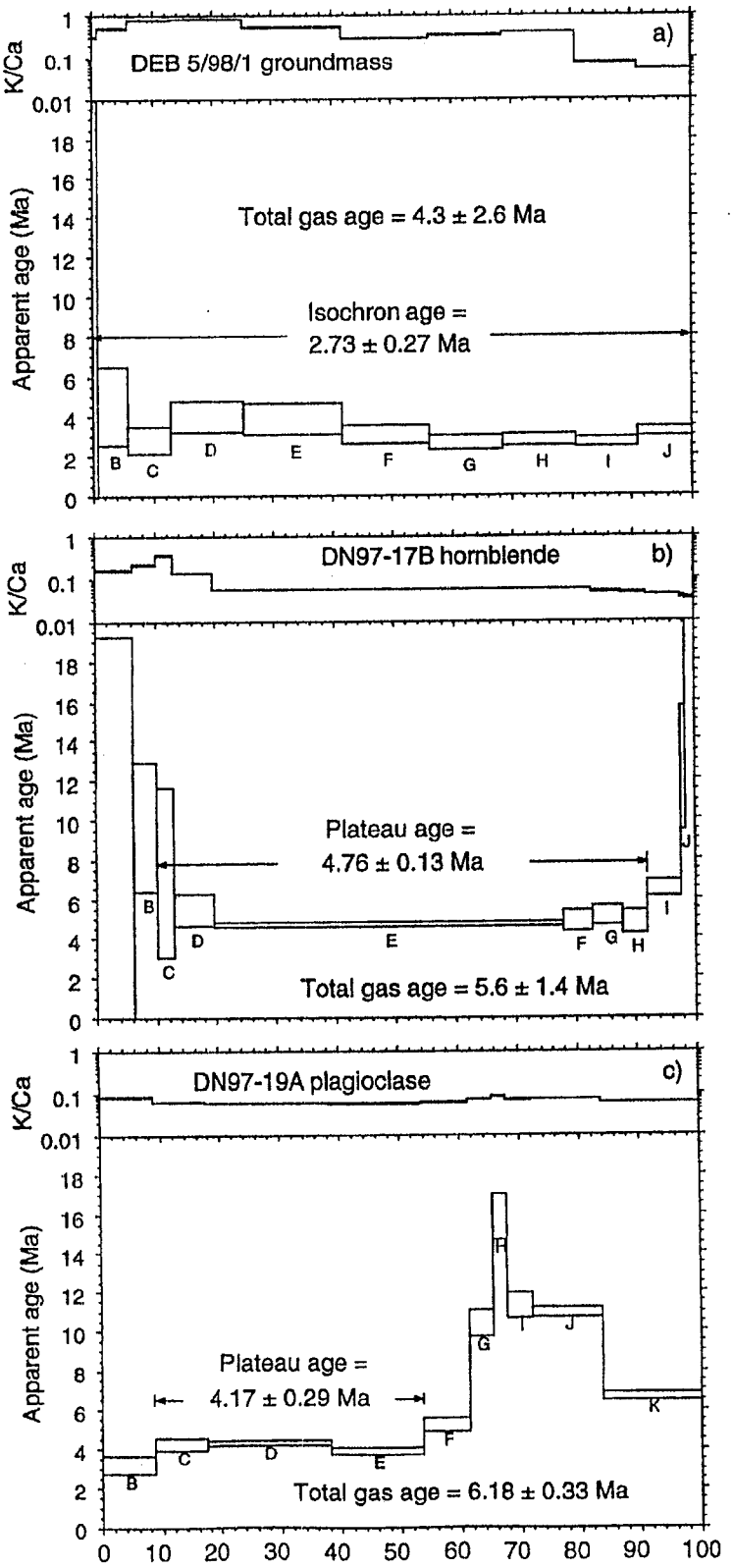
a)
DEB 5/98/1 groundmass
K/Ca
Apparent age (Ma)
Total gas age = 4.3 ± 2.6 Ma
Isochron age =
2.73 ± 0.27 Ma
B
C
D
E
F
G
H
I
J
b)
DN97-17B hornblende
Plateau age =
4.76 ± 0.13 Ma
Total gas age = 5.6 ± 1.4 Ma
c)
DN97-19A plagioclase
Plateau age =
4.17 ± 0.29 Ma
Total gas age = 6.18 ± 0.33 Ma
K

Fig. 2

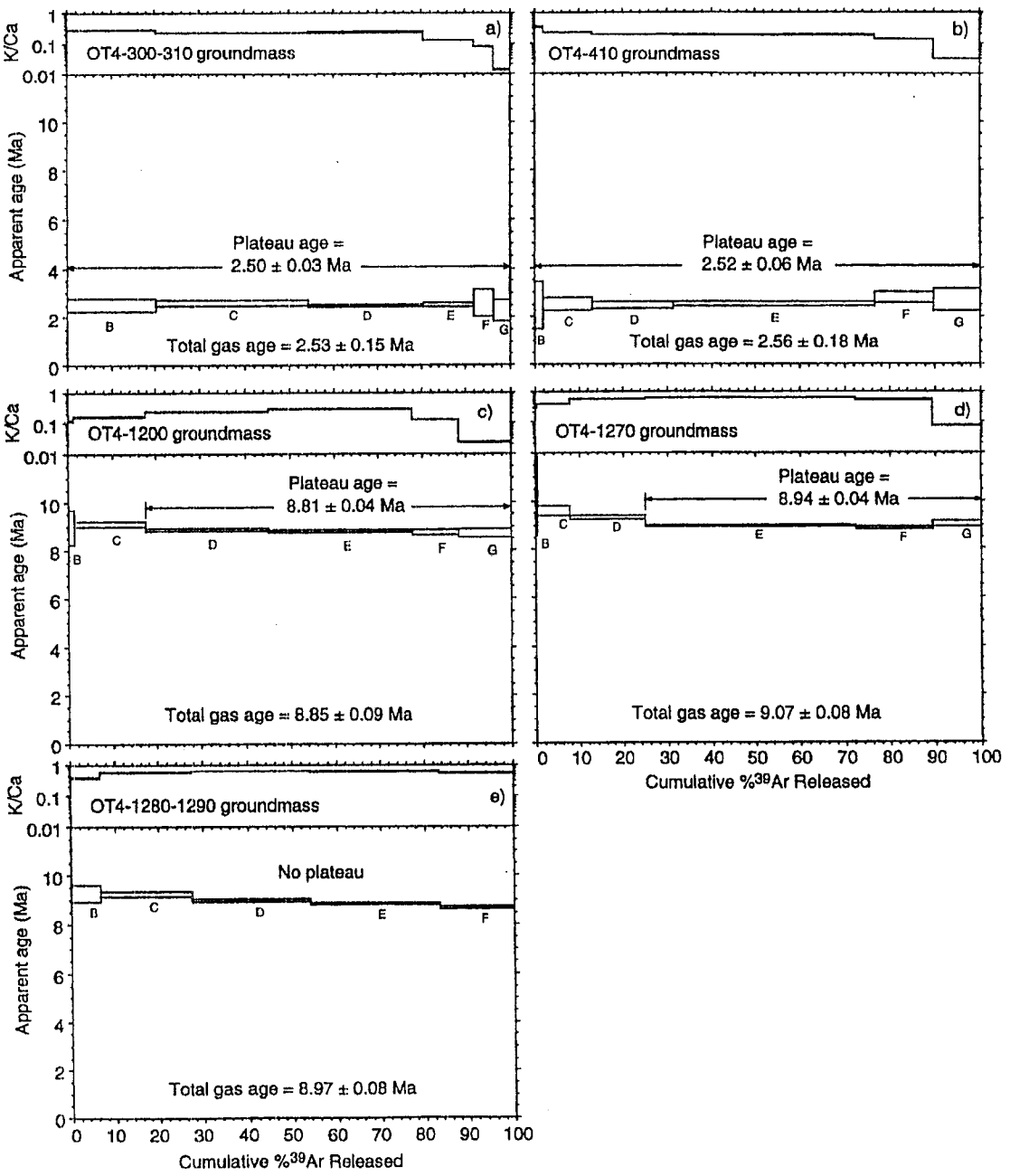
a)
OT4-300-310 groundmass
Plateau age =
2.50 ± 0.03 Ma
Total gas age = 2.53 ± 0.15 Ma
b)
OT4-410 groundmass
Plateau age =
2.52 ± 0.06 Ma
Total gas age = 2.56 ± 0.18 Ma
c)
OT4-1200 groundmass
Plateau age =
8.81 ± 0.04 Ma
Total gas age = 8.85 ± 0.09 Ma
d)
OT4-1270 groundmass
Plateau age =
8.94 ± 0.04 Ma
Total gas age = 9.07 ± 0.08 Ma
e)
OT4-1280-1290 groundmass
No plateau
Total gas age = 8.97 ± 0.08 Ma
K/Ca
Apparent age (Ma)
Cumulative %39Ar Released

Fig. 5

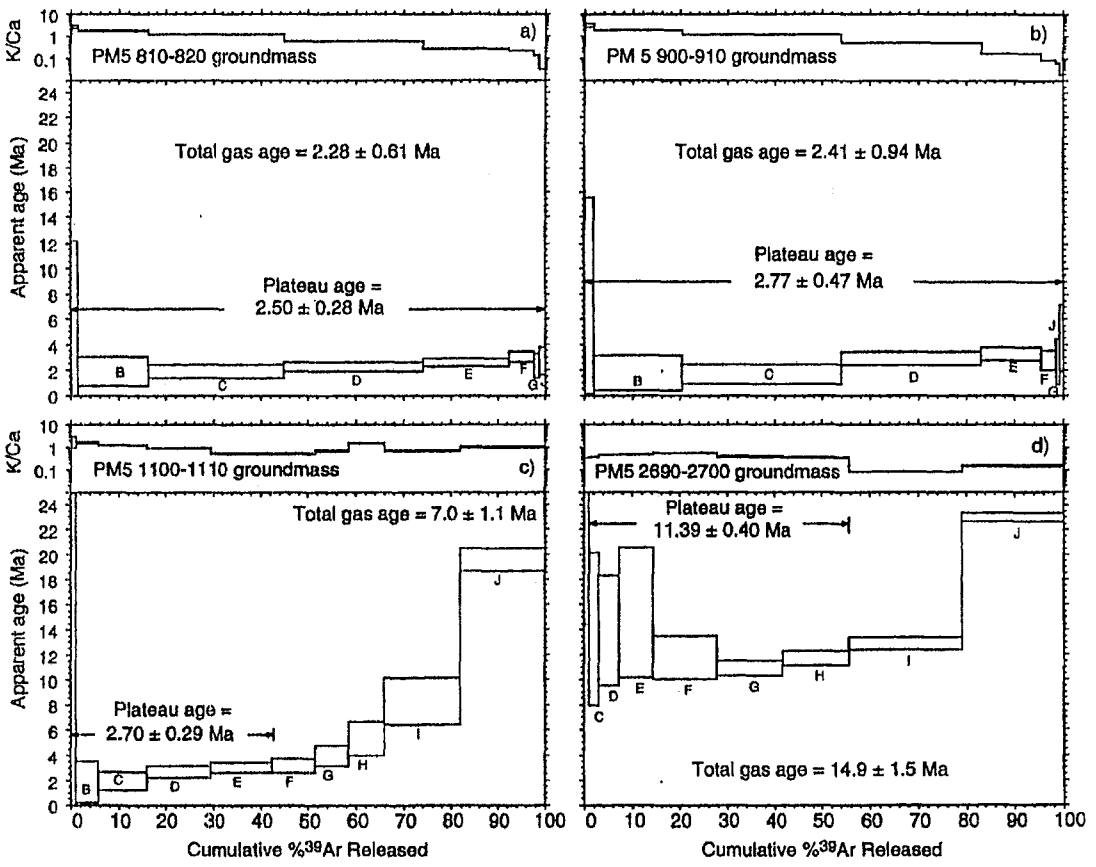
a)
PM5 810-820 groundmass
Total gas age = 2.28 ± 0.61 Ma
Plateau age =
2.50 ± 0.28 Ma
b)
PM 5 900-910 groundmass
Total gas age = 2.41 ± 0.94 Ma
Plateau age =
2.77 ± 0.47 Ma
c)
PM5 1100-1110 groundmass
Total gas age = 7.0 ± 1.1 Ma
Plateau age =
2.70 ± 0.29 Ma
d)
PM5 2690-2700 groundmass
Plateau age =
11.39 ± 0.40 Ma
Total gas age = 14.9 ± 1.5 Ma
K/Ca
Apparent age (Ma)
Cumulative %39Ar Released

Fig.

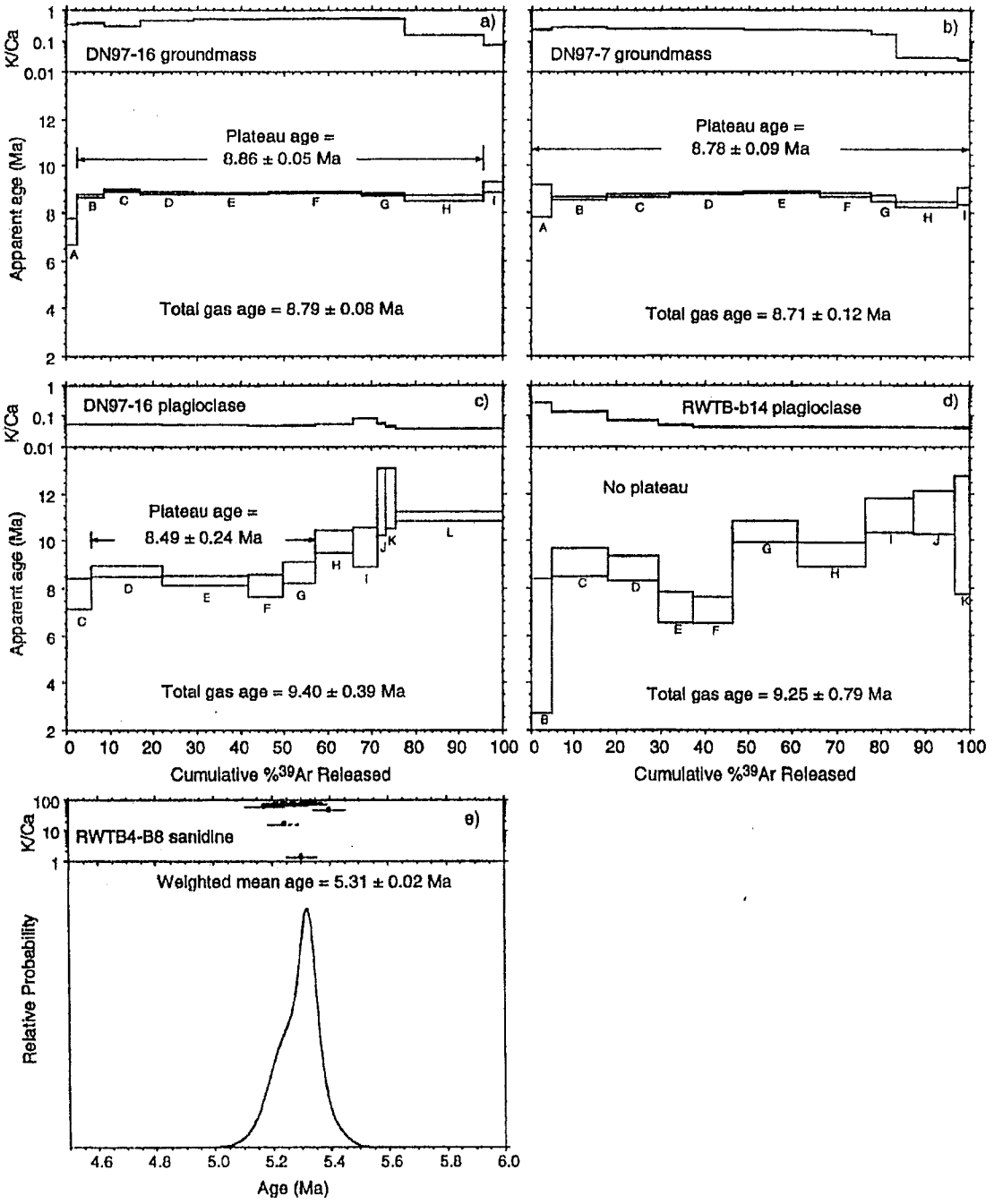
a)
DN97-16 groundmass
Plateau age =
8.86 ± 0.05 Ma
Total gas age = 8.79 ± 0.08 Ma
b)
DN97-7 groundmass
Plateau age =
8.78 ± 0.09 Ma
Total gas age = 8.71 ± 0.12 Ma
c)
DN97-16 plagioclase
Plateau age =
8.49 ± 0.24 Ma
Total gas age = 9.40 ± 0.39 Ma
d)
RWTB-b14 plagioclase
No plateau
Total gas age = 9.25 ± 0.79 Ma
K/Ca
Apparent age (Ma)
Cumulative %39Ar Released

e)
RWTB4-B8 sanidine
Weighted mean age = 5.31 ± 0.02 Ma
K/Ca
Relative Probability
Age (Ma)

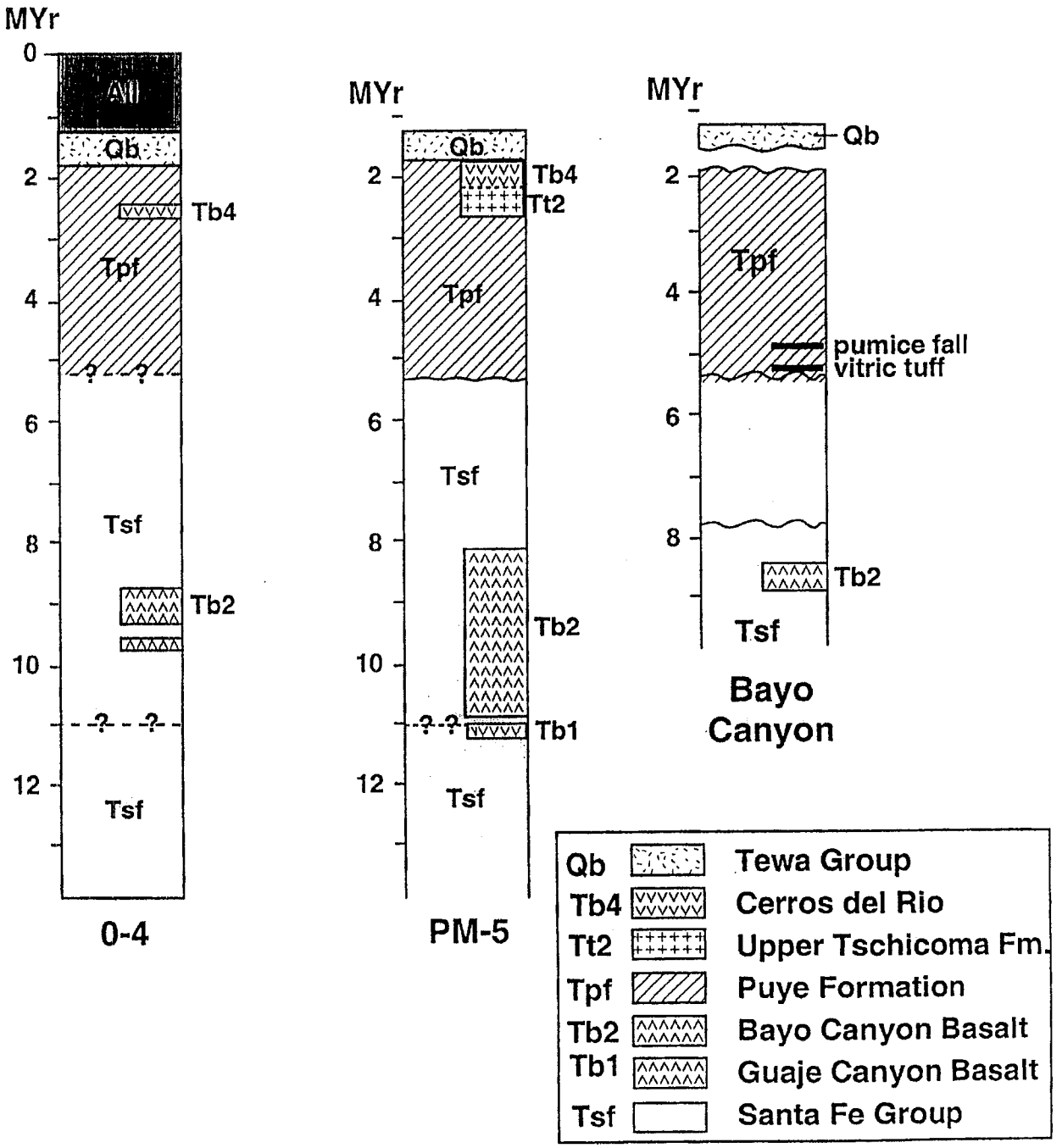
MYr
0
2
4
6
8
10
12
All
Qb
Tb4
Tpf
?
?
Tsf
Tb2
?
?
Tsf
0-4
MYr
Qb
Tb4
Tt2
Tpf
Tsf
Tb2
Tb1
?
?
Tsf
PM-5
MYr
Qb
Tpf
pumice fall
vitric tuff
Tb2
Tsf
Bayo
Canyon
Qb Tewa Group
Tb4 Cerros del Rio
Tt2 Upper Tschicoma Fm.
Tpf Puye Formation
Tb2 Bayo Canyon Basalt
Tb1 Guaje Canyon Basalt
Tsf Santa Fe Group

Via.

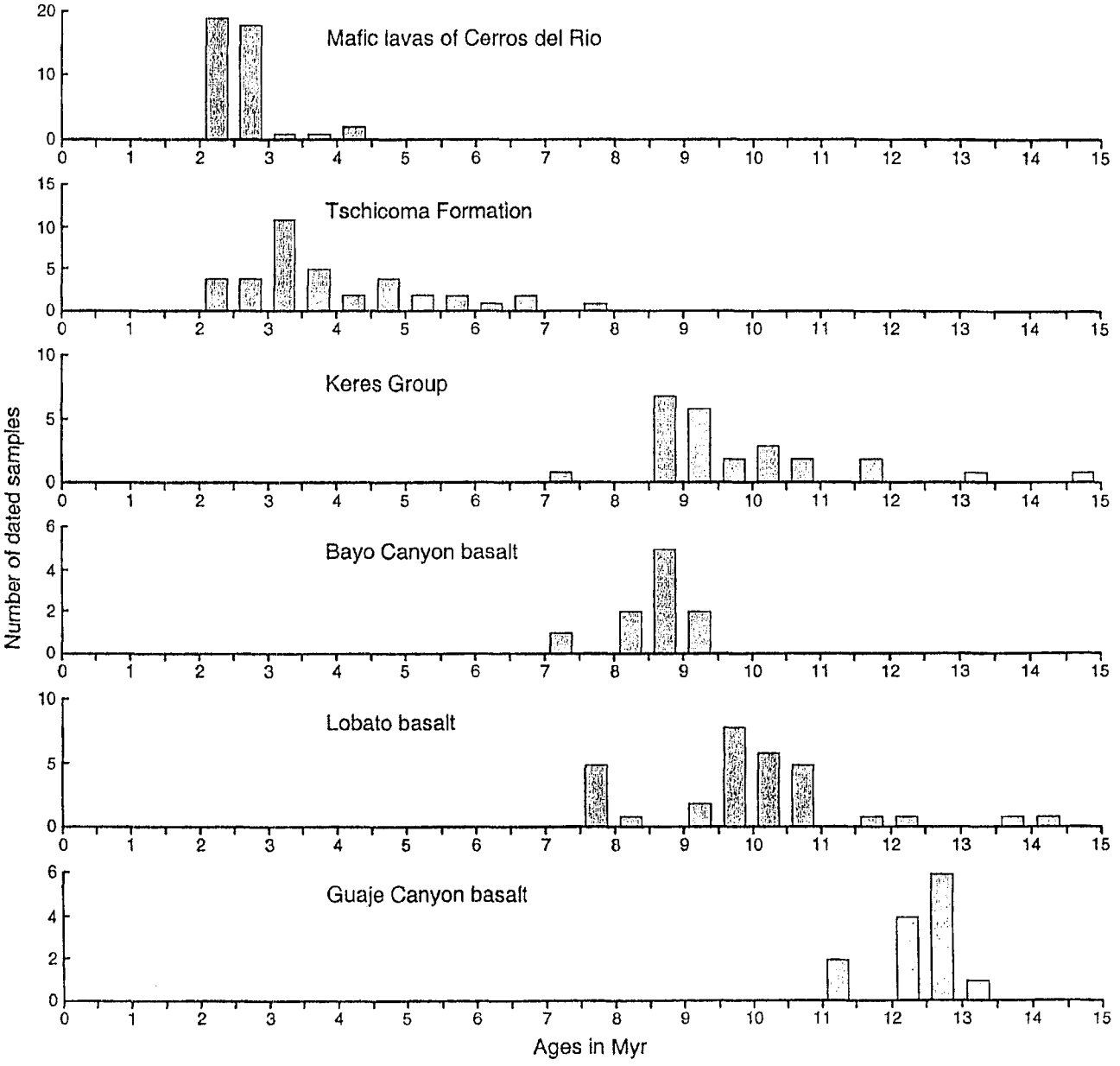
Mafic lavas of Cerros del Rio
Tschicoma Formation
Keres Group
Bayo Canyon basalt
Lobato basalt
Guaje Canyon basalt
Number of dated samples
Ages in Myr

Eii

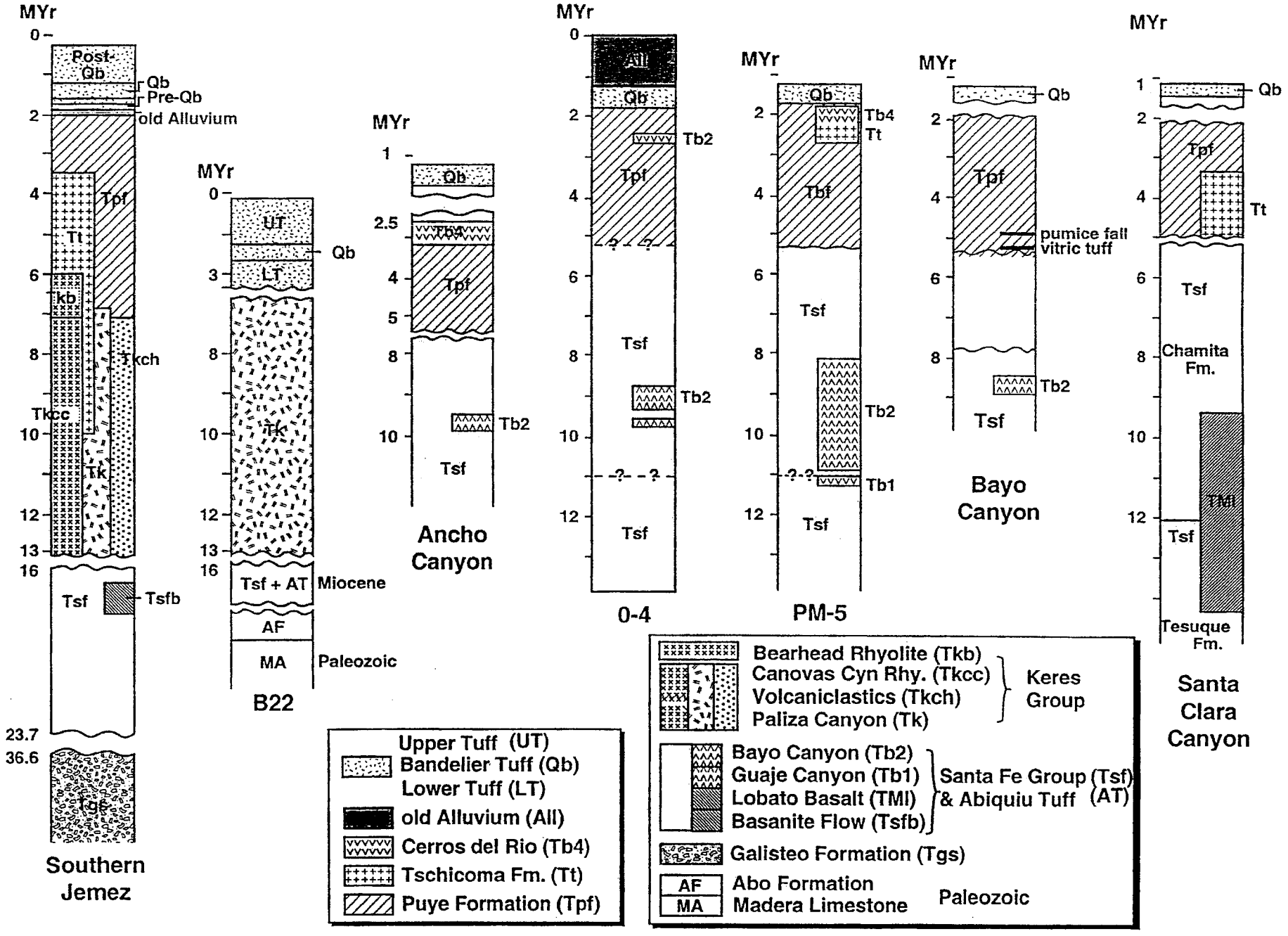
MYr
Post-Qb
Qb
Pre-Qb
old Alluvium
Tpf
Tt
kb
Tkch
Tkcc
Tk
Tsf
Tsfb
Tgs
23.7
36.6
Southern Jemez
UT
LT
Qb
Tk
Tsf + AT
Miocene
AF
MA
Paleozoic
B22
Tb4
Tb2
Ancho Canyon
All
0-4
Tbf
Tb1
PM-5
pumice fall
vitric tuff
Bayo Canyon
Chamita Fm.
TMl
Tesuque Fm.
Santa Clara Canyon
Upper Tuff (UT)
Bandelier Tuff (Qb)
Lower Tuff (LT)
old Alluvium (All)
Cerros del Rio (Tb4)
Tschicoma Fm. (Tt)
Puye Formation (Tpf)
Bearhead Rhyolite (Tkb)
Canovas Cyn Rhy. (Tkcc)
Volcaniclastics (Tkch)
Paliza Canyon (Tk)
Keres Group
Bayo Canyon (Tb2)
Guaje Canyon (Tb1)
Lobato Basalt (TMl)
Basanite Flow (Tsfb)
Santa Fe Group (Tsf) & Abiquiu Tuff (AT)
Galisteo Formation (Tgs)
Abo Formation
Madera Limestone
Paleozoic

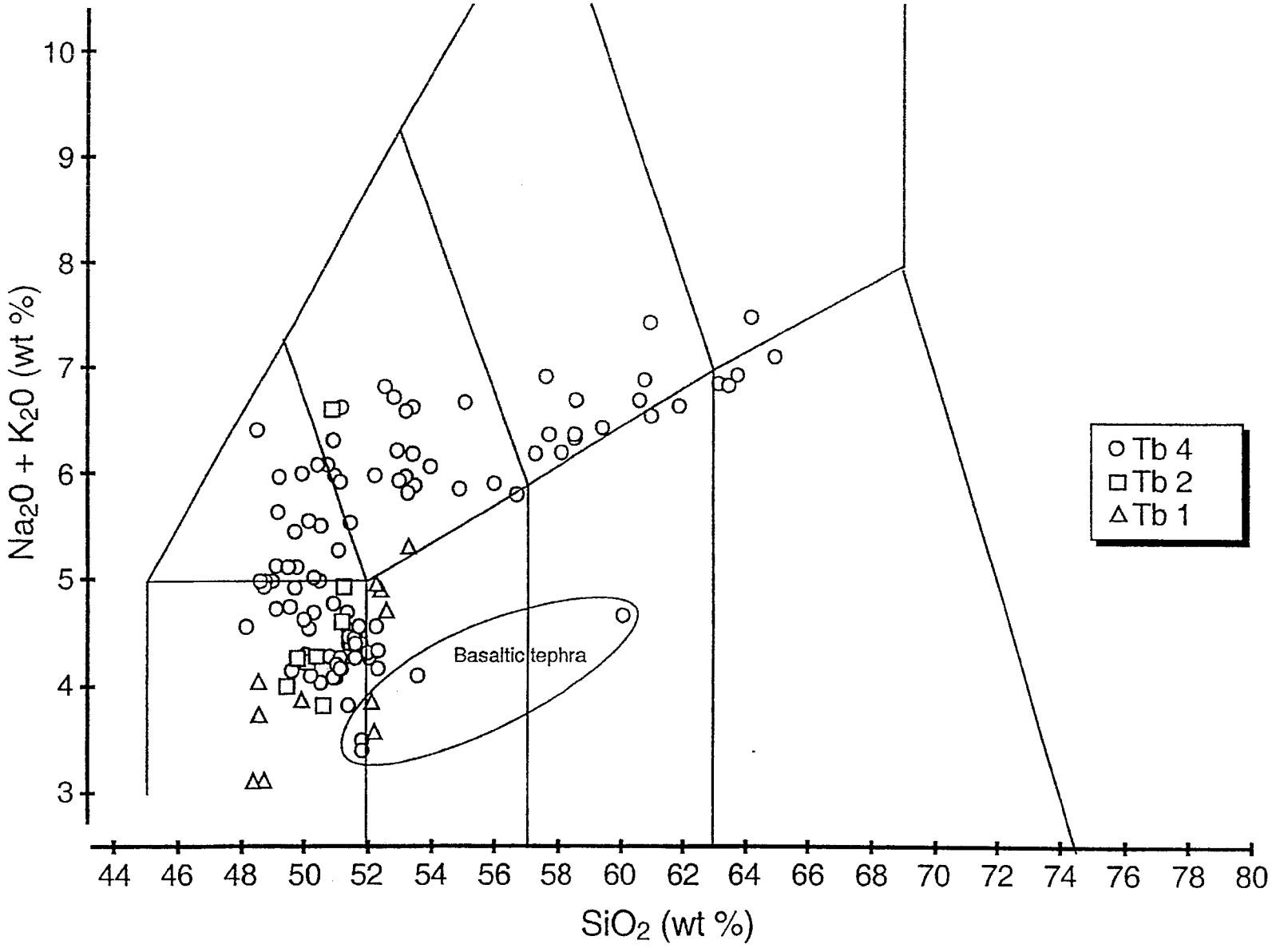
10
9
8
7
6
5
4
3
$Na_2O + K_2O$ (wt %)
44
46
48
50
52
54
56
58
60
62
64
66
68
70
72
74
76
78
80
SiO_2 (wt %)
Basaltic tephra
Tb 4
Tb 2
Tb 1

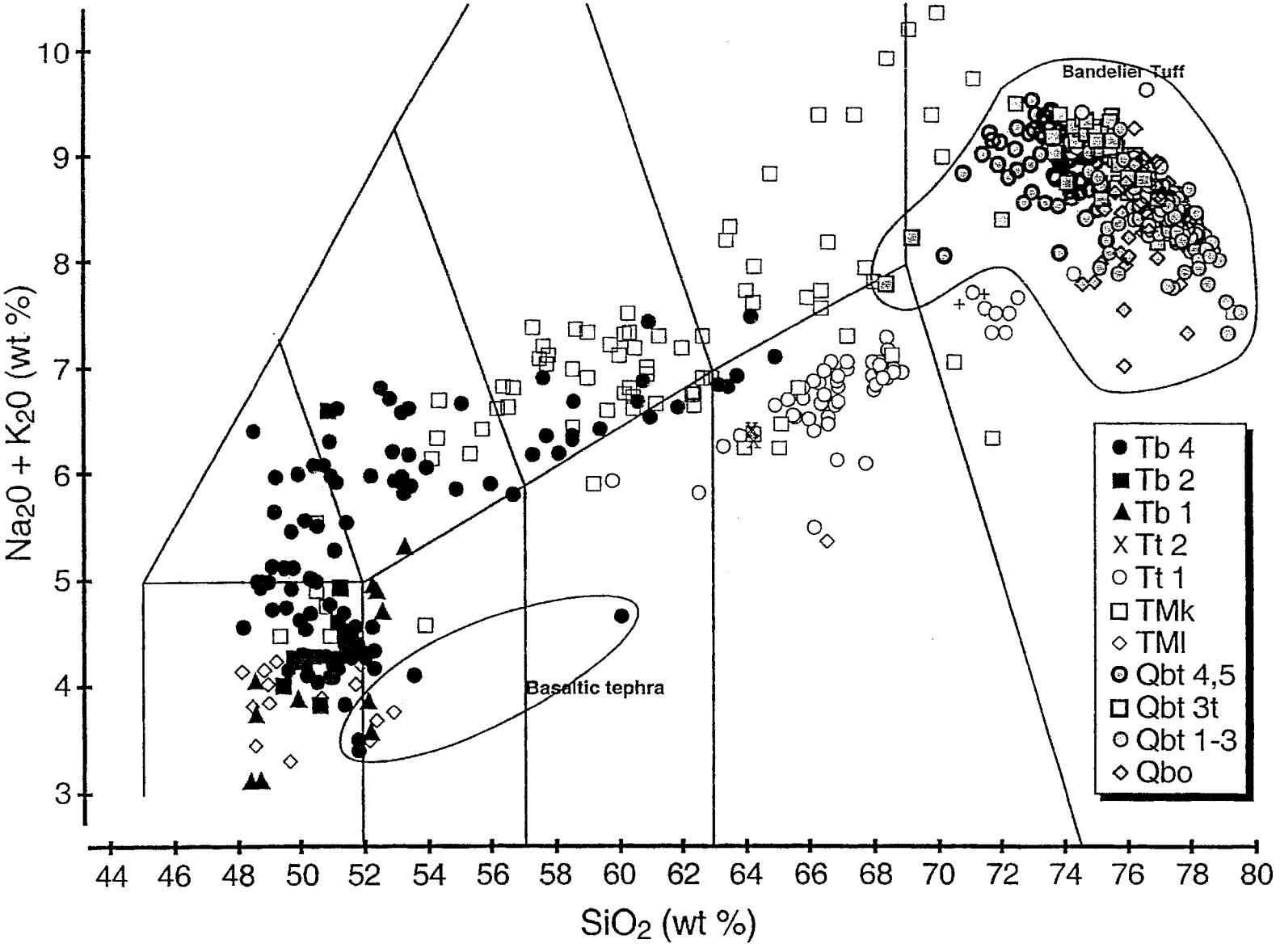
Bandelier Tuff
Basaltic tephra
Tb 4
Tb 2
Tb 1
Tt 2
Tt 1
TMk
TMl
Qbt 4,5
Qbt 3t
Qbt 1-3
Qbo
$Na_2O + K_2O$ (wt %)
SiO_2 (wt %)
10
9
8
7
6
5
4
3
44
46
48
50
52
54
56
58
60
62
64
66
68
70
72
74
76
78
80

Appendix 1. Argon isotopic data

ID	Temp (°C)	$^{40}Ar/^{39}Ar$	$^{37}Ar/^{39}Ar$	$^{36}Ar/^{39}Ar$ (x 10^{-3})	$^{39}Ar_K$ (x 10^{-15} mol)	K/Ca	$^{40}Ar^*$ (%)	^{39}Ar (%)	Age (Ma)	±1σ (Ma)
DEB 5/98/1 groundmass, wt. = 35.25 mg, J = 0.0007683, NM-93, Lab#=9492-01										
A	550	6184.8	1.490	20620	0.604	0.34	1.5	0.8	123	119
B	650	153.3	0.9476	507.8	3.62	0.54	2.1	5.9	4.56	0.97
C	700	48.31	0.6127	156.7	5.03	0.83	4.3	12.8	2.85	0.33
D	750	62.11	0.5767	200.5	8.87	0.88	4.7	25.1	4.01	0.40
E	820	72.19	0.8873	235.0	12.0	0.58	3.9	41.8	3.91	0.39
F	900	38.22	1.698	122.1	10.3	0.30	5.9	56.1	3.15	0.22
G	1000	24.90	1.407	78.00	8.88	0.36	7.9	68.4	2.72	0.17
H	1100	16.51	1.185	49.21	8.94	0.43	12.5	80.8	2.86	0.14
I	1200	12.14	6.384	36.14	7.36	0.080	16.1	91.0	2.72	0.12
J	1650	13.78	9.198	41.17	6.47	0.055	16.8	100.0	3.23	0.13
total gas age			n=10		72.1	0.45			**4.3**	**2.6**
Isochron		MSWD=2.30*	n=10	steps A-J	72.1	0.45		100.0	**2.73**	**0.27**
DN97-17B hornblende, wt. = 69.66 mg, J = 0.0007697, NM-93, Lab#=9501-01										
A	*800*	*579.4*	*3.144*	*1947.2*	*3.40*	*0.16*	*0.7*	*6.2*	*5.9*	*6.7*
B	*850*	*96.04*	*2.409*	*302.1*	*2.11*	*0.21*	*7.2*	*10.1*	*9.7*	*1.6*
C	950	92.00	1.431	293.7	1.51	0.36	5.8	12.9	7.4	2.1
D	1020	34.57	3.678	104.6	3.73	0.14	11.4	19.7	5.46	0.42
E	1080	9.260	9.438	22.36	31.9	0.054	36.5	78.1	4.715	0.056
F	1120	9.606	9.198	23.14	2.65	0.055	36.2	83.0	4.85	0.27
G	1160	7.037	10.95	14.28	2.71	0.047	52.0	87.9	5.11	0.24
H	1200	6.136	11.60	12.20	2.27	0.044	55.8	92.1	4.78	0.28
I	*1300*	*6.547*	*12.75*	*9.810*	*3.03*	*0.040*	*70.7*	*97.6*	*6.47*	*0.20*
J	*1400*	*12.51*	*14.64*	*15.62*	*0.413*	*0.035*	*72.1*	*98.4*	*12.6*	*1.6*
K	*1650*	*24.71*	*15.69*	*30.60*	*0.884*	*0.033*	*68.3*	*100.0*	*23.53*	*0.96*
total gas age			n=11		54.6	0.079			**5.6**	**1.4**
plateau		MSWD=1.44	n=6	steps C-H	44.8	0.070		82.0	**4.76**	**0.13**
DN-97-19A plagioclase, wt. = 80.34 mg, J = 0.0007691, NM-93, Lab#=9518-01										
B	*850*	*14.72*	*6.017*	*43.61*	*4.11*	*0.085*	*15.6*	*8.9*	*3.19*	*0.24*
C	950	4.257	8.022	6.111	4.01	0.064	72.1	17.5	4.28	0.16
D	1050	3.512	8.818	3.689	9.65	0.058	88.2	38.3	4.321	0.065
E	1150	3.065	8.920	3.258	7.08	0.057	90.9	53.6	3.887	0.084
F	*1200*	*4.051*	*8.318*	*3.233*	*3.62*	*0.061*	*92.2*	*61.4*	*5.20*	*0.17*
G	*1250*	*8.136*	*7.026*	*4.146*	*1.85*	*0.073*	*91.6*	*65.3*	*10.36*	*0.33*
H	*1300*	*13.05*	*6.148*	*7.276*	*1.15*	*0.083*	*87.1*	*67.8*	*15.77*	*0.57*
I	*1350*	*9.054*	*7.200*	*5.111*	*1.95*	*0.071*	*89.4*	*72.0*	*11.26*	*0.32*
J	*1400*	*8.657*	*7.173*	*4.612*	*5.41*	*0.071*	*90.6*	*83.7*	*10.91*	*0.12*
K	*1650*	*6.363*	*8.493*	*7.641*	*7.57*	*0.060*	*74.8*	*100.0*	*6.629*	*0.090*
total gas age			n=10		46.4	0.065			**6.18**	**0.33**
plateau		MSWD=8.59*	n=3	steps C-E	20.7	0.059		44.7	**4.17**	**0.29**

Appendix 1. Argon isotopic data

ID	Temp (°C)	$^{40}Ar/^{39}Ar$	$^{37}Ar/^{39}Ar$	$^{36}Ar/^{39}Ar$ (x 10^{-3})	$^{39}Ar_K$ (x 10^{-15} mol)	K/Ca	$^{40}Ar^*$ (%)	^{39}Ar (%)	Age (Ma)	±1σ (Ma)
DN97-16 groundmass, wt. = 71.95 mg, J = 0.0007997, NM-77, Lab#=8369-01										
A	*625*	*45.83*	*1.473*	*138.6*	*5.45*	*0.35*	*10.9*	*2.3*	*7.20*	*0.29*
B	700	8.584	1.332	8.920	14.8	0.38	70.6	8.6	8.730	0.044
C	750	7.198	1.643	3.784	19.4	0.31	86.4	16.9	8.959	0.025
D	800	6.628	1.129	1.925	28.2	0.45	92.8	28.9	8.863	0.021
E	875	6.421	0.9632	1.187	41.0	0.53	95.8	46.4	8.857	0.017
F	975	6.606	0.9393	1.733	49.6	0.54	93.4	67.5	8.889	0.021
G	1075	7.455	0.9481	4.821	23.5	0.54	81.9	77.5	8.799	0.030
H	1250	15.47	3.240	32.99	42.5	0.16	38.7	95.6	8.640	0.061
I	*1650*	*16.22*	*6.771*	*35.51*	*10.2*	*0.075*	*38.7*	*100.0*	*9.10*	*0.11*
total gas age			n=9		234.6	0.41			**8.79**	**0.08**
plateau		MSWD=7.30*	n=7	steps B-H	219.0	0.42		93.3	**8.86**	**0.05**
DN97-7 groundmass, wt. = 66.79 mg, J = 0.0007989, NM-77, Lab#=8368-01										
A	625	55.09	2.111	167.0	5.02	0.24	10.7	4.6	8.52	0.35
B	700	7.343	1.816	5.077	14.1	0.28	81.6	17.6	8.631	0.037
C	750	6.817	2.060	3.128	15.6	0.25	88.9	31.9	8.733	0.030
D	800	6.582	2.055	2.070	18.3	0.25	93.3	48.7	8.844	0.022
E	875	7.075	2.154	3.633	18.9	0.24	87.3	66.1	8.901	0.026
F	975	6.997	2.337	3.728	12.9	0.22	87.0	78.0	8.771	0.033
G	1075	7.584	3.066	6.281	6.31	0.17	78.9	83.8	8.623	0.068
H	1250	9.691	17.33	18.26	14.8	0.029	59.1	97.3	8.365	0.056
I	1650	14.39	21.08	34.44	2.93	0.024	41.4	100.0	8.72	0.19
total gas age			n=9		108.9	0.21			**8.71**	**0.12**
plateau		MSWD=13.8*	n=9	steps A-I	108.9	0.21		100.0	**8.78**	**0.09**
DN97-16 plagioclase, wt. = 19.76 mg, J = 0.0008030, NM-77, Lab#=8361-01										
C	*800*	*8.887*	*9.201*	*14.59*	*0.631*	*0.055*	*60.1*	*5.6*	*7.78*	*0.32*
D	900	8.126	9.065	9.762	1.84	0.056	73.7	22.0	8.73	0.11
E	1000	7.362	9.753	8.252	2.21	0.052	77.8	41.7	8.355	0.097
F	1050	7.025	10.52	7.901	0.906	0.049	79.1	49.8	8.11	0.23
G	1100	7.015	10.31	6.533	0.826	0.049	84.6	57.1	8.66	0.23
H	*1150*	*9.377*	*9.162*	*11.13*	*0.986*	*0.056*	*73.0*	*65.9*	*9.97*	*0.24*
I	*1200*	*12.19*	*6.289*	*20.34*	*0.624*	*0.081*	*55.0*	*71.5*	*9.73*	*0.42*
J	*1250*	*11.77*	*8.951*	*15.22*	*0.209*	*0.057*	*68.1*	*73.3*	*11.66*	*0.72*
K	*1350*	*13.57*	*10.79*	*21.50*	*0.253*	*0.047*	*59.7*	*75.6*	*11.82*	*0.64*
L	*1650*	*10.31*	*12.54*	*12.78*	*2.74*	*0.041*	*73.4*	*100.0*	*11.05*	*0.11*
total gas age			n=10		11.2	0.052			**9.40**	**0.39**
plateau		MSWD=3.18*	n=4	steps D-G	5.8	0.053		51.5	**8.49**	**0.24**

Appendix 1. Argon isotopic data

ID	Temp (°C)	$^{40}Ar/^{39}Ar$	$^{37}Ar/^{39}Ar$	$^{36}Ar/^{39}Ar$ (x 10^{-3})	$^{39}Ar_K$ (x 10^{-15} mol)	K/Ca	$^{40}Ar^*$ (%)	^{39}Ar (%)	Age (Ma)	±1σ (Ma)
RWTB4-B14 groundmass, wt. = 21.00 mg, J = 0.0014764, NM-127, Lab#=51510-01										
B	4	56.86	1.889	185.9	1.65	0.27	3.7	4.9	5.6	1.4
C	7	10.12	3.847	23.76	4.40	0.13	33.7	18.0	9.10	0.29
D	10	6.272	7.382	12.11	3.90	0.069	52.7	29.5	8.84	0.26
E	12	6.805	10.14	16.79	2.62	0.050	39.4	37.3	7.19	0.32
F	15	6.589	11.79	16.70	3.03	0.043	39.9	46.3	7.06	0.28
G	20	8.596	11.59	19.21	5.05	0.044	45.1	61.3	10.41	0.23
H	25	8.679	11.66	20.77	5.15	0.044	40.4	76.6	9.41	0.24
I	30	12.66	11.72	32.16	3.61	0.044	32.6	87.3	11.06	0.37
J	40	15.40	12.04	41.37	3.12	0.042	27.1	96.6	11.20	0.46
K	50	33.01	11.94	102.1	1.15	0.043	11.6	100.0	10.3	1.2
total gas age			n=10		33.7	0.070			**9.25**	**0.79**
no plateau										
OT4-300-310 groundmass, wt. = ~50 mg, J = 0.0001642, NMUM-6, Lab#=531-01										
B	700	87.91	1.775	269.1	13.7	0.29	9.7	20.2	2.52	0.14
C	800	35.58	2.160	91.21	23.1	0.24	24.7	54.3	2.601	0.051
D	900	14.06	2.090	19.79	17.7	0.24	59.4	80.5	2.476	0.019
E	1000	20.31	3.938	41.04	7.82	0.13	41.7	92.0	2.513	0.036
F	1200	87.41	6.540	267.9	2.88	0.078	10.0	96.3	2.60	0.27
G	1400	74.64	37.65	237.0	2.51	0.014	10.0	100.0	2.27	0.22
total gas age			n=6		67.7	0.22			**2.53**	**0.15**
plateau		MSWD=1.36	n=6	steps B-G	67.7	0.22		100.0	**2.50**	**0.03**
OT4-410 groundmass, wt. = ~50 mg, J = 0.0001653, NMUM-6, Lab#=511-01										
B	600	155.1	1.491	497.4	1.58	0.34	5.3	1.9	2.46	0.48
C	700	78.23	2.361	236.7	9.43	0.22	10.8	13.1	2.52	0.14
D	800	41.09	2.621	111.7	15.5	0.19	20.1	31.4	2.466	0.060
E	1000	29.75	2.713	72.80	38.2	0.19	28.3	76.8	2.514	0.041
F	1200	73.27	3.704	217.4	11.0	0.14	12.7	89.8	2.78	0.12
G	1400	141.7	16.95	453.6	8.56	0.030	6.3	100.0	2.70	0.22
total gas age			n=6		84.2	0.17			**2.56**	**0.18**
plateau		MSWD=1.36	n=6	steps B-G	84.2	0.17		100.0	**2.52**	**0.06**
OT4-1200 groundmass, wt. = ~50 mg, J = 0.0001658, NMUM-6, Lab#=510-01										
B	*600*	*74.80*	*4.299*	*153.0*	*0.798*	*0.12*	*40.0*	*1.2*	*8.95*	*0.36*
C	*700*	*44.43*	*3.101*	*47.95*	*11.1*	*0.16*	*68.6*	*17.6*	*9.113*	*0.052*
D	800	30.75	2.083	4.156	18.7	0.24	96.5	45.2	8.862	0.027
E	1000	31.33	1.740	6.846	22.2	0.29	93.9	78.1	8.788	0.028
F	1200	40.24	3.855	38.09	7.01	0.13	72.7	88.4	8.754	0.055
G	1400	69.13	21.09	142.1	7.82	0.024	41.6	100.0	8.703	0.094
total gas age			n=6		67.5	0.21			**8.85**	**0.09**
plateau		MSWD=2.22	n=4	steps D-G	55.7	0.22		82.4	**8.81**	**0.04**

Appendix 1. Argon isotopic data

ID	Temp (°C)	$^{40}Ar/^{39}Ar$	$^{37}Ar/^{39}Ar$	$^{36}Ar/^{39}Ar$ (x 10^{-3})	$^{39}Ar_K$ (x 10^{-15} mol)	K/Ca	$^{40}Ar^*$ (%)	^{39}Ar (%)	Age (Ma)	±1σ (Ma)
OT4-1270 groundmass, wt. = ~50 mg, J = 0.0001637, NMUM-6, Lab#=509-01										
B	*600*	*289.3*	*1.568*	*858.0*	*0.783*	*0.33*	*12.4*	*0.4*	*10.6*	*1.0*
C	*700*	*86.13*	*1.271*	*181.5*	*13.2*	*0.40*	*37.8*	*7.8*	*9.60*	*0.10*
D	*800*	*52.37*	*0.8832*	*70.25*	*31.1*	*0.58*	*60.4*	*25.1*	*9.330*	*0.045*
E	1000	35.00	0.8258	15.72	85.0	0.62	86.8	72.2	8.959	0.021
F	1200	34.65	0.9493	15.50	30.9	0.54	86.9	89.3	8.880	0.029
G	1400	53.46	6.856	79.23	19.2	0.074	57.1	100.0	9.043	0.057
total gas age			n=6		180.3	0.52			**9.07**	**0.08**
plateau		MSWD=4.1*	n=3	steps E-G	135.1	0.52		74.9	**8.94**	**0.04**
OT4-1280-1290 groundmass, wt. = ~50 mg, J = 0.0001646, NMUM-6, Lab#=517-01										
B	700	114.1	1.319	280.5	9.42	0.39	27.4	6.6	9.27	0.17
C	800	50.16	0.8962	64.36	29.9	0.57	62.2	27.5	9.243	0.049
D	900	39.54	0.8163	31.41	38.0	0.63	76.6	54.0	8.980	0.031
E	1000	30.83	0.8314	3.539	42.0	0.61	96.7	83.3	8.839	0.019
F	1200	32.42	0.9613	10.61	24.0	0.53	90.5	100.0	8.695	0.025
total gas age			n=5		143.4	0.58			**8.97**	**0.08**
no plateau										
PM5 810-820 groundmass, wt. = ~50 mg, J = 0.0014184, NM-38, Lab#=5540-01										
A	500	145.3	0.1934	483.9	3.85	2.6	1.6	1.4	6.0	3.1
B	600	27.70	0.2900	91.26	39.6	1.8	2.7	16.2	1.92	0.56
C	675	13.32	0.4171	42.64	77.5	1.2	5.6	45.0	1.91	0.26
D	750	9.221	0.8520	28.42	78.2	0.60	9.6	74.1	2.27	0.18
E	825	7.746	1.846	23.22	49.1	0.28	13.3	92.3	2.63	0.15
F	900	8.892	2.461	26.71	14.3	0.21	13.3	97.6	3.04	0.21
G	1000	11.71	3.696	37.48	3.32	0.14	7.8	98.8	2.35	0.47
J	1650	15.72	16.09	53.89	3.12	0.032	6.5	100.0	2.66	0.53
total gas age			n=8		269.1	0.89			**2.28**	**0.61**
plateau		MSWD=2.38*	n=8	steps A-J	269.1	0.89		100.0	**2.50**	**0.28**
PM5 900-910 groundmass, wt. = ~50mg, J = 0.0014183, NM-38, Lab#=5541-01										
A	500	177.6	0.1687	590.6	3.02	3.0	1.7	1.9	7.9	3.8
B	600	33.62	0.2725	111.5	29.7	1.9	2.0	20.3	1.74	0.70
C	675	18.41	0.4075	60.19	54.0	1.3	3.6	53.9	1.69	0.37
D	750	14.01	0.9795	43.86	46.9	0.52	8.1	83.1	2.89	0.28
E	825	11.44	2.922	35.22	19.8	0.17	11.0	95.5	3.23	0.25
F	900	12.52	5.862	40.28	4.58	0.087	8.5	98.3	2.74	0.39
G	1000	17.17	7.928	56.68	1.47	0.064	6.0	99.2	2.66	0.89
J	1650	29.93	27.37	102.5	1.24	0.019	5.8	100.0	4.5	1.3
total gas age			n=8		160.8	1.00			**2.41**	**0.94**
plateau		MSWD=2.56*	n=8	steps A-J	160.8	1.00		100.0	**2.77**	**0.47**

Appendix 1. Argon isotopic data

ID	Temp (°C)	$^{40}Ar/^{39}Ar$	$^{37}Ar/^{39}Ar$	$^{36}Ar/^{39}Ar$ (x 10^{-3})	$^{39}Ar_K$ (x 10^{-15} mol)	K/Ca	$^{40}Ar^*$ (%)	^{39}Ar (%)	Age (Ma)	±1σ (Ma)
PM5 1100-1110 groundmass, wt. = ~50 mg, J = 0.0014178, NM-38, Lab#=5542-01										
A	500	384.7	0.2886	1285.8	3.95	1.8	1.2	0.9	12.3	8.7
B	600	42.46	0.2928	141.3	20.5	1.7	1.7	5.6	1.85	0.82
C	675	19.77	0.3792	64.42	44.2	1.3	3.9	15.8	1.96	0.36
D	750	13.02	0.5532	40.69	58.5	0.92	8.0	29.3	2.66	0.24
E	825	10.05	0.9287	30.25	57.0	0.55	11.8	42.4	3.02	0.21
F	*900*	*12.47*	*0.9216*	*38.22*	*38.1*	*0.55*	*10.0*	*51.2*	*3.18*	*0.28*
G	*1000*	*20.83*	*0.6738*	*65.44*	*31.0*	*0.76*	*7.4*	*58.3*	*3.95*	*0.42*
H	*1100*	*37.28*	*0.3210*	*119.2*	*32.3*	*1.6*	*5.6*	*65.8*	*5.31*	*0.66*
I	*1300*	*57.97*	*0.6828*	*185.4*	*70.3*	*0.75*	*5.6*	*82.0*	*8.27*	*0.95*
J	*1650*	*34.18*	*0.4764*	*89.72*	*78.3*	*1.1*	*22.5*	*100.0*	*19.61*	*0.45*
total gas age			n=10		434.3	0.97			**7.0**	**1.1**
plateau		MSWD=2.24	n=5	steps A-E	184.3	1.02		42.4	**2.70**	**0.29**
PM5 2690-2700 groundmass, wt. = ~50 mg, J = 0.0014173, NM-38, Lab#=5543-01										
B	600	744.7	1.435	2465.6	2.21	0.36	2.2	0.9	41	13
C	675	176.4	1.357	578.8	4.95	0.38	3.1	2.9	14.0	3.1
D	750	130.8	1.120	424.3	10.3	0.46	4.2	7.2	13.9	2.2
E	825	160.0	1.046	521.4	17.4	0.49	3.8	14.4	15.3	2.6
F	900	56.68	0.9165	176.5	32.5	0.56	8.1	27.7	11.74	0.88
G	1000	19.97	1.263	53.44	33.8	0.40	21.4	41.7	10.90	0.29
H	1100	20.94	1.406	55.69	33.9	0.36	21.9	55.6	11.72	0.29
I	*1300*	*19.16*	*6.646*	*49.54*	*57.0*	*0.077*	*26.3*	*79.1*	*12.89*	*0.26*
J	*1650*	*15.55*	*3.375*	*22.97*	*50.8*	*0.15*	*58.0*	*100.0*	*22.98*	*0.16*
total gas age			n=9		242.9	0.30			**14.9**	**1.5**
plateau		MSWD=2.26	n=7	steps B-H	135.1	0.44		55.6	**11.39**	**0.40**

Notes:
Isotopic ratios corrected for blank, radioactive decay, and mass discrimination, not corrected for interferring reactions.
Individual analysis analytical error only; plateau,total gas, and isochron age errors include error in J.
All plateau, total gas and isochron errors are 2σ
n= number of heating steps
K/Ca = molar ratio calculated from reactor produced 39ArK and 37ArCa.
* outside 95% confidence interval

Irradiation	$(^{40}Ar/^{39}Ar)_K$	$(^{39}Ar/^{37}Ar)_{Ca}$	$(^{36}Ar/^{37}Ar)_{Ca}$	Reactor
NMUM-6	0.0225±0.0007	0.0007±0.00003	0.00026±0.00001	U. of Michigan
NM-38	0.0002±0.0003	0.0007±0.00005	0.00026±0.00002	Texas A&M
NM-77	0.0002±0.0003	0.00089±0.00003	0.00028±0.00001	Texas A&M
NM-93	0.0002±0.0003	0.0007±0.00005	0.00026±0.00002	Texas A&M
NM-127	0.0002±0.0003	0.00089±0.00003	0.00028±0.00001	Texas A&M

APPENDIX 2. DESCRIPTIONS UNDER BINOCULAR MICROSCOPE (BD), FIELD NOTES (FD), AND THIN SECTION NARRATIVES (TN) FOR SAMPLES OF MAFIC UNITS FROM THE PAJARITO PLATEAU

Locations are shown in Figure 2C and stratigraphic assignments are provided in Table 2. Workers are David P. Dethier (DPD), Giday WoldeGabriel (GWG), and Richard G. Warren (RGW).

Sample Number	bd fd tn	Worker	Date	Description
				Samples of outcrop from Bayo Canyon or Black Mesa
DEB5/98/1	BD	RGW	13-MAY-98	Outcrop sample is dark gray basalt with abundant feldspar laths 1.0 to 1.2 mm in length, with albite twinning apparent in wider laths. Black pyroxene to 0.6 mm is scarce.
DEB5/98/1	TN	RGW	19-AUG-2000	This polished thin section represents massive fine-grained pilotaxitic basalt with common to abundant plagioclase laths to 2 mm and common to abundant olivine to 1 mm. Smectite and some celadonite replace rims and fractures of olivine. Smectite also slightly replaces plagioclase. Common to abundant coarse magnetite and common fine acicular ilmenite are both unoxidized groundmass phases.
DN/97/7	TN	RGW	26-AUG-2000	This polished thin section represents slightly to moderately vesicular, coarse-grained pilotaxitic basalt. Scarce to common plagioclase (8%) grades into groundmass size. Common to abundant olivine (5%), almost entirely altered to iddingsite, grades into groundmass size. Only rims preserve relict olivine, far better in groundmass than in phenocrysts. Scarce to common groundmass magnetite (1%) is moderately to strongly exsolved, but common to abundant groundmass laths of ilmenite (1%) are unaltered. No lithics were observed.
DN/97/16	BD	RGW	26-AUG-2000	Outcrop sample is medium gray, medium grained basalt with scarce to common feldspar to 3 mm length, some with albite twins. Common vitreous mafics to 3 mm include very dark green olivine partly altered to iddingsite, very dark green clinopyroxene, and black orthopyroxene. Glomerocrysts of mafics with feldspar are up to 10 mm across. Groundmass olivine is partly altered to iddingsite. A white secondary mineral in 0.1 mm diameter globules, probably calcite, occurs pervasively throughout the groundmass.
DN/97/16	FD	DPD	03-JUL-97	Sample is grey basalt (?) rich in phenocrysts and phenocryst clots. Outcrop has pervasive vapor-phase alteration along cracks, and appears palagonitic below sample site. Basalt overlies Puye Fm and occurs beneath dacite cobble gravel (Quaternary?). Local outcrop pattern is obscure, but unit is exposed between elevations of 6300 and 6420 ft (?) on both sides of arroyo (upper Bayo Canyon) over a lateral distance of 250 to 300 m. Pattern suggests filled paleochannel trend was to SE. Excellent outcrop on N side of arroyo near boundary of Sections 17 and 16 exposes basalt (possible slide block) at ~6300 ft near arroyo level, covered by 25 m of massive medium sand, locally crossbedded, containing channels filled with volcanic pebble gravel. Sand is buff-colored, rich in rounded, frosted quartz grains. Sequence is capped and baked by basaltic flow >6 m thick. Massive sand is ancestral axial Rio Grande, though apparently greatly restricted in transport capacity. Upper (?) flow may correlate with sample at Section 16, since local contact dips to SW. Didn't walk out this contact to determine how far local dip extends.
DN/97/16	TN	RGW	26-AUG-2000	This polished thin section represents massive medium-grained pilotaxitic mugearite with abundant plagioclase (30%), many slightly to occasionally moderately resorbed, and in glomerocrysts to 10 mm2. Mafics are often very large clinopyroxene (5%), olivine (1.5%) that is partly altered to iddingsite, and orthopyroxene (0.2%). Groundmass olivine is also partly altered to iddingsite. Common groundmass magnetite (3%) is moderately to strongly oxidized and exsolved, but scarce to rare ilmenite (0.2%) forms tiny unoxidized groundmass laths. Large acicular groundmass apatite is evident.
RWTB4A14	BD	RGW	16-DEC-99	Sample is dark gray, coarse-grained pilotaxitic basic lava with scarce to common feldspar phenocrysts to 1.5 mm. Common olivine to 2 mm is strongly altered dark reddish brown. Scarce to common round vesicles to 1.2 mm are completely filled with massive pale olive clay, although one 3.5 mm round vesicle is completely filled with brownish calcite.
RWTB4A14	FD	GWG	17-OCT-98	Two flows are exposed within colluvium on a minor southern tributary of Bayo Canyon close to stream level. We sampled near the base of the upper flow. The 25 ft-thick upper flow is fine-grained, massive, jointed, spheroidally weathered, and moderately altered, with amygdules present in surface vesicles and calcite plates along joints. The base of the upper flow is clearly exposed above orange, partly oxidized vesicular basalt of the lower flow. The upper flow is also exposed well above stream level within northern slopes of Bayo Canyon, dips moderately to the southwest, and is faulted both to the east and west. Underlying sediment of the Santa Fe Group, sampled on a later date as RWTB4B5-7, is baked bright red below the upper flow on the northern slopes. Cliffs of upper flow bordering the stream on its northern side are about 40 ft thick, whereas the lower flow is not exposed there.
RWTB4A14	TN	RGW	17-MAY-2000	This polished section represents microporphyritic basalt with common olivine phenocrysts thickly rimmed with iddingsite. Scarce plagioclase phenocrysts are zoned and resorbed. Groundmass pyroxene is medium grained intergranular clinopyroxene. Minor smectite and a trace of celadonite lightly coat to fill scattered vesicles.

APPENDIX 2. DESCRIPTIONS UNDER BINOCULAR MICROSCOPE (BD), FIELD NOTES (FD), AND THIN SECTION NARRATIVES (TN) FOR SAMPLES OF MAFIC UNITS FROM THE PAJARITO PLATEAU (continued)

Locations are shown in Figure 2C and stratigraphic assignments are provided in Table 2. Workers are David P. Dethier (DPD), Giday WoldeGabriel (GWG), and Richard G. Warren (RGW).

Sample Number	bd fd tn	Worker	Date	Description
RWTB4A15	BD	RGW	16-DEC-99	Sample is dark brownish gray, moderately to highly vesicular, fine-grained pilotaxitic basic lava with oblate vesicles to 15/7 mm. Feldspar phenocryst prisms to 4.5 mm are common, some with albite twins. Common mafics include yellow green to black olivine to 2 mm and black clinopyroxene to 1.5 mm which is often intergrown with feldspar phenocrysts. A few vesicles contain spotty coatings of medium granular calcite.
RWTB4A15	FD	GWG	17-OCT-98	Two flows are exposed within colluvium on a minor southern tributary of Bayo Canyon close to stream level. We sampled 5 ft below the top of the lower flow, where 15 ft of vesicular, moderately altered, fine-grained basalt is exposed, but covered below. Top part of flow is baked orange from overlying flow.
RWTB4A15	TN	RGW	17-MAY-2000	This polished section represents medium grained pilotaxitic and cryptocrystalline mugearite with common to abundant large plagioclase phenocrysts, some strongly resorbed. Common mafics are clinopyroxene, olivine, and orthopyroxene. Olivine is mostly altered to iddingsite and orthopyroxene has reacted with matrix, but is intergrown with both clinopyroxene and olivine. Smectite thinly lines some voids.
RWTB4B8	BD	RGW	15-DEC-99	Sample is very light gray vitric massive ash with rare lithics to 0.3 mm. A single 0.3 mm hornblende was observed.
RWTB4B8	FD	RGW	24-JUL-99	A 15 cm-thick gravel with abundant, well-rounded pebbles derived from lavas of the Tschicoma Formation overlies the sandstone sampled as RWTB4B9. Above this gravel, we sampled from the middle of a 120 cm-thick massive gray vitric ash. The ash is overlain by a 120 cm-thick silty claystone with scattered pebbles, and then successively overlain by a 2.4 m-thick deposit of coarse gravel with clasts to 50 cm.
RWTB4B8	TN	RGW	19-MAY-2000	This polished section contains vitric shardy ash fall, mostly well formed colorless shards, but with rare brown shards. Scarce felsic phenocrysts are mostly plagioclase, with minor quartz derived from non-volcanic sources. Scarce to rare mafics are mostly clinopyroxene with lesser hornblende, orthopyroxene, and singly highly shreddy biotite. Scarce lithics are mostly plagioclase-bearing dacite lava, some containing hornblende, and dark to opaque pilotaxitic and argillic lava with clinopyroxene, probably basalt or mugearite.
RWTB4B10	BD	RGW	15-DEC-99	Sample is very pale orange vitric pumice. Several green clinopyroxenes to 1 mm were observed. Five individual pumices were pulverized for chemical and mineralogical analysis.
RWTB4B10	FD	RGW	24-JUL-99	We sampled the largest available pumices from a plinian deposit that overlies the sequence described for sample RWTB4B8. This plinian appears identical to the deposit sampled as RWTB4B10, although here it is very strongly calcite-cemented. The very solid plinian is about 1 m thick here, with a channel incised into its upper surface.
RWTB4B10	TN	RGW	20-FEB-2001	This polished section contains a single glassy and argillic fine tube colorless pumice with scarce, and felsic phenocrysts of generally very highly resorbed plagioclase, a single large quartz, and two small grains of sanidine. Scarce mafics are clinopyroxene and orthopyroxene. Smectite thinly and discontinuously coats the largest vesicle.
RWTB4B14	BD	RGW	15-DEC-99	Sample is pumice fall, mostly vitric, light gray pumice containing scarce prisms of black orthopyroxene and much lesser green clinopyroxene, both to 1 mm. Scarce to common lithics are mostly devitrified lava.
RWTB4B14	FD	RGW	24-JUL-99	On the north side of an unnamed canyon between Los Alamos and Bayo Canyons, downstream from Late Miocene basalt sampled as DN/97/7 and upstream from basalt sampled as RWTB4B13, we sampled a 10 cm-thick plinian deposit. A 30 cm-thick plinian layer overlies this layer of coarse pumice.
RWTB4B14	TN	RGW	20-FEB-2001	This polished section contains an agglutinate of glassy fine tube colorless pumice with common plagioclase phenocrysts, and common pyroxene, mostly orthopyroxene. Scarce to rare lithics of dacite lava and hydrothermally altered lava are found between pumice clasts, Much of the voids between pumice clasts have been filled with smectite. X-ray diffraction analysis reveals minor dolomite, and a trace of vapor phase mineralization.
Samples of outcrop from western Pajarito Plateau				
DN/97/17B	BD	RGW	12-FEB-98	Sample consists of blocks to 60 mm of very light gray vitric pumice from outcrop. Very abundant mafics are mostly black to highly bronze biotite to 3 mm and lesser black to dark brown orthopyroxene prisms to 2 mm. Feldspar to 2 mm is evident.
DN/97/17B	TN	RGW	26-AUG-	This polished thin section represents a single argillic and vitric fine tube colorless pumice with common felsic phenocrysts (10%), entirely

APPENDIX 2. DESCRIPTIONS UNDER BINOCULAR MICROSCOPE (BD), FIELD NOTES (FD), AND THIN SECTION NARRATIVES (TN) FOR SAMPLES OF MAFIC UNITS FROM THE PAJARITO PLATEAU (continued)

Locations are shown in Figure 2C and stratigraphic assignments are provided in Table 2. Workers are David P. Dethier (DPD), Giday WoldeGabriel (GWG), and Richard G. Warren (RGW).

Sample Number	bd fd tn	Worker	Date	Description
			2000	plagioclase (98%) except for a single large quartz grain (2%). Most plagioclase, some large, bears strongly resorbed rims. Abundant mafics (1.5%) are dominantly hornblende (80%), much lesser biotite (20%), and a single orthopyroxene (150 ppmV) mantled by hornblende. Scarce magnetite (0.1%) is unoxidized. No lithics were observed.
DN/97/19A	BD	RGW	12-FEB-98	Sample consists of fragments to 65 mm of light gray vitric pumice from outcrop. Scarce to rare vitreous mafics to 1 mm include very light green clinopyroxene and black orthopyroxene.
DN/97/19A	TN	RGW	15-NOV-99	This polished thin section represents a single vitric pumice with fine tube walls. Common plagioclase occurs mostly as microphenocrysts and as lesser phenocrysts, many very strongly resorbed. Common mafics are mostly orthopyroxene, with minor clinopyroxene.
LAPC98/12	TN	RGW	23-JUL-2000	This polished thin section represents pilotaxitic and microgranophyric lava with vapor phase minerals in small, scattered vesicles. Common felsic phenocrysts of quartz (60%) and plagioclase (40%) occur mostly as very large grains. Most grains of quartz are rounded and some are wormy; many grains of plagioclase have fine, intense reaction rims. Common mafics are mostly strongly reacted and often-blackened biotite and pseudomorphic hornblende, but include a single grain of altered clinopyroxene. Partly altered highly prismatic orthopyroxene is ubiquitous within groundmass. Scarce magnetite is unaltered to moderately oxidized. Five grains of sphene observed are all partly altered, armored with hematite. Several grains of apatite were observed in association with magnetite, biotite, and hornblende; a single grain of zircon was observed. No lithics were observed.
LAPC98/13	TN	RGW	23-JUL-2000	This polished thin section represents pilotaxitic and microgranophyric lava with minor vapor phase minerals in small, scattered vesicles. Scarce to common felsic phenocrysts of quartz (50%) and plagioclase (50%) occur generally as very large grains. Most grains of quartz are rounded and some are wormy; many grains of plagioclase have fine, intense reaction rims. Mafics include common to abundant biotite, mostly represented by three very large grains, scarce pseudomorphic hornblende, and single partly altered grains of equant clinopyroxene and highly prismatic orthopyroxene. Partly altered highly prismatic pyroxene, ubiquitous within groundmass, is almost entirely orthopyroxene but includes minor clinopyroxene. Scarce magnetite is unaltered to slightly altered. Accessories observed include five grains of sphene, and several grains of apatite and two grains of zircon that are both associated with magnetite and biotite. No lithics were observed.
Samples of outcrop from White Rock Canyon at mouth of Ancho Canyon (chemical analyses in WoldeGabriel et al., 1996)				
SLR/93/1	BD	RGW	04-AUG-97	Outcrop sample is brownish gray basalt with abundant chalky, partly altered feldspar to 8 mm and common, partly altered very dark green clinopyroxene to 3 mm and iddingsite after olivine to 2 mm.
Samples of cuttings or core from drill holes				
OT4-310D	TN	RGW	01-MAR-99	This polished thin section consists of fragments of bulk cuttings, typically 1 to 2 mm in long dimension, to a maximum of 4 mm. Most fragments are medium-grained pilotaxitic basalt with scarce to common phenocrysts of plagioclase and olivine. Most fragments of basalt are holocrystalline. Fragments of partly vitric basalt have mineralogy similar to holocrystalline basalt, and thus probably represent the margin of the same flow or perhaps subordinate clasts within a flow breccia. About 12% of the cuttings are fragments of dacite lava of Tschicoma Formation, which represent contamination from clasts within the overlying Puye Fanglomerate. The dacite fragments contain substantial quartz, and appear similar to dacite of Caballo Mountain. Other fragments of contaminant include argillite and silty argillite, the latter containing clasts of the subject basalt, and both displaying lithologies characteristic of Old Alluvium rather than overlying Puye Fanglomerate.
OT4-1210D	TN	RGW	03-MAR-99	This polished thin section consists of more than 100 fragments of bulk cuttings with a maximum long dimension of 7 mm. All fragments are pilotaxitic basalt with phenocrysts of abundant plagioclase, mostly microphenocrysts, and common to abundant olivine. The largest plagioclase phenocrysts have strongly resorbed cores, and the largest olivine phenocrysts are completely altered to iddingsite. A single, very large clinopyroxene phenocryst is intergrown with plagioclase, and many medium-sized olivine phenocrysts are also intergrown with plagioclase. Much of the basalt is finely granulated. No alteration or veining is associated with the granulation, indicating an origin from flow brecciation.

APPENDIX 2. DESCRIPTIONS UNDER BINOCULAR MICROSCOPE (BD), FIELD NOTES (FD), AND THIN SECTION NARRATIVES (TN) FOR SAMPLES OF MAFIC UNITS FROM THE PAJARITO PLATEAU (continued)

Locations are shown in Figure 2C and stratigraphic assignments are provided in Table 2. Workers are David P. Dethier (DPD), Giday WoldeGabriel (GWG), and Richard G. Warren (RGW).

Sample Number	bd fd tn	Worker	Date	Description
OT4-1280D	TN	RGW	06-MAR-99	All fragments in this polished thin section are coarse-grained pilotaxitic basalt with large phenocrysts of abundant clinopyroxene and plagioclase, and smaller phenocrysts of scarce to common olivine that is entirely altered to iddingsite and clay. A few plagioclase phenocrysts are resorbed. Scarce orthopyroxene included within clinopyroxene is partly altered to clay and strongly reacted with groundmass, showing reaction rims with abundant iddingsite after groundmass olivine. Massive clay associated with orthopyroxene is associated with sparry calcite and contains vapor-phase biotite, demonstrating that the alteration is deuteric. Acicular apatite is conspicuous in groundmass.
OT4-1300D	BD	RGW	14-SEP-98	Washed cuttings from 1290 to 1300 ft depths in drill hole OT4, treated with 10% nitric acid, are fragments to 6 mm. Cuttings are mostly dark grayish brown, fine-grained, massive basalt with common, very conspicuous feldspar laths to 2 mm. Common black to very dark green clinopyroxene to 1.5 mm and scarce iddingsite after olivine to 1 mm are intergrown in a few grains. Cuttings are slightly contaminated with fragments to 6 mm of gray, devitrified dacite lava, quartzite, and sandstone. These contaminants have been removed from samples submitted for laboratory analyses.
OT4-1470D	TN	RGW	20-MAR-99	This polished thin section consists of small fragments of bulk cuttings, with few fragments >1 mm in long dimension. Most fragments are large free felsic crystals and dacite fragments, and about 15% are medium grained pilotaxitic mugearite with phenocrysts of scarce olivine and plagioclase, and rare clinopyroxene, and relatively large, abundant groundmass magnetite. Fragments of microporphyritic basalt may represent a different lithology of this basaltic rock, or more likely different basalt. Fragments also include granite and quartzite. This assemblage of fragments probably represents a conglomeratic fluvial deposit of the ancestral Rio Grande.
PM5-820D	BD	RGW	10-FEB-98	Handpicked cuttings from 810 to 820 ft depths in drill hole PM5 are fragments to 12 mm. These fragments are dark gray medium-grained microvesicular basalt with rare very light green olivine. Occasional fragments of massive basalt are oxidized dark reddish brown.
PM5-820D	TN	RGW	21-MAR-99	This polished thin section displays about 40 fragments of hand picked cuttings of vitric pilotaxitic lava. Glass is brown, microlite-charged. Scarce microphenocrysts are equant to prismatic pyroxene, with the larger grains almost entirely orthopyroxene. Scarce to rare reaction rims of clinopyroxene surround voids within microlite-poor glass and some orthopyroxene. A single sandy argillite fragment of Santa Fe Group contaminates this sample.
PM5-910D	BD	RGW	10-FEB-98	Handpicked cuttings from 900 to 910 ft depths in drill hole PM5 are fragments to 11 mm. These fragments are medium dark gray to dark reddish gray massive to slightly microvesicular basalt with rare feldspar to 1 mm and olivine to 0.8 mm.
PM5-910D	TN	RGW	21-MAR-99	This polished thin section displays 23 fragments from hand picked cuttings of vitric pilotaxitic lava with subequal pale brown glass and tiny feldspar groundmass laths. Vesicles in some fragments contain tiny aggregates of equigranular vapor phase minerals, probably cristobalite. Scarce microphenocrysts are equant to prismatic pyroxene, with the larger grains almost entirely orthopyroxene. A single phenocryst of plagioclase is present. A single, very large pseudomorph consists of an opaque sponge of clinopyroxene and magnetite that have replaced hornblende in a magmatic reaction.
PM5-1010D	BD	RGW	11-SEP-98	Handpicked cuttings from 1000 to 1010 ft depths in drill hole PM5 are fragments to 6 mm. These fragments are dark gray vitric and lesser devitrified lava with common dark green clinopyroxene and brown orthopyroxene, both mostly equant, but some in prisms to 1.2 mm, and scarce to common feldspar, some resorbed.
PM5-1110D	BD	RGW	10-FEB-98	Handpicked cuttings from 1100 to 1110 ft depths in drill hole PM5 are fragments to 7 mm. Some dark gray fragments contain light green olivine. Some light gray fragments also contain olivine and resemble the basalt of sample PM5-910D, but other light gray fragments may be dacite. Remnant fragments from those selected for age dating are mostly light gray fragments. These fragments are medium dark gray vitric to medium gray crystalline basalt with conspicuous feldspar.
PM5-1110D	TN	RGW	13-AUG-2000	This polished thin section represents 33 fragments, many very small, of pilotaxitic lava. Most fragments are also microgranophyric and minor granospherulitic, but some are vitric. Scarce to common plagioclase generally forms small, blocky phenocrysts, with the largest grain strongly resorbed. Common to abundant mafics are orthopyroxene, clinopyroxene, and much lesser opaque pseudomorphic hornblende, with the largest clinopyroxene strongly resorbed. Scarce to rare magnetite is slightly oxidized and gradational into groundmass.
PM5-1790D	BD	RGW	11-FEB-98	Handpicked cuttings from 1780 to 1790 ft depths in drill hole PM5 are fragments to 2.5 mm. These fragments are mostly black vitric and

APPENDIX 2. DESCRIPTIONS UNDER BINOCULAR MICROSCOPE (BD), FIELD NOTES (FD), AND THIN SECTION NARRATIVES (TN) FOR SAMPLES OF MAFIC UNITS FROM THE PAJARITO PLATEAU (continued)

Locations are shown in Figure 2C and stratigraphic assignments are provided in Table 2. Workers are David P. Dethier (DPD), Giday WoldeGabriel (GWG), and Richard G. Warren (RGW).

Sample Number	bd fd tn	Worker	Date	Description
				minor pale reddish brown devitrified lava with rare feldspar to 1 mm and very dark green prismatic clinopyroxene to 2 mm.
PM5-1790D	TN	RGW	13-AUG-2000	This polished thin section represents more than 100 small fragments, mostly slightly vesicular vitric and pilotaxitic lava with brown glass and common plagioclase that mostly forms small, blocky phenocrysts. Common mafics are clinopyroxene, orthopyroxene, and lesser hornblende. Several fragments of coarse-grained pilotaxitic basalt and one fragment with large biotite are caved from overlying intervals.
PM5-1900D	BD	RGW	10-FEB-98	Handpicked cuttings from 1890 to 1900 ft depths in drill hole PM5 are fragments to 3 mm. These fragments are grayish black basalt with common olivine that is partly altered to iddingsite and greenish clay. Scarce small vesicles are filled with greenish clay.
PM5-1900D	TN	RGW	21-MAR-99	This polished thin section consists of approximately 150 fragments of hand picked cuttings, mostly coarse-grained holocrystalline basalt that seems to grade to microporphyritic in some fragments and fine-grained in others, with all lithologies petrographically similar. The basalt has phenocrysts of common olivine, almost entirely altered to iddingsite, and scarce to common plagioclase, slightly altered to smectite, which fills most vesicles. An earlier generation of smectite forms fibrous rosettes with higher birefringence than later, more massive smectite. About 15% of the fragments in this section are dacite lava of the Tschicoma Formation; many are vitric, and all are certainly caved from the overlying Puye Fanglomerate.
PM5-2050D	BD	RGW	11-FEB-98	Handpicked cuttings from 2040 to 2050 ft depths in drill hole PM5 are fragments to 2 mm. These fragments are mostly grayish black vitric and partly dark reddish brown spherulitic lava with conspicuous feldspar to 2 mm. One 1 mm long black orthopyroxene prism was observed.
PM5-2050D	TN	RGW	13-AUG-2000	This polished thin section represents more than 100 small fragments, all slightly vesicular, vitric and minor microgranophyric pilotaxitic lava with brown glass. Common plagioclase phenocrysts include many that are moderately resorbed. Common to abundant mafics are clinopyroxene and orthopyroxene. Common magnetite is moderately oxidized and moderately exsolved, but scarce ilmenite is unaltered.
PM5-2190D	BD	RGW	10-FEB-98	Handpicked cuttings from 2180 to 2190 ft depths in drill hole PM5 are fragments to 3 mm. These fragments are dark gray coarse-grained basalt with scarce olivine to 1 mm, partly altered to iddingsite at rims and to green clay in cores. Very abundant olivine microphenocrysts are conspicuous. Voids are filled with light green clay.
PM5-2190D	TN	RGW	13-AUG-2000	This polished thin section represents more than 100 small fragments, mostly slightly to moderately vesicular argillic coarse-grained pilotaxitic basalt. Smectite fills vesicles, but coarse calcite fills a single vesicle. Scarce to common olivine phenocrysts are entirely altered to iddingsite. Common to abundant plagioclase microphenocrysts, mostly laths slightly larger than coarse groundmass, are slightly to strongly replaced by smectite, with the alteration intensity strongly variable among individual fragments. Groundmass clinopyroxene is unaltered, even within the most highly altered fragments. Fragments of vitric and minor microgranophyric pilotaxitic lava with brown glass constitute 15% of the fragments. These vitric fragments contain common plagioclase phenocrysts and common to abundant mafics of clinopyroxene and orthopyroxene; they are identical to fragments of sample PM5-2050D, and are caved from that interval. Other single fragments caved from uphole are medium-grained pilotaxitic and cryptocrystalline basalt with unaltered olivine, and cryptocrystalline basalt with common, small plagioclase phenocrysts and common iddingsite after olivine phenocrysts.
PM5-2240D	BD	RGW	10-FEB-98	Handpicked cuttings from 2230 to 2240 ft depths in drill hole PM5 are fragments to 3 mm. These fragments are blackish gray fine-grained basalt with large conspicuous feldspar and vitreous olivine. Some clay thinly coats fractures and vesicles.
PM5-2240D	TN	RGW	13-AUG-2000	This polished thin section represents nine fragments; eight are moderately vesicular fine-grained pilotaxitic basalt. Phenocrysts include scarce to common but generally very large olivine, completely replaced by smectite or iddingsite, scarce but generally large clinopyroxene, and scarce to rare plagioclase in laths to 0.5 mm. Smectite partly fills vesicles, and large vesicles in one fragment are lined with extremely coarse heulandite, with single grains >0.1 mm2. The ninth fragment represents a massive medium-grained pilotaxitic mugearite with phenocrysts of abundant, very large clinopyroxene, scarce to common iddingsite after olivine, and scarce to common plagioclase, and including a single grain of orthopyroxene.
PM5-2440D	BD	RGW	11-FEB-98	Handpicked cuttings from 2430 to 2440 ft depths in drill hole PM5 are fragments to 12 mm. These fragments are brownish gray coarse-grained basalt with common olivine pseudomorphs to 3 mm, cores replaced by clay and rims replaced by iddingsite, scarce to common very dark green clinopyroxene to 4 mm, some intergrown with olivine, and common feldspar to 1.5 mm. Vesicles are partly to completely filled with coarse drusy quartz and with soft white mineral, probably calcite.

APPENDIX 2. DESCRIPTIONS UNDER BINOCULAR MICROSCOPE (BD), FIELD NOTES (FD), AND THIN SECTION NARRATIVES (TN) FOR SAMPLES OF MAFIC UNITS FROM THE PAJARITO PLATEAU (continued)

Locations are shown in Figure 2C and stratigraphic assignments are provided in Table 2. Workers are David P. Dethier (DPD), Giday WoldeGabriel (GWG), and Richard G. Warren (RGW).

Sample Number	bd fd tn	Worker	Date	Description
PM5-2440D	TN	RGW	21-MAR-99	This polished thin section consists of approximately 100 fragments of hand picked cuttings, all mugearite except for a single contaminating fragment of dacite lava of Tschicoma Formation, certainly caved from the overlying Puye Fanglomerate. Except for two fragments, the mugearite is hypocrystalline with glass completely altered to smectite, phenocrysts of common plagioclase and clinopyroxene, and scarce olivine completely altered to iddingsite. Plagioclase is slightly altered to smectite, especially at cores. Two generations of smectite pervasively fill vesicles; earlier smectite forms fibrous rosettes with higher birefringence than later, more massive smectite. Two fragments are slightly hypocrystalline, coarse grained, but seem to represent a different lithology of the same mugearite rather than a different basalt.
PM5-2640D	BD	RGW	14-SEP-98	Ultrasonically cleaned cuttings >2 mm that are retained on a 10 mesh sieve are from 2630 to 2640 ft depths in drill hole PM5. Cuttings are mostly fragments of brownish gray, argillic basalt to 20 mm. Light greenish clay replaces abundant laths of feldspar microphenocrysts to 1 mm, and fills scattered, round vesicles to 4 mm. Olivine pseudomorphs of clay and iddingsite to 2 mm are common to abundant. Cuttings are somewhat contaminated with fragments of unaltered basalt and red sandstone that have been removed from samples submitted for laboratory analyses.
PM5-2700D	BD	RGW	11-FEB-98	Handpicked cuttings from 2690 to 2700 ft depths in drill hole PM5 are fragments to 10 mm. These fragments are dark gray coarse-grained basalt with scarce to common olivine to 2 mm that has light green cores where unaltered, but which is completely altered to greenish clay in some fragments. White drusy quartz occurs in veins to 2.5 mm thick.
PM5-2700D	TN	RGW	27-MAR-99	This polished thin section displays 27 fragments from hand picked cuttings of microporphyritic basalt. Coarse groundmass phases are primarily unaltered clinopyroxene, unaltered to slightly altered feldspar laths, primarily plagioclase, and slightly to strongly altered olivine. Most fragments are unaltered to slightly argillic, but one brecciated fragment is strongly argillic. Prominent calcite is confined to thick veins. Phenocrysts of olivine are common, with alteration ranging from slight, with iddingsite rims in most fragments, to complete in the most strongly altered fragments. Scarce microphenocrysts of plagioclase overlap in size with the largest groundmass grains. Plagioclase is unaltered in most fragments, but some laths are mostly or entirely altered to smectite in the most altered fragments.
PM5-2740D	BD	RGW	14-SEP-98	Washed cuttings are from 2730 to 2740 ft depths in drill hole PM5. Cuttings are mostly fragments of light brownish gray, argillic basalt to 19 mm. Light greenish gray clay replaces abundant laths of feldspar microphenocrysts to 1 mm, and fills scattered, round to ovoid vesicles to 6 mm. Olivine pseudomorphs of clay and iddingsite to 2 mm are common. Cuttings are somewhat contaminated with fragments of very coarsely crystalline quartz to 7 mm with associated sparry calcite, and scarce red sandstone that have been removed from samples submitted for laboratory analyses.
R9-50.5D	BD	RGW	05-NOV-97	Unwashed cuttings from 41 to 50.5 ft depths in drill hole R9 are fragments of generally massive dark gray basalt to 15 mm, and occasionally to 40 mm. The basalt contains scattered vesicles to 1 mm, scarce to common pale olive olivine to 1.4 mm, and scarce to rare prismatic feldspar to 1.5 mm.
R9-92D	BD	RGW	25-AUG-98	Ultrasonically cleaned cuttings from 90 to 92 ft depths in drill hole R9 are dark gray, fine-grained basalt with common ovoid vesicles to 11 mm, scarce to common olive olivine to 2.5 mm, and scarce feldspar laths to 1 mm.
R9-92D	TN	RGW	12-MAR-99	This polished thin section consists of four large fragments of cuttings, all medium-grained hypocrystalline pilotaxitic basalt with phenocrysts of common olivine and scarce plagioclase. Olivine and pyroxene in groundmass, presumed all to be clinopyroxene, are distinguishable by a slightly higher reflectance and generally slight alteration to iddingsite for olivine. Scarce Fe-Ti oxides all occur as groundmass phases, including tiny ilmenite prisms and much more abundant, highly skeletal magnetite. Granular spinel inclusions within olivine phenocrysts are relatively large. Intergranular brown glass is partly devitrified along grain boundaries to a cryptocrystalline assemblage of basaltic minerals. Smectite completely fills smaller vesicles, those with diameters of about 0.1 mm, but large vesicles, with diameters >1 mm, are thinly lined with smectite. Olivine rims are thinly altered to iddingsite, and large voids within olivine are usually completely filled with smectite, clearly associating the slight alteration with smectite.
R9-122D	BD	RGW	09-FEB-98	This sample of washed and ultrasonically cleaned cuttings to 25 mm, from 121 to 122 ft depths in drill hole R9, is medium dark gray, medium-grained, moderately vesicular basalt with scarce to common vesicles that range from round to 1 mm to very elongate to 6/1 mm. Mafics are scarce pale olive olivine to 1.5 mm and pale brownish black pyroxene rhombs that might be pigeonite. Feldspar, to 0.6 mm, is very rare.

APPENDIX 2. DESCRIPTIONS UNDER BINOCULAR MICROSCOPE (BD), FIELD NOTES (FD), AND THIN SECTION NARRATIVES (TN) FOR SAMPLES OF MAFIC UNITS FROM THE PAJARITO PLATEAU (continued)

Locations are shown in Figure 2C and stratigraphic assignments are provided in Table 2. Workers are David P. Dethier (DPD), Giday WoldeGabriel (GWG), and Richard G. Warren (RGW).

Sample Number	bd fd tn	Worker	Date	Description
R9-122D	TN	RGW	16-MAR-99	This polished thin section consists of three large fragments of cuttings, all medium-grained hypocrystalline, ophitic basalt with common phenocrysts of olivine and rare microphenocrysts of plagioclase. Olivine and clinopyroxene in groundmass are distinguishable by the generally dusky brown color of clinopyroxene and slightly higher reflectance and generally slight alteration to iddingsite for olivine. Scarce Fe-Ti oxides all occur as groundmass phases, including tiny ilmenite prisms and more abundant magnetite. Intergranular brown glass is partly devitrified along grain boundaries to a cryptocrystalline assemblage of basaltic minerals. Minor smectite partly fills some vesicles.
R9-162D	BD	RGW	25-AUG-98	Ultrasonically cleaned cuttings from 160 to 162 ft depths in drill hole R9 are medium dark gray, massive, coarse-grained basalt with common olive olivine to 3 mm. A few surfaces, which probably represent fractures, are thinly coated with moderate orange pink clay.
R9-162D	TN	RGW	04-APR-99	This polished thin section consists of four fragments of cuttings, all medium grained ophitic basalt with common phenocrysts of olivine. Rare microphenocrysts of plagioclase could also be classified as the largest groundmass plagioclase. Smectite mostly fills vesicles and slightly replaces some olivine.
R9-181.3	BD	RGW	10-NOV-97	Core from 281.2 to 281.3 ft depths in drill hole R9 is light brownish gray vesicular basalt with common, generally slightly ovoid vesicles to 10/5 mm diameters. Near vertical fracture surface that has split off about 10% of core piece is heavily coated with light brown authigenic clay. Common, completely unaltered olivine indicates a complete lack of secondary alteration of basalt. Feldspar is scarce to common as prisms to 1 mm.
R9-201.5	BD	RGW	06-NOV-97	Core from 201.2 to 201.5 ft depths in drill hole R9 is medium dark gray massive basalt with scattered, aligned ovoid vesicles to 4/1 mm. Scarce to rare feldspar occurs to 1 mm, and scarce to common pale olive to dark olive olivine to 3 mm, strongly locally altered to iddingsite, probably in association with fractures that are thickly coated with moderate orange pink authigenic clay.
R9-219	BD	RGW	22-DEC-97	Core from 218.8 to 219.0 ft depths in drill hole R9 is brownish gray vesicular basalt, pervasively coated with pinkish gray to moderate reddish brown clay. In thick accumulations, the clay is laminated, with the darker color towards the interior of the clay deposit. Black dendrites of manganese oxides thinly and spottily coat some clay.
R9-228	BD	RGW	06-NOV-97	Core from 227.7 to 228.0 ft depths in drill hole R9 is medium dark gray basalt with rare, somewhat ovoid vesicles to 6/3.5 mm. Olive olivine to 1.5 mm is common; no feldspar was observed. Some fractures and vesicles are thickly coated with very pale orange pink authigenic clay.
R9-228.2	BD	RGW	22-DEC-97	Core from 228.0 to 228.2 ft depths in drill hole R9 is mostly massive medium gray basalt with scarce unaltered pale olive olivine to 1.5 mm. The few irregular elongate vesicles to 16 mm that occur are filled with moderate orange pink and much lesser moderate reddish brown clay. These clays are laminated in part; the darker color always occurs at the top of the deposit. Dendrites of manganese oxides spottily coat interior surfaces of clay.
R9-257.6	BD	RGW	06-NOV-97	Core from 257.2 to 257.6 ft depths in drill hole R9 is medium light gray basalt with rare round vesicles to 3.5 mm, and common light green olivine to 3 mm. No feldspar was observed. A 40/17 mm clast of very light gray quartzite at 257.3 ft depth is equigranular, with grains mostly 1 to 3 mm diameter.
R9-273.7	BD	RGW	05-NOV-97	Core from 273.3 to 273.7 ft depths in drill hole R9 is massive medium gray basalt with scarce to common pale olive olivine to 2 mm. No feldspar phenocrysts were observed.
R9-281.8	BD	RGW	10-NOV-97	Core from 281.5 to 281.8 ft depths in drill hole R9 is dark gray basalt with common very light green olivine to 5 mm. Irregular fracture 2 to 6 mm wide is partly filled with brecciated basalt, but mostly with moderate orange pink authigenic clay. This fracture dips 68 degrees, and is terminated by another irregular fracture that dips 15 degrees.
R9-282.2	BD	RGW	06-NOV-97	Core from 282.0 to 282.2 ft depths in drill hole R9 is dark gray, well sorted basaltic ash, mostly subangular hydroclastic shards of basalt, scarce felsics, and rare lithics, all mostly 0.1 to 0.5 mm diameter.
R9-282.2	TN	RGW	22-OCT-2000	This polished thin section represents massive vitric shardy basaltic ash with abundant shards and scoria, both brown in plane light. Groundmass plagioclase is generally scarce within individual scoria. Within matrix, unaltered olivine phenocrysts (3%) are common and dominant, generally have adhering brown shards, and often contain nearly opaque inclusions of spinel. Rare felsic crystals (0.4%) include equal abundances of quartz and plagioclase. Quartz invariably displays wavy extinction indicating xenocrystic derivation entirely from nonvolcanic sources; much plagioclase has sericitic alteration, suggesting similar nonvolcanic sources, but some plagioclase grains certainly

APPENDIX 2. DESCRIPTIONS UNDER BINOCULAR MICROSCOPE (BD), FIELD NOTES (FD), AND THIN SECTION NARRATIVES (TN) FOR SAMPLES OF MAFIC UNITS FROM THE PAJARITO PLATEAU (continued)

Locations are shown in Figure 2C and stratigraphic assignments are provided in Table 2. Workers are David P. Dethier (DPD), Giday WoldeGabriel (GWG), and Richard G. Warren (RGW).

Sample Number	bd fd tn	Worker	Date	Description
				represent phenocrysts. Rare magnetite (100 ppmV) is generally strongly oxidized, and a single grain of ilmenite observed (5 ppmV) is slightly altered. Rare, generally moderately well rounded lithics include microgranophyric lava, one included within a brown shard, axiolitic welded tuff, and medium-grained basalt.
R9-282.6	BD	RGW	10-NOV-97	Core from 282.4 to 282.6 ft depths in drill hole R9 is very dark yellowish brown, poorly sorted basaltic tephra, mostly ash but with scarce to common black basaltic shards, many in elongate pumiceous forms to 8/2 mm diameters. Generally very irregular vesicles are completely filled with clay; common to abundant clay fillings to 12/2 mm diameters are very pale orange at top of interval, grading down to scarce to common clay fillings to 3/2 mm diameters at base. Lowermost several mm of core piece is basaltic ash described for sample R9-282.8; contact between the two layers is horizontal, with undulations of 2 mm.
R9-285.5	BD	RGW	06-NOV-97	Core from 285.3 to 285.5 ft depths in drill hole R9 is light olive gray well sorted basaltic ash, mostly 0.1 to 0.3 mm, mostly subangular black hydroclastic shards of basalt, and common felsics. Scarce to rare white globules of white secondary mineral are probably calcite.
R9-285.5	TN	RGW	22-OCT-2000	This polished thin section represents massive vitric shardy basaltic ash with abundant shards and scoria, both pale brown in plane light. Ash enrichment defines faint layering best displayed by a layer that is 2 mm wide. Groundmass plagioclase varies from scarce to abundant within individual scoria. Within matrix, unaltered olivine phenocrysts (3%) are common and dominant, generally have adhering pale brown shards, and often contain abundant nearly opaque inclusions of spinel. Rare felsic crystals (0.3%) include quartz (0.2%) and plagioclase (0.1%). Quartz invariably displays wavy extinction and/or contains abundant fluid inclusions, indicating xenocrystic derivation entirely from nonvolcanic sources, but plagioclase includes grains with sericitic alteration, suggesting similar nonvolcanic sources, and prismatic grains that certainly represent phenocrysts. The only Fe-Ti oxide grain observed was a single, tiny highly oxidized magnetite. Rare, generally moderately well rounded lithics (0.1%) include argillic basalt, probably Miocene, microgranophyric lava, probably of Tschicoma Formation, and granitoid.
R9-690.4	BD	RGW	10-FEB-98	Core from 690.2 to 690.4 ft depths in drill hole R9 is dark gray, massive fine-grained basalt with common feldspar to 2.5 mm and common olivine to 1.5 mm, which ranges from light green unaltered to red iddingsite pseudomorphs. The sample is moderately veined with a white secondary mineral, probably calcite, filling hairline fractures.
R9-690.4	TN	RGW	04-APR-99	This polished thin section is microporphyritic basalt with phenocrysts of common to abundant olivine and scarce plagioclase. Large vesicles are completely filled with calcite, and smaller vesicles are completely filled with smectite. Plagioclase is slightly altered to smectite where adjacent to smectite-filled vesicles such as at photomap location SE3. Thick iddingsite rims of approximately constant thickness surround all olivine grains, so that groundmass is mostly altered, but the largest phenocrysts have relatively little alteration. Clinopyroxene, all present as equant grains and grain aggregates in groundmass, is entirely unaltered.
R9-699.1	BD	RGW	10-FEB-98	Core from 698.9 to 699.1 ft depths in drill hole R9 is medium gray, fine-grained, moderately vesicular basalt with round vesicles to 4 mm and ovoid vesicles to 14/4 mm. Vesicle surfaces are uniformly covered with an ultrathin coating of a secondary mineral that gives the vesicles a bluish appearance. Feldspar to 1 mm and olivine to 3 mm, mostly altered to iddingsite, are both common.
R9-767D	BD	RGW	15-DEC-99	Cuttings that pass size 10 sieve are uniformly fragments to 24 mm of medium dark gray somewhat finely vesicular, very coarse grained mafic lava with common feldspar phenocrysts to 2 mm and common olivine pseudomorphs to 1 mm of light green clay surrounded by reddish brown iddingsite rims.
R9-771D	BD	RGW	15-DEC-99	Cuttings that pass size 10 sieve are uniformly fragments to 19 mm of medium dark gray somewhat finely vesicular, very coarse-grained mafic lava with scarce to common feldspar phenocrysts to 1.5 mm. Common olivine to 0.5 mm is olive green where unaltered, but mostly altered to reddish brown iddingsite.
R9-771D	TN	RGW	28-FEB-2000	This polished thin section is a single fragment of very coarsely microporphyritic basalt with scarce to common plagioclase phenocrysts. Common to abundant olivine occurs entirely as microphenocrysts mostly altered to iddingsite, but with some relict cores and more common unaltered rims. Very pale brownish and greenish groundmass clinopyroxene is very coarse. No groundmass orthopyroxene was found among about 25 groundmass pyroxene grains examined for optical signs. Although magnetite predominates, ilmenite laths are conspicuous; both phases are coarse and unaltered.

APPENDIX 2. DESCRIPTIONS UNDER BINOCULAR MICROSCOPE (BD), FIELD NOTES (FD), AND THIN SECTION NARRATIVES (TN) FOR SAMPLES OF MAFIC UNITS FROM THE PAJARITO PLATEAU (continued)

Locations are shown in Figure 2C and stratigraphic assignments are provided in Table 2. Workers are David P. Dethier (DPD), Giday WoldeGabriel (GWG), and Richard G. Warren (RGW).

Sample Number	bd fd tn	Worker	Date	Description
R12-138.5D	BD	RGW	25-JUN-98	Ultrasonically cleaned cuttings from 138.3 to 138.5 ft depths in drill hole R12 are fragments of dark gray basalt to 18 mm with scattered ovoid vesicles, generally 2 to 4 mm long, common plagioclase to 2.5 mm, and scarce to rare olivine to 1 mm.
R12-138.5D	TN	RGW	30-AUG-2000	This polished thin section represents 4 fragments of cuttings; all are slightly to moderately vesicular fine-grained pilotaxitic and cryptocrystalline basalt with common phenocrysts of olivine (3%) and plagioclase (8%). Most vesicles are irregular and 0.1-0.2 mm in long dimension; many are filled with smectite. Within groundmass, generally fine-grained skeletal unaltered magnetite is scarce to common (2%), and tiny acicular ilmenite is scarce to rare. No lithics were observed.
R12-228D	BD	RGW	25-JUN-98	Ultrasonically cleaned cuttings from 227.3 to 228 ft depths in drill hole R12 are fragments of slightly vesicular, medium dark gray basalt to 26 mm with scattered ovoid vesicles to 6 mm long, and common light olive olivine to 1.5 mm, occasionally to 4 mm.
R12-228D	TN	RGW	30-AUG-2000	This polished thin section represents 5 large and 1 small fragments of cuttings; all are slightly to moderately vesicular fine-grained pilotaxitic and cryptocrystalline basalt with phenocrysts of common olivine (3%) and scarce to rare plagioclase (1%). Most vesicles are irregular and 0.1-0.2 mm in long dimension; most are filled with smectite. Generally fine-grained skeletal unaltered magnetite is scarce to common (1.5%) within groundmass. No lithics were observed.
R12-270D	BD	RGW	26-JUN-98	Ultrasonically cleaned cuttings from 269 to 270 ft depths in drill hole R12 are fragments of dark gray basalt to 19 mm with scattered round vesicles to 9 mm diameter, and common green olivine to 1.8 mm. Very light brown clay occurs in scarce to rare massive fragments to 3 mm thick, and very thinly and discontinuously on fragment surfaces within the size fraction >0.5 mm, retained on 35 mesh sieve.
R12-270D	TN	RGW	30-AUG-2000	This polished thin section represents 3 fragments of cuttings; all are slightly to moderately vesicular fine-grained pilotaxitic and cryptocrystalline basalt with phenocrysts of scarce to common olivine (2%) and scarce to rare plagioclase (2%) that occurs mostly as laths to 1.4 mm, but includes occasional resorbed grains. Smectite partly fills the largest vesicle and a few other vesicles within the same fragment, but vesicles are generally free of alteration or secondary mineral coatings. Generally fine-grained skeletal, slightly oxidized to unaltered magnetite is scarce to common (1.5%) within groundmass. No lithics were observed.
R12-380D	BD	RGW	26-JUN-98	Ultrasonically cleaned cuttings from 379.2 to 380 ft depths in drill hole R12 are fragments of medium dark gray, coarse grained, massive basalt to 16 mm with rare irregular vesicles to 3 mm and common light green olivine to 3 mm.
R12-380D	TN	RGW	30-AUG-2000	This polished thin section represents 9 fragments of cuttings; all are slightly vesicular medium- to coarse-grained pilotaxitic basalt with phenocrysts of common olivine (4%) and rare plagioclase (0.5%) and clinopyroxene (0.05%). Plagioclase occurs mostly as strongly resorbed grains, and clinopyroxene occurs within a single small glomerocryst that also contains resorbed plagioclase. A single aggregate of groundmass clinopyroxene indicates the presence of a reactive phase that has either been completely assimilated or occurs outside the plane of the thin section. Very coarse-grained unaltered magnetite is common (3%) within groundmass. No lithics were observed.
R12-442D	BD	RGW	26-JUN-98	Ultrasonically cleaned cuttings from 438 to 442 ft depths in drill hole R12 are fragments of medium dark gray, massive basalt to 20 mm.
R12-442D	TN	RGW	30-AUG-2000	This polished thin section represents 5 large and 1 tiny fragments of cuttings; all are slightly vesicular medium-grained pilotaxitic basalt with phenocrysts of common olivine (4%) and rare small laths of plagioclase (0.3%). Olivine phenocrysts are unaltered in 3 large fragments, but are partly to completely replaced by smectite in the other two; other secondary minerals include a trace of later calcite and celadonite. Common groundmass magnetite (3%) is unaltered, even within argillic fragments. No lithics were observed.
R12-810D	BD	RGW	06-AUG-98	Cuttings from 809.6 to 810 ft depths in drill hole R12 are medium dark gray, coarse-grained, very slightly vesicular basalt with common iddingsite after olivine to 2 mm. Vesicles, to 1 mm, are very irregular.
R12-810D	TN	RGW	27-AUG-2000	This polished thin section represents 4 fragments of cuttings; all are slightly to moderately vesicular microporphyric basalt. Smectite or calcite partly to entirely fill most vesicles. Common plagioclase phenocrysts (12%) grade into groundmass. Common to abundant olivine phenocrysts (7%) are partly to entirely altered to iddingsite along rims. Scarce to common magnetite (1.5%) and abundant, generally large stubby laths of ilmenite (1.5%) are both slightly oxidized within groundmass; inclusions of spinel are scarce to common within olivine phenocrysts. No lithics were observed.
R12-877D	BD	RGW	13-JAN-2000	Cuttings from 872 to 877 ft depths in drill hole R12 are fragments to 30 mm of dark olive gray, pilotaxitic, medium- to coarse-grained, slightly vesicular basic lava with scarce to common iddingsite after olivine to 4 mm and scarce to common feldspar phenocrysts to 1.2 mm. The

APPENDIX 2. DESCRIPTIONS UNDER BINOCULAR MICROSCOPE (BD), FIELD NOTES (FD), AND THIN SECTION NARRATIVES (TN) FOR SAMPLES OF MAFIC UNITS FROM THE PAJARITO PLATEAU (continued)

Locations are shown in Figure 2C and stratigraphic assignments are provided in Table 2. Workers are David P. Dethier (DPD), Giday WoldeGabriel (GWG), and Richard G. Warren (RGW).

Sample Number	bd fd tn	Worker	Date	Description
				largest vesicles, ovoid to 10 mm, are partly filled to 9 mm length with white, waxy, nonefforvescent secondary minerals, probably smectite.
R12-880D	BD	RGW	13-JAN-2000	Cuttings from 877 to 880 ft depths in drill hole R12 are fragments to 19 mm of dark gray, pilotaxitic, medium- to coarse-grained, slightly vesicular basic lava with scarce, highly irregular vesicles to 4 mm. Scarce to common iddingsite after olivine occurs in glomerocrysts to 3.5 mm. Feldspar phenocrysts to 1 mm are scarce. Rare white coatings of nonefforvescent secondary minerals to 3 mm are probably smectite.
R12-880D	TN	RGW	17-FEB-2000	This polished thin section consists of 3 fragments of slightly vesicular microporphyric basalt with scarce, somewhat resorbed plagioclase phenocrysts. Common phenocrysts and microphenocrysts of olivine are entirely altered to iddingsite. Rare smectite mostly fills voids.
R15-532D	BD	RGW	20-AUG-99	This sample of ultrasonically cleaned cuttings retained on size 7 sieve (>2.8 mm) is grayish black, fine to medium-grained basalt with scattered, round vesicles to 3 mm diameter scarce to common phenocrysts of olive olivine to 3.5 mm and plagioclase laths to 1.5 mm.
R15-562D	BD	RGW	20-AUG-99	This sample of ultrasonically cleaned cuttings retained on size 7 sieve (>2.8 mm) is dark gray, somewhat microvesicular, coarse-grained basalt, probably ophitic, with phenocrysts of common dark reddish brown olivine to 3 mm and scarce plagioclase laths to 2.5 mm. Very rare grayish pink clay thinly coats vesicles.
R15-577D	BD	RGW	20-AUG-99	This sample of ultrasonically cleaned cuttings retained on size 7 sieve (>2.8 mm) is dark gray, fine-grained basalt with scarce to common phenocrysts of olive olivine and plagioclase, both to 3 mm. A few fragments of medium gray coarse-grained basalt have caved from the overlying interval.
R15-610D	BD	RGW	20-AUG-99	This sample of ultrasonically cleaned cuttings retained on size 7 sieve (>2.8 mm) is light gray coarse-grained basalt with phenocrysts of common dark reddish brown unaltered olivine to 1.5 mm and scarce plagioclase to 1 mm. Grayish orange pink clay occurs as rare, thin fracture coatings.
SHB1-693.7	BD	RGW	04-AUG-97	Core is medium dark gray vitric, pumiceous lava with rare feldspar to 3 mm, and scarce to rare pyroxene, which includes pale green clinopyroxene and black vitreous orthopyroxene. The rock is streaked pale yellowish brown where it is devitrified along thin, discontinuous fractures. Pale greenish void filling to 1 mm is possibly opal. Below 693.8 ft, the rock is increasingly devitrified, with banding from the devitrification dipping 37 degrees.